GREAT LAKES FISHERY COMMISSION

Research Completion Report[1]

A Model for the Transport of Lampricides in St. Marys River

by

Hung Tao Shen
Poojitha D. Yapa
Xun Xia and Shunan Lu
Department of Civil and Environmental Engineering
Clarkson University
Potsdam, New York

March 1995

---

[1] Project completion reports of Commission-sponsored general research are made available to the Commission's cooperators in the interest of rapid dissemination of information that may be useful in Great Lakes fishery management, research, or administration. The reader should be aware that project completion reports have not been through a peer review process and that sponsorship of the project by the Commission does not necessarily imply that the findings or conclusions are endorsed by the Commission.

A MODEL FOR TRANSPORT OF LAMPRICIDES IN ST. MARYS RIVER

by

Hung Tao Shen
Poojitha D. Yapa
Xun Xia
and
Shunan Lu

Sponsored by
Great Lakes Fishery Commission
Ann Arbor, Michigan

Department of Civil and Environmental Engineering
Clarkson University
Potsdam, New York
March 1995

Acknowledgement

This study was partially supported by the Great Lakes Fishery Commission. The authors would like to thank members of the St. Marys River Control Task Force for their continuous input and valuable suggestions.

Contents

List of Tables

List of Figures

Chapter 1

Introduction

In 1930's sea lamprey made their way into the Great Lakes by means of ships. In the subsequent years, the sea lamprey grew at a tremendous rate, that by 1950's the fishing in the region was drastically affected and was getting closer to extinction. A major program of using lampricide to control sea lamprey initiated by the Great Lakes Fisheries Commission has had an important impact in reversing the trend.

This successful program consisted of application of lampricide to kill sea lamprey during the vulnerable larval stage. Major studies conducted by the Geat Lakes Fishery Commission revealed that a certain critical concentration of lampricide needs to be maintained for a specific minimum duration to provide a lethal dose.

Mathematical models provide an inexpensive and useful tool for studying the behavior on the chemical transport in river. Many mathematical models have been developed for simulating the transport and fate of toxic chemicals in rivers and lakes [Schnoor, 1984; Thomann and DiToro, 1983; Ambrose et al., 1983; 1988; McCorquodale et al., 1986; Halfon and Brueggemann, 1990; Dickson et al., 1982; Onishi and Wise, 1979; Baker, 1980]. Most of these models are either one dimensional or simple box-type models, in which the stream or lake is considered as a series of interconnected well-mixed volume segments. In this report, a two-dimensional computer model is developed for simulating the transport and spreading of lampricides in the St. Marys River. The St. Marys River is the connecting waterway between Lake Superior and Lake Huron (Figure 1.1). The upper portion of the river extends approximately 24 km from Whitefish Bay to the St. Marys Rapids at Sault Ste. Marie. This portion has a series of hydraulic structures such as compensating gates, shipping locks, and power generating facilities to control the outflow of Lake Superior. The lower portion of the river, about 76 km in length, consists of several channels, three large and numerous small islands, and lake-like areas. Total surface area of the river is about 732 km^2. Mean annual discharge for the river is 2,140 m^3/s.

The St. Marys River is known to harbor large numbers of sea lamprey larvae and is the only such tributary to Lake Huron that is not treated with lampricides. A computer model can simulate the lampricide transport, provide critical information needed to plan lampricide treatment by predicting the effectiveness of different possible treatment plans. This can reduce or eliminate the use of field experiments of dye injection for treatment planning.

In a recent study, a computer model for oil spills in the upper St. Lawrence River was developed [Shen et al., 1992; Yapa et al., 1992]. This model has been extended to consider chemicals. The integrated chemical/oil spill model, RSPILL, considers chemical transport, transformation and kinetic processes in both river water and bed sediment. In this study, RSPILL is modified to simulate the transport of lampricide in the St. Marys River.

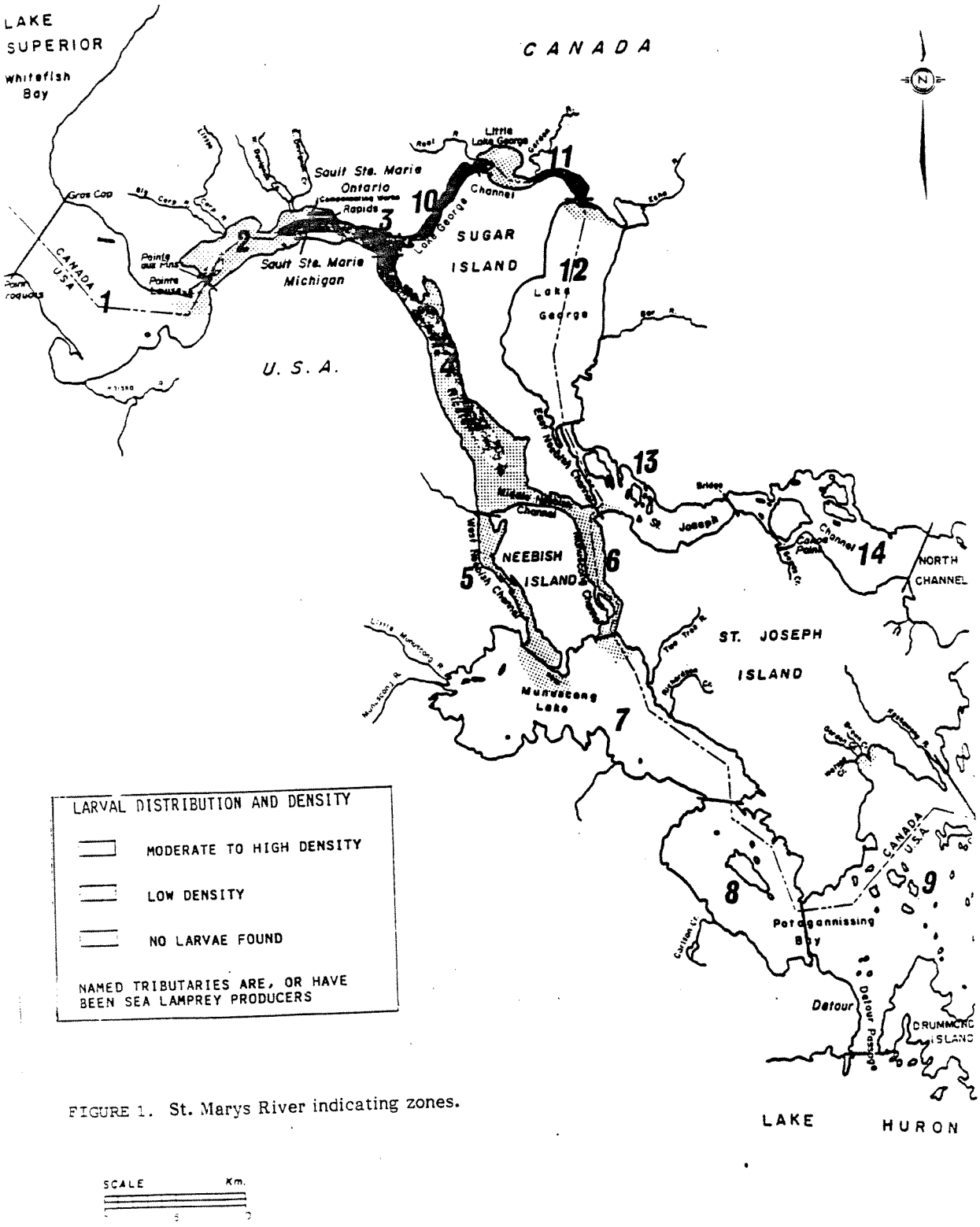

FIGURE 1. St. Marys River indicating zones.

Figure 1.1: The St. Marys River

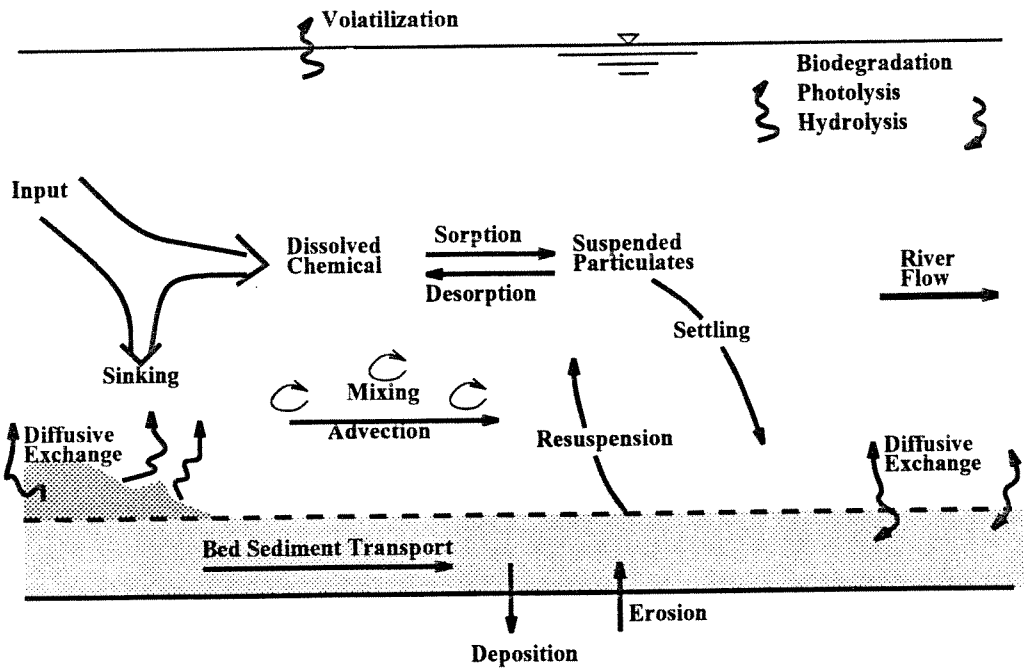

Figure 1.2: Fate and transport of chemicals in rivers

1.1 Transport and Fate of Chemicals

The fate of a chemical in a river is affected by the hydrodynamic, geological, chemical, and biological characteristics of the river and the chemical characteristics [Neely and Blau, eds. 1984; Dickson 1982; Thomann and Mueller 1986]. The hydrodynamics affect the chemical transport through advection and diffusion in the water body as well as in sediment. Reaction and transfer mechanisms are incorporated with the transport phenomena to define the temporal and spatial distribution of the chemical. A brief discussion of the physical, chemical and biological processes as summarized in Fig. 1.2 is given as follows:

1.1.1 Fluid Transport and Sediment Movement

Both the dissolved and particulate components of the chemical are transported along the river by the current through advection and diffusion. The horizontal transport of sediment along the bed, settling and resuspension of sediment, and diffusive exchange across the benthic boundary layer between the water column and the bed significantly affects the distribution of the chemical. Although there were many studies on transport of sands and silts (Egashira, and Ashida, 1991; and Engelund, 1976), there is a significant lack of fundamental understanding on the transport of clays and detrital materials. The exchange across the benthic boundary layer, which is governed by turbulent diffusion at the interface between the bed and the water column, is difficult to simulate by a simple hydrodynamic model. In addition to the above processes, the characteristics of the bed can affect the transport of the dissolved component through the interstitial water and interaction with other constituents in both dissolved and particulate phases.

1.1.2 Chemical Transfer Mechanisms

Chemical transfers occur within the water column and bed sediment. These include sorption-desorption processes between dissolved material and suspended sediment, volatilization of the dissolved fraction, and possibly the deep burial and loss of the material to the bed. Soluble materials will be sorbed onto particulate surfaces until an equilibrium between the dissolved and the particulate phases is reached. Assuming equilibrium is established, various isotherms can be used to describe the relationship between the sorbed and dissolved fractions.

1.1.3 Chemical Kinetic Transformations

The principal transformations are photolysis, hydrolysis, oxidation and biodegradation. These processes are the major ultimate sinks of reacting chemicals in the river. Photolysis is the degradation process by which chemical bonds of a substance are broken as the result of transfer of light or radiant energy to these bonds. The rate of photochemical reaction is expressed in first-order kinetics. The rate coefficient is a function of the quantum yield of the reaction, the available light intensity and the presence of intermediary compounds that contribute to sensitization or indirect photolysis. Hydrolysis of synthetic organic compounds is a common process, and is usually mediated by an acid or base, or less commonly in a neutral environment. In biochemical systems it is usually enzyme-mediated and may be considered a biological reaction. The two major factors influencing chemical hydrolysis are pH and water temperature. Biodegradation is the transformation of chemical compounds by the action of living organisms. It is one of the major processes that affect the fate of organic chemicals, such as pesticides, solvents and detergents. The rate of biodegradation is difficult to determine, since it will be dependent on the concentration of organic compounds in the environment. A number of environmental variables are known to affect the biodegradation of organic chemicals. These include mixing, temperature, oxygen concentration, redox potential, pH, ionic strength, and the presence of organic and inorganic nutrients.

1.2 Chemical transport Model

In the present study, a chemical transport model is developed by taking into consideration the major processes discussed in the preceding section. The model consists of components hydrodynamics of the river flow ; advection and diffusion of chemicals. A brief outline of the model structure is presented in Fig. 1.3.

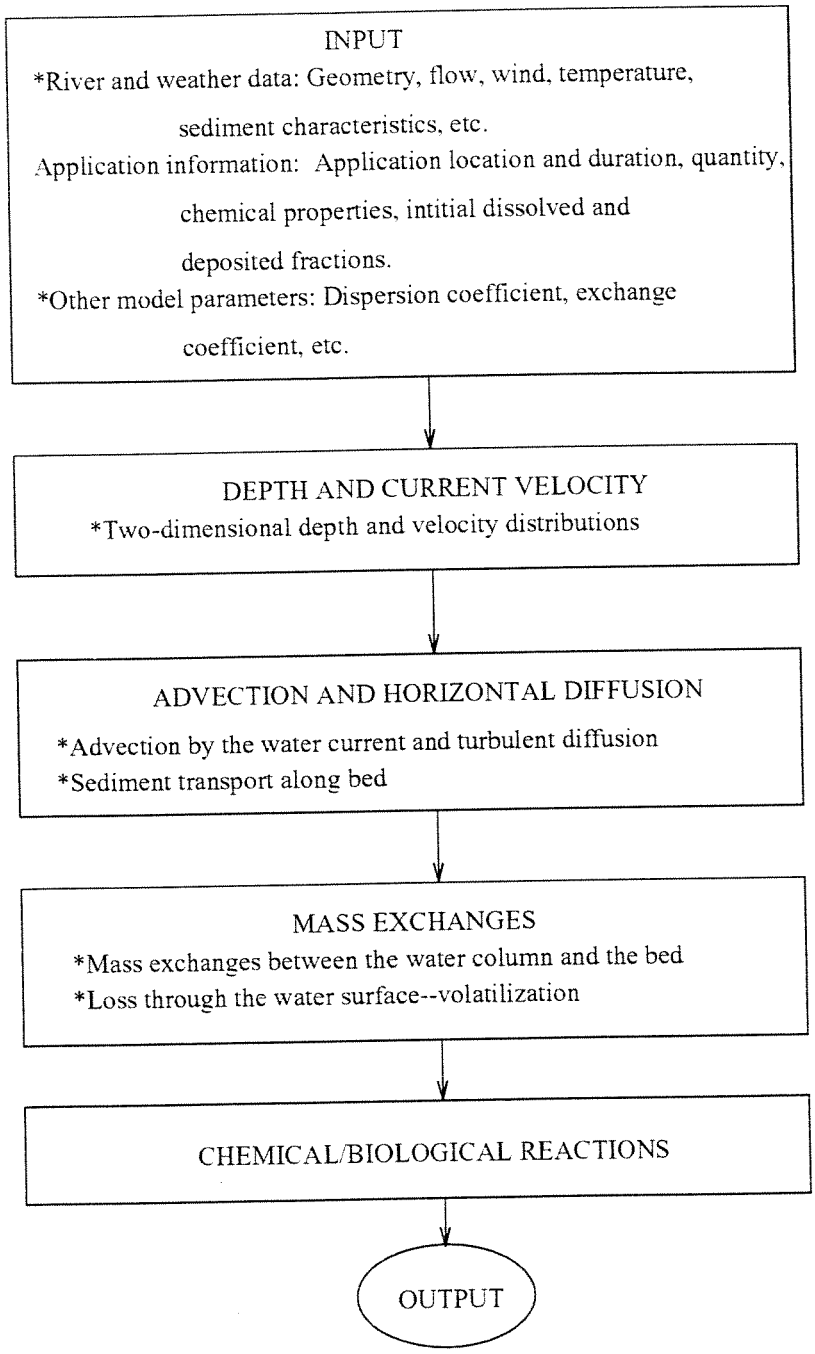

Figure 1.3: Structure of the chemical transport model

Chapter 2

Simulation of Hydrodynamics

Since the water current affects advection, spreading, and the exchange of chemical between the water column and the bed, analysis of the transport of the chemical in a river requires water velocity and depth distributions. A two-dimensional hydrodynamics model [Wake and Xiao, 1989] is used to simulate the hydrodynamics based on a finite element method. This chapter describes the model equations, data preparation, and simulation results.

2.1 Depth-Averaged Shallow Water Equation

For incompressible turbulent flow, the mass conservation equation of water in the Cartesian coordinates system (x_1, x_2, x_3) is:

$$\frac{\partial \rho}{\partial t} + \frac{\partial(\rho v_i)}{\partial x_i} = 0 \tag{2.1}$$

The momentum equation is:

$$\rho \frac{Dv_k}{Dt} = -\frac{\partial p}{\partial x_k} + \frac{\partial \tau_{ik}}{\partial x_i} + \rho b_k \tag{2.2}$$

In these equations, both subscripts i and k vary from 1 to 3; x_i and t = space and time variables; $\frac{D}{Dt} = \frac{\partial}{\partial t} + u\frac{\partial}{\partial x} + v\frac{\partial}{\partial y} + w\frac{\partial}{\partial z}$; ρ = density of fluid; v_i = component of the velocity in the x_i direction; b_k = body force components in the x_k direction; p = pressure; $\tau_{ik} = \mu\frac{\partial u_k}{\partial x_i} - \rho\overline{u'_k u'_i}$, internal stress acting in the k^{th} direction on an elemental surface area with outward normal in the i^{th} direction; and u' = turbulent fluctuation of the water velocity.

For a shallow water body with nearly horizontal flow, Eq. 2.2 can be simplified by neglecting the acceleration and gradients in the vertical direction. Horizontal and vertical components of Eq. 2.2 can be reduced to:

$$\rho \frac{Dv_k}{Dt} = -\frac{\partial p}{\partial x_k} + \frac{\partial \tau_{ik}}{\partial x_i} + \rho b_k; \qquad i,k = 1,2 \tag{2.3}$$

$$-\frac{dp}{dx_3} = \rho g \tag{2.4}$$

Integrating Eq. 2.4, the pressure distribution can be obtained as:

$$\begin{aligned} p &= p_a + \int_{x_3}^{\eta} \rho g dx_3 \\ &= p_a + \rho g(\eta - x_3) \end{aligned} \tag{2.5}$$

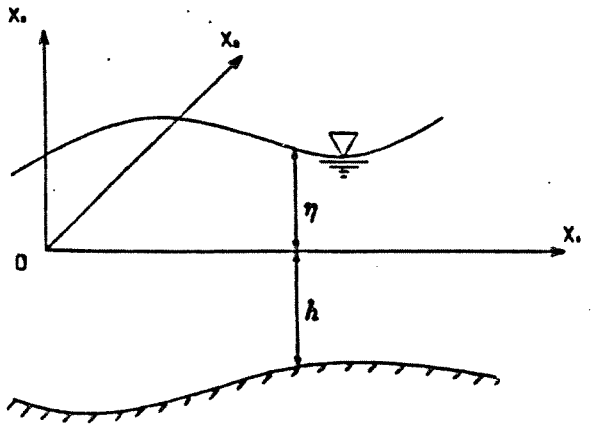

Figure 2.1: Definition sketch for shallow water flows

in which, η = elevation of the free surface from the mean water level, x_3=0; g = gravity; p_a = atmospheric pressure as shown in Fig. 2.1.

Integrating Eq. 2.1 over the depth of the flow, from $x_3 = -h$ to η, and applying appropriate boundary conditions at the bed and the free surface, the following continuity equation can be obtained

$$\frac{\partial(\rho H)}{\partial t} + \frac{\partial(\rho q_1)}{\partial x_1} + \frac{\partial(\rho q_2)}{\partial x_2} = 0 \tag{2.6}$$

in which, $H = h + \eta$ = total flow depth, and $q_i = \int_{-h}^{\eta} v_i dx_3$ = unit width flux. In Eq. 2.6 the mass exchange at $x_3 = \eta$ has been neglected.

Define the excess pressure force as the deviation from the static condition:

$$N_p = \rho \int_{-h}^{\eta} p dx_3 - \frac{1}{2} g h^2 \tag{2.7}$$

The pressure force can be obtained by integrating Eq. 2.6 over the depth of the flow as:

$$N_p = g\eta h + \frac{1}{2} g\eta^2 + \frac{1}{\rho} p_a H \tag{2.8}$$

Depth-integrated momentum equations can be obtained by integrating Eq. 2.3 from $-h$ to η and replacing x_1, x_2 and x_3 dimension by x, y and z:

$$\frac{\partial q_x}{\partial t} + \frac{\partial}{\partial x}\left(\frac{q_x^2}{H}\right) + \frac{\partial}{\partial y}\left(\frac{q_x q_y}{H}\right) = -\frac{\partial N_p}{\partial x} + \frac{1}{\rho}\left(\frac{\partial N_{xx}}{\partial x} + \frac{\partial N_{yx}}{\partial y}\right) + f q_y + \frac{1}{\rho}(\tau_{s_x} - \tau_{b_x}) + g\eta\frac{\partial h}{\partial x} \tag{2.9}$$

and

$$\frac{\partial q_y}{\partial t} + \frac{\partial}{\partial x}\left(\frac{q_x q_y}{H}\right) + \frac{\partial}{\partial y}\left(\frac{q_y^2}{H}\right) = -\frac{\partial N_p}{\partial y} + \frac{1}{\rho}\left(\frac{\partial N_{yy}}{\partial y} + \frac{\partial N_{xy}}{\partial x}\right) - f q_x + \frac{1}{\rho}(\tau_{s_y} - \tau_{b_y}) + g\eta\frac{\partial h}{\partial y} \tag{2.10}$$

with

$$N_{ij} =< \tau_{ij} + \rho u_i' u_j' >\equiv \int_{-h}^{\eta} (\tau_{ij} + \rho u_i' u_j') dz;$$
$$\simeq \varepsilon_{ij}(\frac{\partial q_i}{\partial x_j} + \frac{\partial q_j}{\partial x_i}); \quad i,j = x,y \tag{2.11}$$

in which, u_i' = deviation of u_i from its depth-averaged value; $<\ >$ = depth-integrated value; f = Coriolis factor: τ_s and τ_b = shear stresses at the free surface and the bottom.

The bottom shear stresses in Eqs. 2.9 and 2.10 can be expressed as:

$$\tau_{b_x} = c_f \rho \frac{q_x ({q_x}^2 + {q_y}^2)^{1/2}}{H^2}$$
$$\tau_{b_y} = c_f \rho \frac{q_y ({q_x}^2 + {q_y}^2)^{1/2}}{H^2} \tag{2.12}$$

in which, the friction coefficient c_f can be expressed in terms of Manning's coefficient of the bed as

$$c_f = \frac{n_b^2}{H^{1/3}} g \tag{2.13}$$

2.2 Finite Element Formulation

The basic idea of finite element method is to approximate the solution of a global system of the first order ordinary differential equations which are transformed from a system of the second order partial differential equations by a simple polynomial in a smaller triangular subdomain called element.

The FEM formulation used here is based on the weighted residual method and Galerkin's criteria. Assuming that q_x, q_y, and η have the same interpolation shape function $[\phi]$, then

$$q_x = [\phi]\{q_x\}^e$$
$$q_y = [\phi]\{q_y\}^e$$
$$\eta = [\phi]\{\eta\}^e \tag{2.14}$$

The system of equations in FEM over a triangular element can be expressed as:

$$[M]^e \frac{\partial \{q_x\}^e}{\partial t} - \{F_x\}^e = 0$$
$$[M]^e \frac{\partial \{q_y\}^e}{\partial t} - \{F_y\}^e = 0$$
$$[M]^e \frac{\partial \{\eta\}^e}{\partial t} - \{F_\eta\}^e = 0 \tag{2.15}$$

in which

$$[M]^e = \int\int \{\phi\}[\phi] dA$$
$$\{F_x\}^e = \int\int (\{\phi\} B_x^* - \{\phi\} A_x) dA$$
$$\{F_y\}^e = \int\int (\{\phi\} B_y^* - \{\phi\} A_y) dA$$
$$\{F_\eta\}^e = -\int\int (\frac{\partial \{\phi\}}{\partial x} q_x + \frac{\partial \{\phi\}}{\partial y} q_y) dA - \int_s \{\phi\} \bar{q}_n dS \tag{2.16}$$

and

$$A_x = \frac{\partial}{\partial x}(\frac{q_x^2}{H}) + \frac{\partial}{\partial y}(\frac{\partial q_x q_y}{H})$$
$$A_y = \frac{\partial}{\partial y}(\frac{q_x q_y}{H}) + \frac{\partial}{\partial x}(\frac{q_y^2}{H})$$
$$B_x^* = fq_y + \tau_{s_x} - \tau_{b_x} - (gh\frac{\partial \eta}{\partial x} + g\eta\frac{\partial \eta}{\partial x})$$
$$B_y^* = -fq_x + \tau_{s_y} - \tau_{b_y} - (gh\frac{\partial \eta}{\partial y} + g\eta\frac{\partial \eta}{\partial y}) \tag{2.17}$$

The shape function $\{\phi\}$ for a linear triangular element is defined as:

$$\phi_i = \frac{1}{2\Delta}(a_i + b_i x + c_i y) \tag{2.18}$$

in which, Δ is the area of the triangular element, a, b,and c are parameters determined by the geometry of the element and i denotes the three nodes of the triangular element. The corresponding mass matrix $[M]^e$ can be written as:

$$[M]^e = \int\int \{\phi\}[\phi]dA = \frac{\Delta}{12}\begin{pmatrix} 2 & 1 & 1 \\ 1 & 2 & 1 \\ 1 & 1 & 2 \end{pmatrix} \tag{2.19}$$

An explicit finite difference scheme is employed to integrate Eq.2.15 with respect to time. Then

$$[M]\frac{(\{\Psi\}^{t+\Delta t} - \{\Psi\}^t)}{\Delta t} = \{F\} \tag{2.20}$$

and

$$\{\Psi\}^{t+\Delta t} = \frac{1}{|M|}(\Delta t\{F\} + \{\Psi\}) \tag{2.21}$$

in which, Ψ can be q_x, q_y or η, and the assembled global matrix $[M]$ is a banded-symmetric all positive real matrix. It is time consuming to solve such a large complex matrix. The shape functions can be modified to have an unit value in the adjacent regions of one node and zero in others. The new shape functions ϕ_1^*, ϕ_2^* and ϕ_3^* are orthogonal, i.e. $\phi_i^*\phi_j^* = 1$ when $i = j$, and 0 when $i \neq j$. By doing so, the lumped mass matrix becomes a diagonal matrix $[M']^e$.

$$[M']^e = \int\int \{\phi^*\}[\phi^*]dA = \frac{\Delta}{3}\begin{pmatrix} 1 & 0 & 0 \\ 0 & 1 & 0 \\ 0 & 0 & 1 \end{pmatrix} \tag{2.22}$$

The global mass matrix $[M']$ also becomes diagonal. The solution of $\{q_x\}, \{q_y\}$ and $\{\eta\}$ can be solved easily. This lumped formulation has proven itself to be one of the most powerful techniques in the FEM simulation of shallow water hydrodynamics.

Similarly, the water surface slope $\frac{\partial \eta}{\partial x}$ and $\frac{\partial \eta}{\partial y}$ can be solved by their FEM formulation as:

$$\{\frac{\partial \eta}{\partial x}\}^e = \int\int \frac{\partial\{\phi\}}{\partial x}\eta dA$$
$$\{\frac{\partial \eta}{\partial y}\}^e = \int\int \frac{\partial\{\phi\}}{\partial y}\eta dA \tag{2.23}$$

By applying lumped technique, they will be calculated at the same time when solving $\{\eta\}$.

2.3 Initial Conditions and Boundary Conditions

Theoretically, the solution at any time level can be obtained through the FEM scheme if a set of initial values of q_x, q_y and η in the solution domain are given. Practically, it is impossible to define initial values accurately. Therefore, the initial conditions are obtained by the following two methods:

- At the initial moment, a quiescent flow is assumed;
- The initial conditions are given as the result from a previous run.

It should be noted that the zero initial values from a "Cold-Start" state and the suddenly imposed flux boundary conditions will cause a drain or recharge near outflow and inflow boundaries at the very beginning of the computation. When the recharged flow near the entrances does not have enough time to reach the drained areas, the bottom of the domain at some shallow region becomes dry, i.e. water depth is zero, and the numerical scheme will blow up. Therefore, the recharge or discharge flow need to be adjusted to their full rate gradually.

There are three types of boundary conditions in the model. Either mass flux q or surface elevation η needs to be prescribed on boundary nodes. The global coordinate system needs to be transformed to the local one according to its boundary normal direction.

2.4 Time Integration

By using finite element method and the lumping technique, the original set of non-linear, second-order partial differential equations is reduced to a system of first-order ordinary differential equations. Therefore, an explicit type time-stepping scheme can give enough accuracy. A modified explicit time integration technique called leap-frog method which is accurate to second order in time step $\mathcal{O}(\Delta t^2)$ is applied.

Suppose the initial condition for water surface elevation and mass flux are given, the solution at any time can be achieved by solving the FEM equations. The solutions of water surface elevation η as well as surface tilt $\frac{\partial \eta}{\partial x}, \frac{\partial \eta}{\partial y}$ are calculated at half time steps, i.e time $t^{n-1/2}, t^{n+1/2}, \ldots$. The solutions of mass flux q_x, q_y are solved at time $t^n, t^{n+1}, \ldots$.

Since the leap-frog method is considered conditionally stable, a proper critical time step Δt_{cr} must be satisfied to stabilize the whole process of solution advancement. The critical time step for leap-frog method must satisfy

$$\Delta t_{cr} = 1.5 \frac{\Delta L}{\sqrt{2gh}} \tag{2.24}$$

in which, ΔL = the minimum size of element, i.e. minimum length of the side of all the triangular elements, and h = the maximum water depth under mean water surface level. When combined with the lumped formulation, the critical time step can be increased to $\sqrt{3}\frac{\Delta L}{\sqrt{2gh}}$. The effort of increasing the time step will provide savings of computation time and efficiency.

The convective terms of governing equations often cause oscillation or instability of the solution. Numerical viscosity or added dissipation is always used to increase stability. Besides the viscosity term in the second derivatives, an added viscosity is included as total viscosity $\alpha_{total} = \alpha + \alpha_{add}$. The upwind method is employed to estimate added viscosity as $\alpha_{add} = K\frac{|u|\Delta L}{2}$, where u is velocity and K is a undetermined coefficient. According to the optimum added dissipation method (Wake and Xiao 1989), K is calculated as $K = \coth(\gamma) - \frac{1}{\gamma}$ and $\gamma = \frac{|u|\Delta L}{2\alpha}$.

The extension of optimum added dissipation method on two-dimensional case can be applied to two vertically-integrated momentum equations. The modifications of eddy viscosities ε_{ij} in the internal stress term, $N_{xx} = \frac{\partial}{\partial x}(2\varepsilon_{xx}\frac{\partial q_x}{\partial x})$, $N_{yy} = \frac{\partial}{\partial y}(2\varepsilon_{yy}\frac{\partial q_y}{\partial y})$ and $N_{xy} = \frac{\partial}{\partial y}(\varepsilon_{xy}\frac{\partial q_y}{\partial x})$, are

$$\begin{cases} \varepsilon_{xx_{total}} = \varepsilon_{xx} + \varepsilon_{xx_{add}} \\ \varepsilon_{yy_{total}} = \varepsilon_{yy} + \varepsilon_{yy_{add}} \\ \varepsilon_{xy_{total}} = \frac{1}{4}(\varepsilon_{xx_{total}} + \varepsilon_{yy_{total}}) \end{cases} \tag{2.25}$$

Here

$$\varepsilon_{ij_{add}} = K(\gamma_{ij})\gamma_{ij}\varepsilon_{ij} \tag{2.26}$$

Therefore, the eddy viscosities are adjusted according to corresponding velocities in each time step to suppress the numerical oscillation and keep stability.

2.5 Input and output files

The two-dimensional hydrodynamics model is written in Fortran-77. All I/O files have the same primary name, but different extension names. Here, we use "*" to present file name; The extension name should always be the same as the ones given here.

2.5.1 Input files

There are 7 input files:

1. ***.time**
   Starting type (cold start or hot start), the end time of the simulation and the time step of the hydraulic simulation.

2. ***.ptm**
   output control

3. ***.geo**
   Geometry information of the whole domain including finite element meshes, islands, water depth under standard water level at each finite element node, land boundary, open boundary, manning's coeffients, and eddy viscosity.

4. ***.elv**
   Boundary elevation specified

5. ***.flx**
   Boundary flux specified

6. ***.dsc**
   boundary discharge specified

7. ***.wnd**
   Wind data including updated time, magnitude and direction

There are two categories of the above input files. The first category can be considered as fixed data for a given river such as *.geo. This is the information required to describe the geometry of the river. Normally, there is no need to adjust this data. The second category includes various hydrodynamic boundary conditions, which may be adjusted according to the flow conditions.

2.5.2 Data preparation

The first step for data preparation is to setup the geometry of St. Marys River. The map of this river from National Ocean Service is digitized to produce the node points of about 4,000 and to determine the shoreline geometry and bottom topography of the domain. A finite element mesh of about 8,000 elements are created using the FASTAB software. Fig. 2.2 shows the triangulation finite element system. Figure 2.3 shows the contour of water depth. These informations of geometry are organized to form the *.geo file.

Throughout the simulation, the unit discharge at the nodes of inflow boundaries are specified. The land boundary nodes are prescribed as zero-normal flux. For the downstream boundary, water levels are specified at every outflow nodes.

The flow model is calibrated for three typical discharges at 1614 m^3/s, 2152 m^3/s, and 3143 m^3/s. The Manning's coefficients are selected so that the model can provide a good agreement with previous one dimensional simulation for water level at differet stations and discharge distribution between East Channel and South Channel. Table 2.1 to 2.3 show the comparisons of water level and discharge distributions of the two-dimensional model and th one-dimensional simulation.

2.5.3 Output files

There are 3 output files:

1. ***.hdw**
   Print the desired hydrodynamics results including unit discharge components in both x,y directions and water level. The results can be used as the initial conditions of hydraulic for hot start. From the above output of hydrodynamics result, the velocity are gotten at each node. The Fig. 2.4 shows the velocity contour under hydrological condition during the fall of 1981 which is descripted in the case studies in the chapter 6.

2. ***.prt**
   Print the information in detail, including some input information.

3. ***.err**
   Print the error information during the simulation.

2.5.4 Running the program

When running the program, the display on the computer is

File name (without extension) ?

type your file name and press the "return" key.

Case 1. Q=57,000 cfs (1614 cms)

Discharge (cms)	1-D simulation	2-D simulation
Total inflow	1770	1622
Total outflow	1815	1630
East channel	426	418
South channel	1389	1212

Water level (m)	1-D simulation	2-D simulation
Section 1	177.40	177.37
Section 3	177.30	177.31
Section 4	177.23	177.20
Section 5	177.15	177.17
Section 6	177.15	177.15
Section 7	177.09	177.07
Section 8	177.00	176.98
Section 9	177.26	177.25
Section 10	177.17	177.16
Section 11	177.12	177.11
Section 12	177.00	176.98
Section 13	176.88	176.88

Table 2.1: **Comparison of 1-D and 2-D simulation result for 1614 cms**

Case 2. Q=76,000 cfs (2152 cms)

Discharge (cms)	1-D simulation	2-D simulation
Total inflow	2362	2163
Total outflow	2430	2167
East channel	577	573
South channel	1853	1594

Water level (m)	1-D simulation	2-D simulation
Section 1	177.78	177.77
Section 3	177.71	177.73
Section 4	177.60	177.57
Section 5	177.52	177.54
Section 6	177.52	177.52
Section 7	177.46	177.44
Section 8	177.37	177.35
Section 9	177.64	177.62
Section 10	177.55	177.54
Section 11	177.49	177.48
Section 12	177.40	177.40
Section 13	177.25	177.25

Table 2.2: **Comparison of 1-D and 2-D simulation result for 2152 cms**

Case 3. Q=111,000 cfs (3143 cms)

Discharge (cms)	1-D simulation	2-D simulation
Total inflow	3393	3169
Total outflow	3532	3176
East channel	865	898
South channel	2667	2278

Water level (m)	1-D simulation	2-D simulation
Section 1	178.04	178.07
Section 3	177.89	170.01
Section 4	177.76	177.75
Section 5	177.68	177.72
Section 6	177.68	177.68
Section 7	177.61	177.60
Section 8	177.45	177.44
Section 9	177.87	177.83
Section 10	177.71	177.72
Section 11	177.65	177.64
Section 12	177.45	177.44
Section 13	177.31	177.31

Table 2.3: **Comparison of 1-D and 2-D simulation result for 3143 cms**

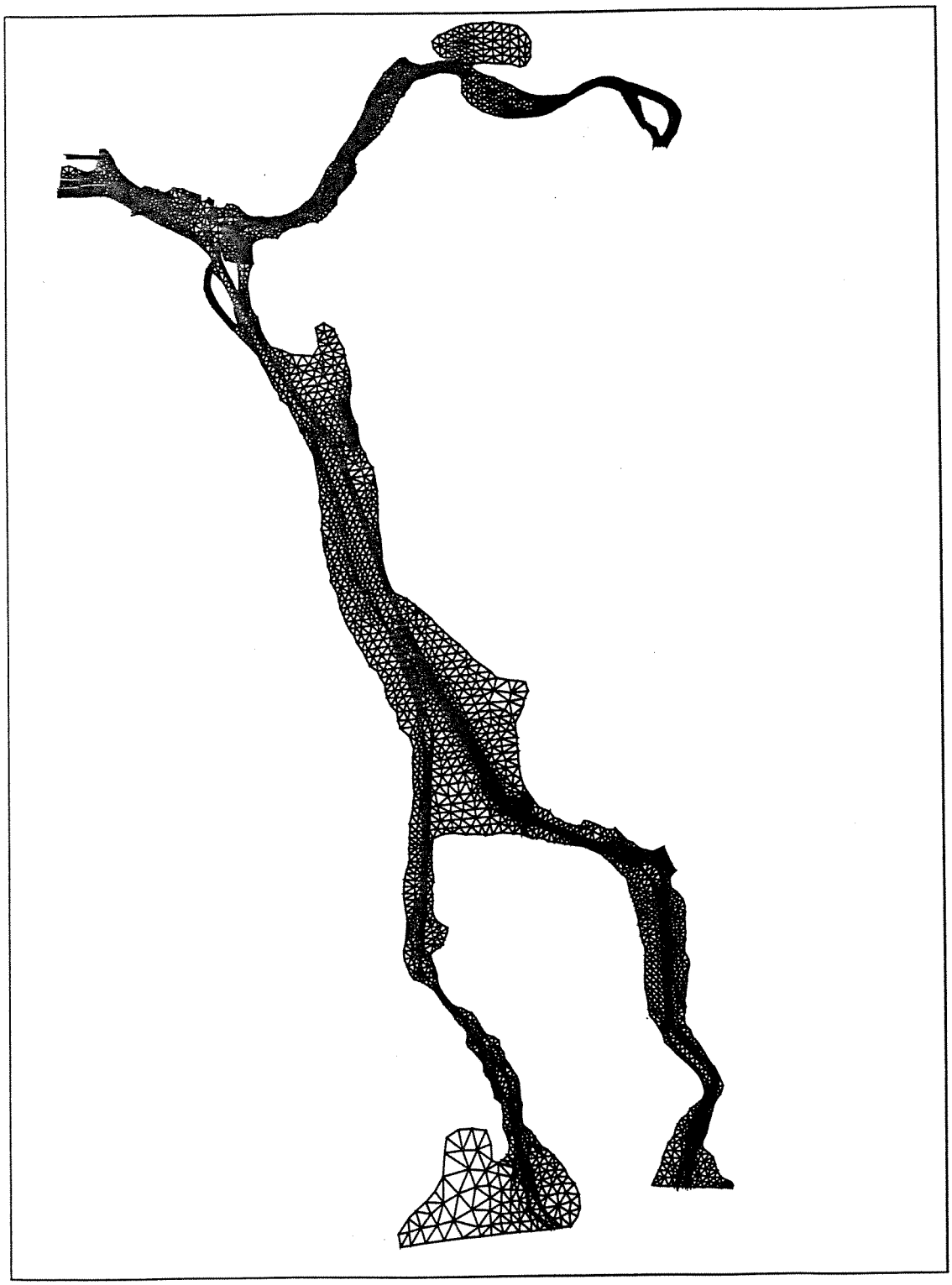

Figure 2.2: Finite element system of St. Marys River

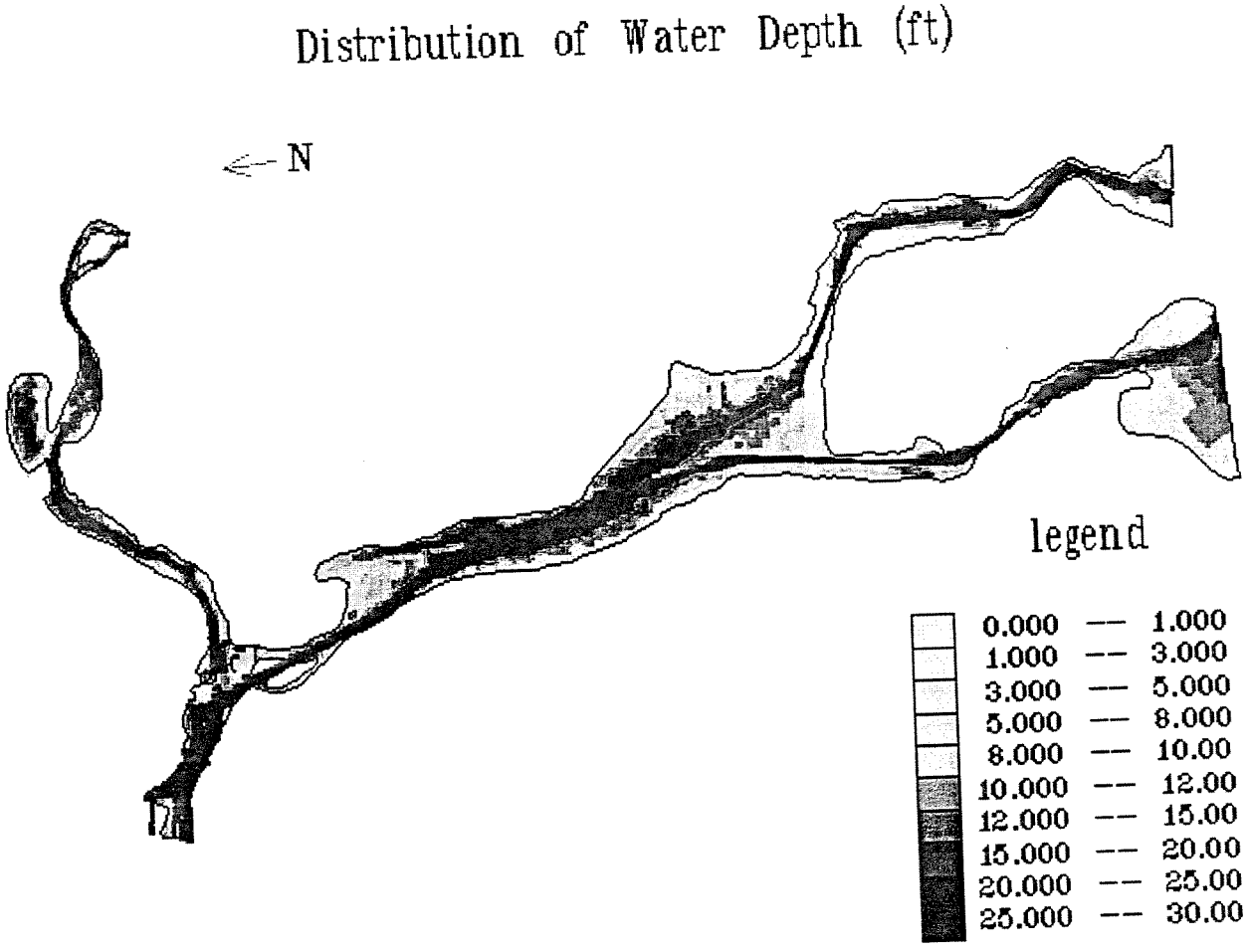

Figure 2.3: Distribution of Water Depth

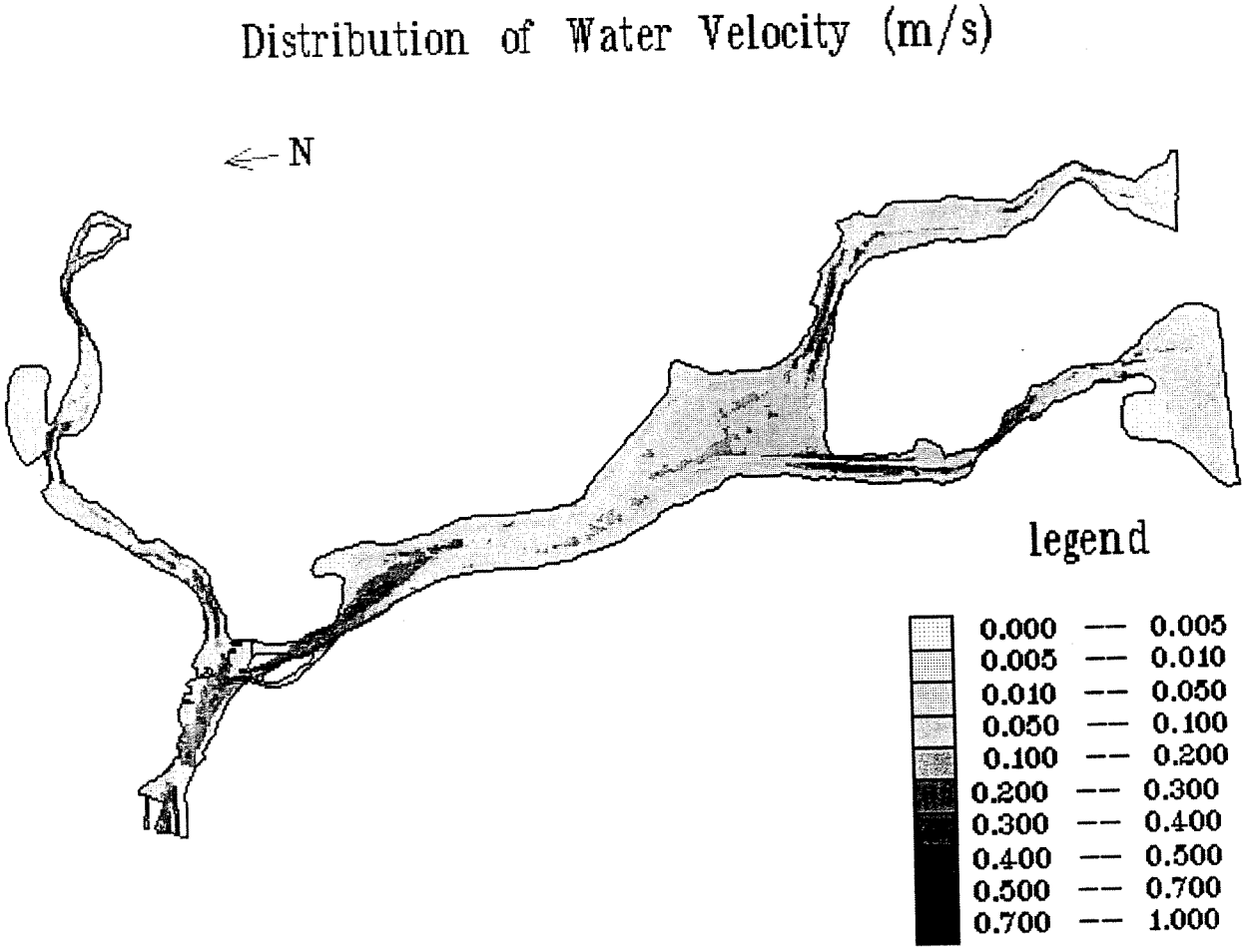

Figure 2.4: Distribution of Water Velocity

Chapter 3

Chemical Transport Simulation

The chemical that is being transported in the river is considered to be distributed in the water column and the bed sediment. These two layers are designated as layers 1 and 2, respectively. Concentrations in these two layers are represented by their depth-averaged values. The sediment on the bed is considered to be transported along the bed under the influence of the fluid shear. Exchanges of sediment and chemical at the interface between the bed and the water column is considered. Chemical can exist in both dissolved form or in particulate form absorbed to solids.

3.1 Governing Equations

Consider an element of length Δx and width Δy, as shown in Figure 3.1. The governing equation of the total chemical concentration C_1 in the water column can be written as

$$\begin{aligned}\frac{\partial(C_1h_1)}{\partial t}+\frac{\partial}{\partial x}(u_1C_1h_1)+\frac{\partial}{\partial y}(v_1C_1h_1)= \\ \frac{\partial}{\partial x}(h_1D_x\frac{\partial C_1}{\partial x})+\frac{\partial}{\partial y}(h_1D_y\frac{\partial C_1}{\partial y}) \\ +K_f(f_{d2}\frac{C_2}{\phi_2}-f_{d1}C_1)-K_{d1}f_{d1}h_1C_1 \\ -k_l[(-\frac{C_g}{H_e}+f_{d1}C_1)]-V_sf_{p1}C_1+V_uf_{p2}C_2\end{aligned} \tag{3.1}$$

Similarly, the equation for the total concentration in the moving bed sediment C_2 is

$$\begin{aligned}\frac{\partial(C_2h_2)}{\partial t}+\frac{\partial}{\partial x}(u_2C_2h_2)+\frac{\partial}{\partial y}(v_2C_2h_2)= \\ -K_f(f_{d2}\frac{C_2}{\phi_2}-f_{d1}C_1)-K_{d2}f_{d2}h_2C_2 \\ +V_sf_{p1}C_1-V_uf_{p2}C_2-V_df_{p2}C_2\end{aligned} \tag{3.2}$$

in which, subscripts 1, 2 denote water column and bed sediment, respectively; C = chemical concentration; h_1 = depth of flow; h_2 =depth of moving sediment layer; x, y, t = space and time variables; D_x, D_y = diffusion coefficients in x and y directions; u, v = components of depth-averaged velocity in x and y directions respectively; f_d = dissolved chemical as a fraction of the total chemical; f_p = chemical in particulate phase as a fraction of the total chemical; K_f

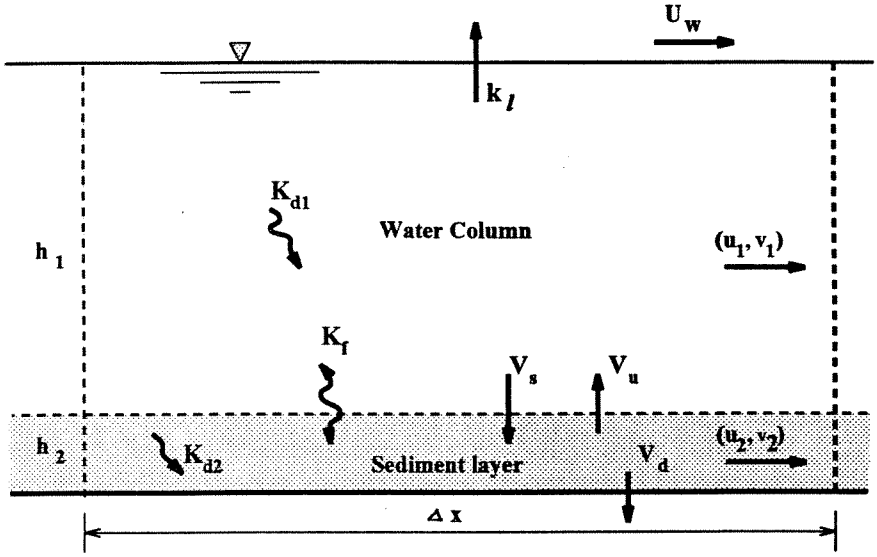

Figure 3.1: Chemical transfers in a differential element of width Δy

= diffusion rate of dissolved chemical between the sediment and water column; K_d = dissolved chemical loss rate due to microbial decay, photolysis and hydrolysis; ϕ = porosity; k_l = overall volatilization transfer coefficient across air-water interface; V_s = settling velocity of particulate from water column to the bed sediment; V_u = resuspension velocity of sediment into the water column; V_d = loss velocity of chemical from sediment due to net sedimentation or burial; H_e = Henry's constant; C_g = vapor phase concentration.

In Eq. 3.1, the third term on the right-hand side is the diffusive exchange of dissolved chemical between the sediment and the water column. The fourth and fifth terms are net chemical losses due to volatilization, photolysis, hydrolysis and biodegradation. The last two terms are the exchanges of the chemical in the particulate phase between the sediment and the water column.

Equations 3.1 and 3.2 can be written in Lagrangian form as

$$\begin{aligned} h_1\frac{DC_1}{Dt} = & \frac{\partial}{\partial x}(h_1 D_x\frac{\partial C_1}{\partial x}) + \frac{\partial}{\partial y}(h_1 D_y\frac{\partial C_1}{\partial y}) \\ & + K_f(f_{d2}\frac{C_2}{\phi_2} - f_{d1}C_1) - K_{d1}f_{d1}h_1C_1 \\ & - k_l[(-\frac{C_g}{H_e} + f_{d1}C_1)] - V_s f_{p1}C_1 + V_u f_{p2}C_2 \end{aligned} \tag{3.3}$$

and

$$\begin{aligned} h_2\frac{DC_2}{Dt} = & -K_f(f_{d2}\frac{C_2}{\phi_2} - f_{d1}C_1) - K_{d2}f_{d2}h_2C_2 \\ & + V_s f_{p1}C_1 - V_u f_{p2}C_2 - V_d f_{p2}C_2 - C_2(V_s\frac{m_1}{m_2} - V_u - V_d) \end{aligned} \tag{3.4}$$

in which, m_1 and m_2 = solid concentrations defined as mass of solids per bulk volume of solids and water.

3.2 Chemical Sorption

The fate of a chemical in an environmental system is highly dependent on sorptive behavior. If the sorption process is assumed to be an equilibrium first order kinetic process, a partition coefficient can be used to specify the fraction of dissolved and particulate components of the chemical to the total. The total chemical concentration can be expressed as

$$C = C_p + C_d \tag{3.5}$$

in which, subscripts p and d denote the solution and the sorbed phases, respectively. Hence, $C_d = f_d\, C$ and $C_p = f_p C$. The fraction of the total chemical concentration that is in the particulate phase can be expressed as

$$f_p = \frac{\Gamma m}{1 + \Gamma m} \tag{3.6}$$

in which, Γ= the porosity corrected partition coefficient, $C_p/(mC_d)$; and m=solid concentration defined as mass of solids per bulk volume of solids and water. For heavy metals Thomann[1985] suggested that the water column partition coefficient can be approximated by

$$\Gamma = 250000 m^{-1} \tag{3.7}$$

in which, the units of Γ and m are l/kg and mg/l respectively. This is equivalent to $f_d = 0.8$, independent of the solids concentration. The sediment partition coefficient is generally less than the water column partition coefficient. For organic chemicals, the partition coefficient can be related to the relative distribution of the chemical between water and octanol, i.e. the octanol-water partition coefficient, K_{ow}, and the solubility of the chemical in the water, S_w. The sorption of organic chemicals to sediment is a function of the weight fraction of the organic carbon of the sediment. Karickoff et al. [1979] relate the organic carbon partition coefficient Γ_{oc} to K_{ow} by $\Gamma_{oc} = 0.617 K_{ow}$ Hence,

$$\Gamma = 0.617 f_{oc} K_{ow} \tag{3.8}$$

in which, f_{oc} = the weight fraction of organic carbon of the total solids concentration. This fraction ranges from about 0.001 to 0.1. Based on the study of Di Toro [1985], Thomann and Salas [1986] suggested

$$\Gamma = \frac{f_{oc} K_{ow}}{1 + m(f_{oc} K_{ow})/1.4} \tag{3.9}$$

in which, m = solid concentration in the water column. This indicates that organic chemicals with a low partition coefficient and a normal range of suspended solid concentration principally exists in the dissolved form. The coefficient K_{ow} may be estimated according to Chiou et al. [1977]

$$\log K_{ow} = 5.0 - 0.67 \log S_w \tag{3.10}$$

Other formulas for K_{oc} are summarized by Karickhoff [1984]. Values of K_{oc} and K_{ow} for selected chemicals are given by Lyman et al.[1982].

3.3 Numerical Scheme

The movement of the chemical in the river as described by Eqs. 3.1 and 3.2 is mainly governed by the advection and diffusion processes. These equations can be solved when chemical properties are known. A Lagrangian discrete-parcel method [Shen et al. 1991] is used. In the Lagrangian discrete-parcel algorithm, both the chemical on the bed and the chemical in the suspension are represented as an ensemble of a large number of small parcels. Each parcel has a set of time dependent spatial coordinates, and a mass associated with it. The movement of each parcel in the river is affected by the water current and the concentration of surrounding parcels. During each time step, all the parcels are first displaced according to the current or sediment velocities and a turbulent fluctuation component applied at their respective locations. The turbulent fluctuation component is simulated by using the random walk method (Fischer et al. 1979). The fluctuation component depends on the diffusion coefficient. After all the parcels are displaced according to advection and diffusion, further modifications to parcel volume and location are introduced to account for mass exchanges and chemical reactions. Therefore, the mass of parcels changes with time. The number of parcels also increases with time during the simulation. If a large number of parcels are released in the river, and their discrete path and mass are followed and recorded as functions of time relative to a grid system in fixed space, then the concentration distribution of the pollutant in the water column or bed sediment can be computed. The approach requires an efficient book-keeping procedure rather than the the solution of a large matrix associated with a conventional Eulerian finite-difference or finite-element method. The Lagrangian discrete parcel algorithm is inherently stable with respect to time, although the time step should be compatible with the grid size and velocity for numerical accuracy.

3.4 Sediment Transport and Exchange at the Bed

Sediments can be transported as a suspension in the water column or along the bed as a bed load. The transport of the suspended sediment can be described by an advective diffusion equation presented as

$$\frac{\partial(m_1 h_1)}{\partial t} + \frac{\partial}{\partial x}(u_1 m_1 h_1) + \frac{\partial}{\partial y}(v_1 m_1 h_1) = \frac{\partial}{\partial x}(h_1 D_x \frac{\partial m_1}{\partial x}) + \frac{\partial}{\partial y}(h_1 D_y \frac{\partial m_1}{\partial y}) - V_s m_2 + V_u m_1 \tag{3.11}$$

in which, m_1 =suspended sediment concentration; and m_2=bed sediment concentration.

Eq. 3.14 can be solved by the Lagrangian discrete-parcel method in a manner similar to solving Eqs. 3.1 and 3.2 . The transport of the bed sediment can be described by

$$\frac{\partial(m_2 h_b)}{\partial t} + \frac{\partial}{\partial x}(u_b m_2 h_b) + \frac{\partial}{\partial y}(v_b m_2 h_b) = -V_u m_2 + V_s m_1 - V_d m_2 \tag{3.12}$$

in which, h_b = thickness of the bed load layer; and u_b, v_b = components of the bed load velocity V_b. Extensive literature on the transport of sediment in alluvial rivers exist [Vanoni 1977]. Relatively little is known concerning the transport of clays and other cohesive materials that often exist in

estuaries [Mehta 1986]. For alluvial rivers, the velocity of the bed sediment can be estimated by [Engelund 1976]

$$V_b = \alpha U_* \left(1 - 0.7\sqrt{\frac{\Theta_c}{\Theta}}\right) \tag{3.13}$$

in which, V_b = velocity of the bed load, its direction is the same as the velocity of water column; U_*= shear velocity at the interface between water and sediment; Θ = nondimensional shear stress, Θ_c = nondimensional constant, equal to 0.046; and α = 9.3. U_* and Θ are given by

$$U_* = \sqrt{\frac{\tau_o}{\rho}} \tag{3.14}$$

$$\Theta = \frac{\tau o}{(\gamma_s - \gamma)d} \tag{3.15}$$

and

$$\tau_o = \frac{\gamma n^2 V_w^2}{H^{1/3}} \tag{3.16}$$

in which, V_w = current velocity, H = depth of water, d = diameter of sand, γ and γ_s are the specific weights of water and solid respectively.

According to Engelund's bed-load theory, the thickness of bed-load is given by

$$h_2 = \frac{\gamma d}{\beta}(\Theta - \Theta_c) \tag{3.17}$$

in which, h_2 = the depth of bed-load layer, β = an empirical constant, equal to 0.8.

Egashira et al.[1991] suggested the following expression

$$h_2 = \frac{\Theta d}{\overline{c}\cos\theta(\tan\phi_s/(1+\alpha) - \tan\theta)} \tag{3.18}$$

in which, θ = bed slope; ϕ_s = friction angle; $\overline{c}$ = bed sediment concentration; and α is an empirical constant = 0.25. Equation 3.18 is the same as Eq. 3.17, when $\overline{c}$=0.5.

For cohesive sediments, the deposition rate D_s can be estimated by [Krone 1983]

$$D_s = W_s C_b (1 - \frac{\tau_b}{\tau_d}) \tag{3.19}$$

in which, W_s = settling velocity; C_b = suspended sediment concentration near the bed; τ_b = bed shear stress; and τ_d = critical shear stress for deposition. The erosion rate can be estimated by

$$E_s = M_e(\frac{\tau_b}{\tau_e} - 1) \qquad ;\texttt{for } \tau_b > \tau_e \tag{3.20}$$

in which, M_e = erodibility constant; τ_e = critical shear stress for erosion. The constant M_e may be determined experimentally. Teisson [1991] suggested that $M_e = aC_b^{1/3}$. For alluvial rivers, the velocity V_d in Eq. 3.2 can be determined from Eq. 3.12. The velocity V_u for alluvial rivers can be estimated from the Eqs. 3.21–3.26, which are based on the work of Garcia and Parker [1991].

$$V_u = \frac{V_s E_s}{c_a} \tag{3.21}$$

$$E_s = \frac{AZ_n^5}{1 + \frac{A}{0.3}Z_n^5} \tag{3.22}$$

$$Z_n = \frac{u_*^{'}}{V_s} R_p^{0.6} \tag{3.23}$$

$$R_p = \frac{\sqrt{gRd_s}d_s}{\nu} \tag{3.24}$$

$$u_*^{'} = (\frac{g^{0.5}}{c^{'}})U_w \tag{3.25}$$

$$c^{'} = 18\log(\frac{12R_b}{3d_s}) \tag{3.26}$$

in which, c_n= near-bed sediment concentration; E_s =sediment entrainment coefficient; R = submerged specific gravity of sediment; R_b = hydraulic radius; d_s= sediment grain size; and A = an empirical constant (1.3×10^{-7}).

The present model assumes the suspended concentration of the sediment remains at an equilibrium constant value during the simulation period, and $V_d = 0$, for simplicity. This implies that the resuspension velocityV_u can be calculated as

$$V_u = \frac{V_s m_1}{m_2} \tag{3.27}$$

in which, m_1 and m_2 are sediment concentrations in the water column and the bed, respectively. The settling velocity for non-cohesive sediment can be estimated by the Stokes' law

$$V_s = \frac{g}{18}(\frac{\rho_s - \rho}{\mu})d^2 \tag{3.28}$$

or

$$V_s = 0.0336(\rho_s - \rho)d^2 \tag{3.29}$$

in which, V_s is in m/day; ρ and ρ_s =water and sediment densities, g/cm^3 ; d=sediment diameter,μm; g=gravity,981 cm/s^2; and μ=dynamic viscosity of water.

The settling velocity can be affected by particle shape, concentration, water temperature and turbulence [Vanoni 1977]. For cohesive sediment, the fall velocity may increase significantly due to flocculation[Migniot 1989]. The diffusive transfer at the sediment-water interface is limited by the diffusion in the sediment, since the vertical diffusion in the water column is orders of magnitude higher. Di Toro et al. [1981] suggested that

$$K_f = 19\phi_2 M^{-2/3} \tag{3.30}$$

in which, M = molecular weight of the chemical. The value of K_f typically varies between 0.1 and 1.0 cm/day. For the localized deposit of chemical on the bed, such as the deposition after the initial spill of the chemical, the vertical mass exchange of the chemical is governed by the turbulent mass transfer [McCorquodale et al., 1986]. This is not considered in this study.

3.5 Volatilization

Many materials volatilize readily. Therefore, volatilization needs to be considered in the simulation of dissolved phase, since it is an important loss mechanism. The mass exchange of the chemical across the air-water interface can be derived from the difference between exchanges from water to air and from air to water. Thus

$$V_1 \frac{dC_1}{dt} = k_l A(\frac{C_g}{H_e} - f_{d1} C_1) \tag{3.31}$$

$$\frac{1}{k_l} = \frac{1}{K_l} + \frac{1}{K_g H_e} \tag{3.32}$$

in which, V_1= the total volume of water; K_l= the liquid film coefficient; and K_g=the gas film coefficient.

$$K_l = (\frac{32}{M})^{1/4} (D_L \frac{U}{h})^{1/4} \tag{3.33}$$

$$K_g = 168(\frac{18}{M})^{1/4} U_w \tag{3.34}$$

in which, M = molecular weight; D_L = oxygen diffusivity, 0.000181 m^2/day; U = velocity of flow, m/s; and U_w =wind speed, m/s.

$$H_e' = \frac{P_{vp}}{S} \tag{3.35}$$

in which, P_{vp} = vapor pressure in atm; S = water solubility in mol/m^3; and H_e' is in atm-m^3/mol.

$$H_e = \frac{H_e'}{RT} \tag{3.36}$$

in which, R = universal gas constant, 8.206×10^{-5} $atm - m^3$/K-mole; and T in K. In Eq. 3.36, H_e is dimensionless. Therefore, k_l is in m/day.

3.6 Chemical Kinetic Transformations

The chemical kinetic transformations also affect the environmental distribution of chemical substances. The principal transformations are photolysis, hydrolysis, and biodegradation. Because these process may be the major ultimate sinks of reacting chemicals in the water environment, it is necessary that they be included in the model.

Total chemical kinetic transformations rate, K_d, of dissolved chemical in water column is

$$K_d = K_P + K_H + K_B \tag{3.37}$$

K_P, K_H, K_B denote the loss rate of photolysis, hydrolysis and biodegradation, respectively.

3.6.1 Photolysis

Photolysis is the degradation process by which chemical bonds of a substance are broken due to light or radiant energy. The direct energy transfer is that the absorption of sunlight by pollutants causing chemical reactions which affect their toxicity. The rate of a photochemical reaction is usually expressed in the first-order kinetics. The photolysis rate can be determinated as follows

$$K_P = \phi \epsilon_\lambda L_\lambda \tag{3.38}$$

in which, ϕ = quantum yield; ϵ_λ= the absorbability of chemical; L_λ= light intensity.

3.6.2 Hydrolysis

Hydrolysis is a chemical transformation process in which an organic molecule reacts with water, forming a new carbon-oxygen bond. Hydrolysis is likely to be the most important reaction of organic compounds with water in aqueous environments. The hydrolysis rate constant are estimated as follows

$$K_H = K_n + K_a[H^+] + K_b[OH^-] \tag{3.39}$$

in which, K_n = neutral hydrolysis rate, K_a =acid catalyzed hydrolysis rate constant, K_b =base catalyzed hydrolysis rate constant, $[H^+]$ = molar concentration of hydrogen ions, and $[OH^-]$ = molar concentration of hydroxide ions.

3.6.3 Biodegradation

Biodegradation is one of the most important environmental processes that cause the breakdown of organic compounds. Mills and Dean [1982] estimated the rate of biodegradation as follows

$$K_B = \frac{\mu_{max}}{yK_s} \tag{3.40}$$

in which, μ_{max} = maximum specific growth rate$[T^{-1}]$; y = bacterial yield coefficient[cells/M]; and $K_s[M/L^3]$ = half-saturation constant, i.e. the concentration at which the growth rate is one-half of the maximum growth rate.

Chemical kinetic transformation is a very complex process. There are no accurate methods to compute these transformations due to lack of data. Chemical kinetic transformations coefficients, K_P, K_H, K_B, are given by Lyman and Rosenblatt [1982].

3.7 Model Implementation

Based on the analytical formulation presented, a computer model for chemical transport is developed for the St. Marys River.

3.7.1 The Grid System

The river is schematized into a square grid system as shown in Fig. 3.2, which is used in the chemical transport simulation. The velocity and depth of the entire river is mapped onto this square grid system. The velocity and depth information stored at these grid points are used in the model computations. Velocities and depths are obtained from the hydrodynamics model described

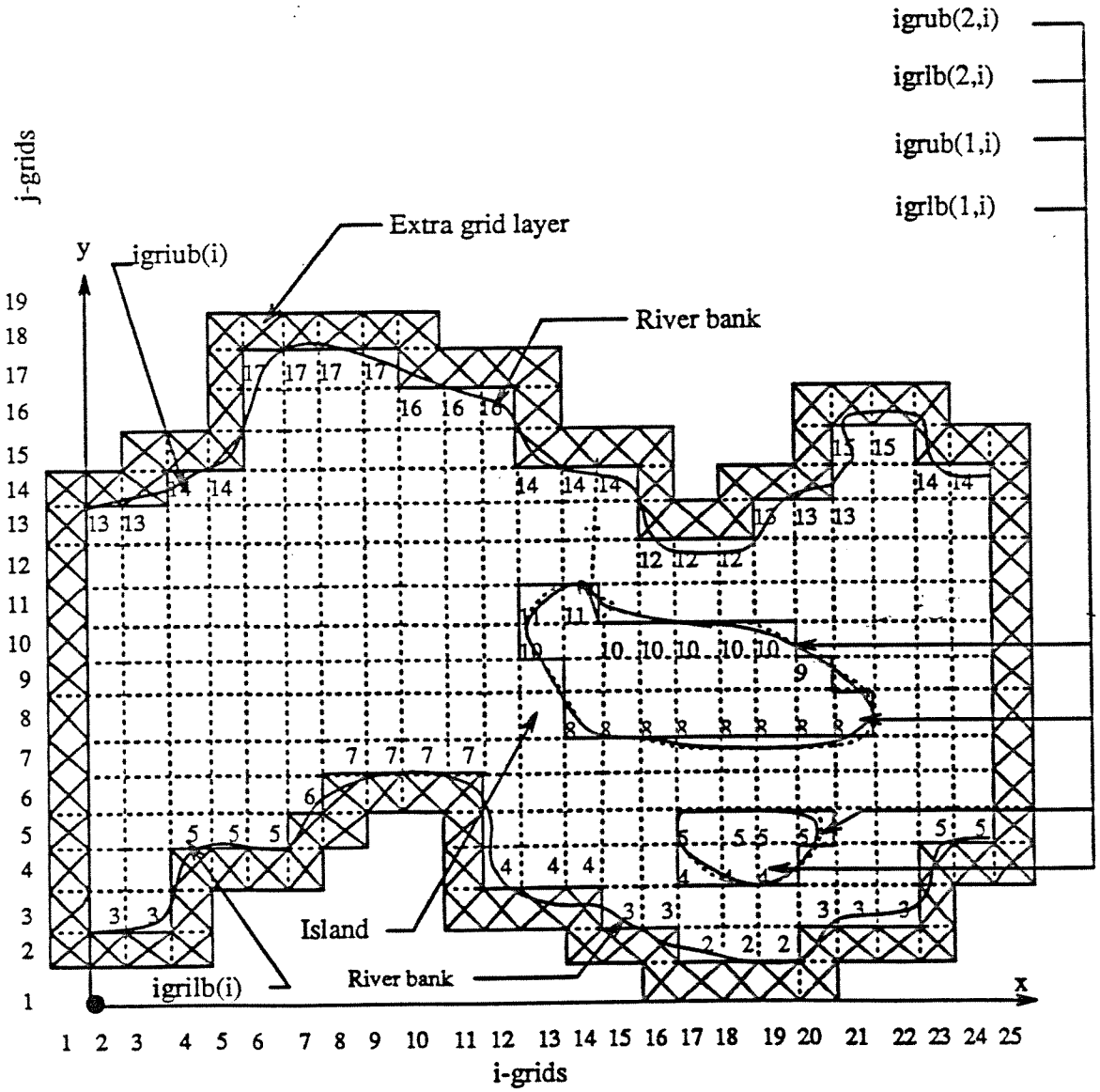

Figure 3.2: Grid boxes and river boundary representation

in the previous chapter. The output of finite element based on the hydrodynamics model gives the velocities at the nodes of the triangular element system. These values are interpolated to all grid boxes. Only boxes found within the defined river boundaries are assigned velocities and depths. River boundaries for this grid system are defined by boundary grid boxes. For each grid along the x-direction, two corresponding y-grid boxes are used to define the river banks.

An island is represented by land boxes in a given column of grids as the region between two y-box numbers. These two y-box numbers refer to the lower and upper boundaries of the island. The model can handle any number of islands in the river. However, if more islands are intersected by a vertical line along which the x-coordinate is constant, more space will be needed for the input data. A maximum of 4 islands are allowed for any column.

z

3.7.2 Release of a chemical

At the beginning of the simulation, the user selects a number of parcels to represent the chemical at the release time. This number can be up to 15,000 parcels for each layer at the beginning of the simulation. During the simulation, the number may increase to as much as 50,000 due to the exchanges between the bed and the suspended layers. In the St. Marys River simulations, chemical in the bed is assumed to be negligible due to the low sediment concentration.

Based on users input of the concentration of chemical released and the discharge of water, the total amount of chemical input at a chemical discharge location is obtained. In the model, dye or lampricide are considered as miscible nonreactive chemicals. Parcels in a layer have equal volumes at the beginning. The total number of parcels in each layer are the same at the beginning. A chemical discharge is treated either as an instantaneous input or a continuous input. When the discharge duration is zero the discharge is treated as instantaneous input. Otherwise, it is treated as a continuous effluent.

3.8 Model Structure

The computer code is written in standard Fortran77. No compiler specific extensions have been used. The code has been tested only on 32 bit machines with Fortran 77 compilers that support 32 bit computations.

The model structure is shown in Fig. 3.3 The model can be run for a new simulation or continue from a previously terminated run by changing weather and chemical characteristics.

3.8.1 Main Program

Major steps of the the main program can be summarized as the following:

- Read chemical discharge information in the data file **stm.spl**.
- Read model parameters in the data file **stm.dat**
- Read velocities and depths at grid boxes from **stmgrid.vel**.
- Call **con** to read back the simulation results if it continues a job from a previously terminated run.
- Call **forms** to calculate chemical forms in water column .
- Call **relsus** and **relsur** to release chemical parcels at equal intervals for the chemical discharge duration; call **advsus** to advect chemical parcels in suspended layer; call **advsur** to calculate sediment velocities and to advect chemical parcels in sediment layer.
- Call **redepn**, **rmproces** and **exchan** to calculate volatilization, chemical loss from water column, settling to bed, resuspend to suspension layer, and to calculate exchange between suspended layer and bed sediment layer.
- Call **rearrg** to adjust particle sizes, i.e. lump small particles together and divide large particles to satisfy the requirements of the random walk simulation and the computer memory.
- Save simulation results into corresponding output files (refer to next section) at designed output frequency.

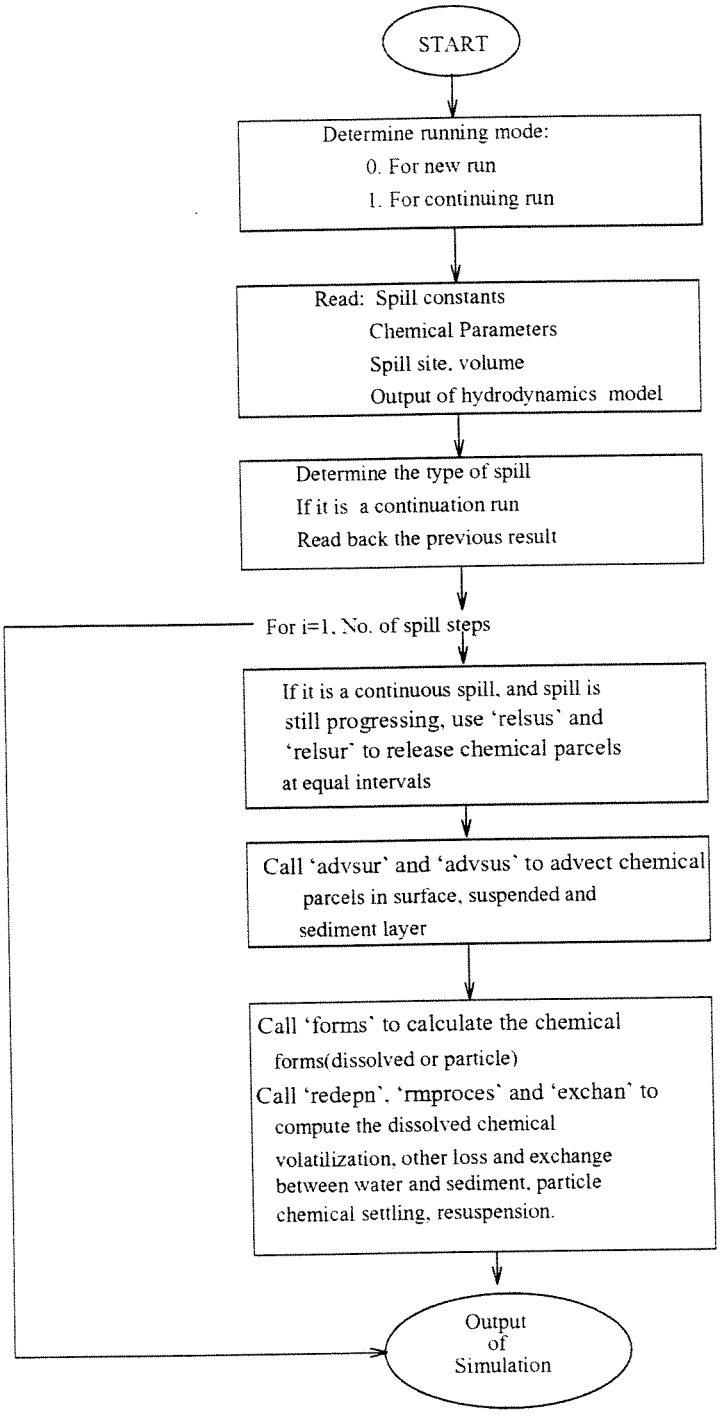

Figure 3.3: Block diagram of the computer model

3.8.2 Subroutines

The simple subroutines can be easily understood without explanation. Block diagrams for two main subroutines are given in Fig. 3.4 and Fig. 3.5 to assist the understanding of the program.

3.8.3 Input Data Files

There are two categories of input that are required to run the model; the first category can be considered as fixed data for a given river reach. This is the information required to describe the shoreline and geometry of the river. Normally, there is no need to adjust this data. The second category includes various parameters, which may be adjusted according to the flow condition and spill characteristics.

All file names to be opened for input and output will be in the file **stm.fnm**. Sample input data files included in this section are:

1. `stmgrid.geo`
   River geometry of the St. Marys River schematized using square grids.

2. `stm.spl`
   apply lampricide information, wind condition, and ambient air temperature.

3. `stmgrid.vel`
   Velocity and water depth at the grid boxes.

4. `stm.dat`
   Model parameters for model.

3.8.4 Additional Input

In additional to the above, the user must respond through keyboard to one question prompted by the program. This input is discussed in the following paragraphs.

Continuation Runs

The model can be used either for a simulation from the beginning of a spill, or for continuing a previously stopped simulation. The user is required to choose from these two options. The screen will show the following:

```
★★★★★★★★★★★★★★★★★★★★★★★★★★★★
★ The model can be run from t = 0 or    ★
★ restarted after a stop                ★
★ Enter 0 or 1 and hit return           ★
★ 0 for a run starting from t = 0       ★
★ 1 to start from a previously          ★
★ stopped point                         ★
★ ————————————————————————————————    ★
```

the user must choose a 0 or 1 for this prompt.

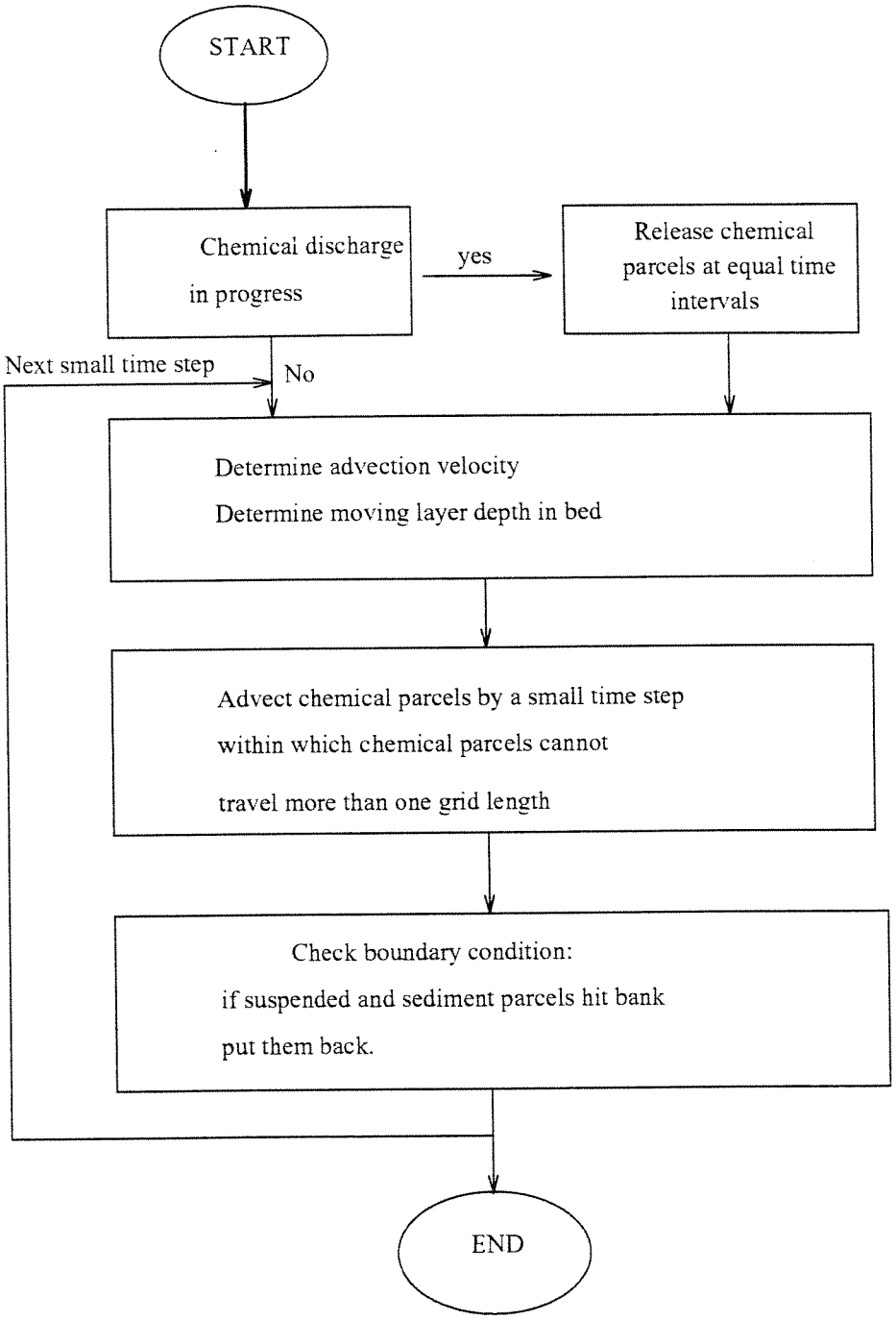

Figure 3.4: Block diagram of release and advection of chemical parcels

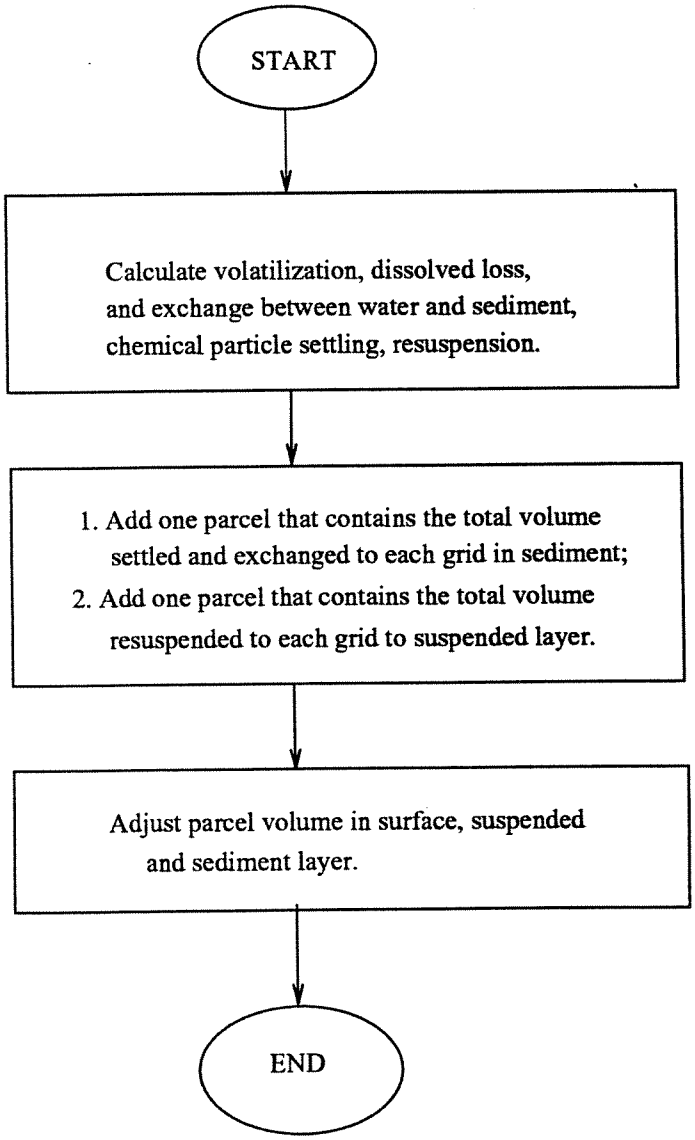

Figure 3.5: Block diagram of exchange between suspension and sediment layers

3.8.5 Model Outputs

Output from the model can be directed to different devices, i.e., screen, printer, and files. Chemical spill simulation results are output to files at the selected output frequency. These results include the following files:

- `stmprt.out`: This file contains spill site and chemical parameters. A summary of distributions of the chemical, including updated total volume, volume in the bed sediment, volume in the suspended layer, total volatilization and the volatilization in the current time step, total other chemical reaction loss and the loss in the current time step, volume resuspension and settling.
- `stm.sur`: the parcel information in this file correspond to the chemical parcels in the sediment layer. For each output time step, the file contains the total parcel number, the co-ordinates and volume of chemical in each parcel.
- `stm.sus`: This file has the same format as `stm.sur`. The information in this file corresponds to the suspended layer.

Chapter 4

Model Calibration

A series of four dye studies were conducted in the St. Marys River during December 7 to 10, 1981[1]. The purpose of the study was to observe the general dispersal pattern of dye released from various sites. A sketch for the maximum concentration pattern was given for each test. The results are generally indicative of the maximum concentration existed during the progression of the dye cloud. The distributions of concentration with respect to time are not available. These dye dispersal plots available are somewhat qualitative but provide a reasonable set of data to compare with the computer model results. The dye used was fluorescent Rhodamine WT , 20% aqueous. The dye injection sites were Edison Sault Electric Generating Station, Corps of Engineers Power Station, Compensating Gates, and the Canadian Lock, respectively. In order to determine the general accuracy of the model, four simulations corresponding to the field study were carried out.

4.1 Case 1–Edison Sault Electric Application

On December 7, 1981, a total of 38.4 liters of dye was applied to the Edison Power Canal at Fort street in Sault Marie, Michigan during a 10 hour period from 0600 to 1600 hours. A fairly good mix of dye, horizontally and vertically, occurred in the Canal. Since the Canal is too narrow to include in the model, the dye discharge site for the simulation is considered to be at the Edison Sault Electric Power House with an average concentration of 2.84 ppb and the release period from 0600 to 1200 hours.

Maximum observed and simulated dye concentrations are shown in Figs. 4.1 and 4.2. The simulated results every hour are attached in the Appendix A from Figures 1 to 10. From these results, most of the dye from this source appears to go down the main shipping channel south of Sugar Island. The leading edge of the dye flows relatively fast along the main shipping channel and take about 5 hours to reach Lake Nicolet. The simulation of dye dispersion compares relatively well with the observed data.

[1] Report of a study of current patterns in the Sault Ste. Marie Harbour area of St. Marys River using a tracer dye.

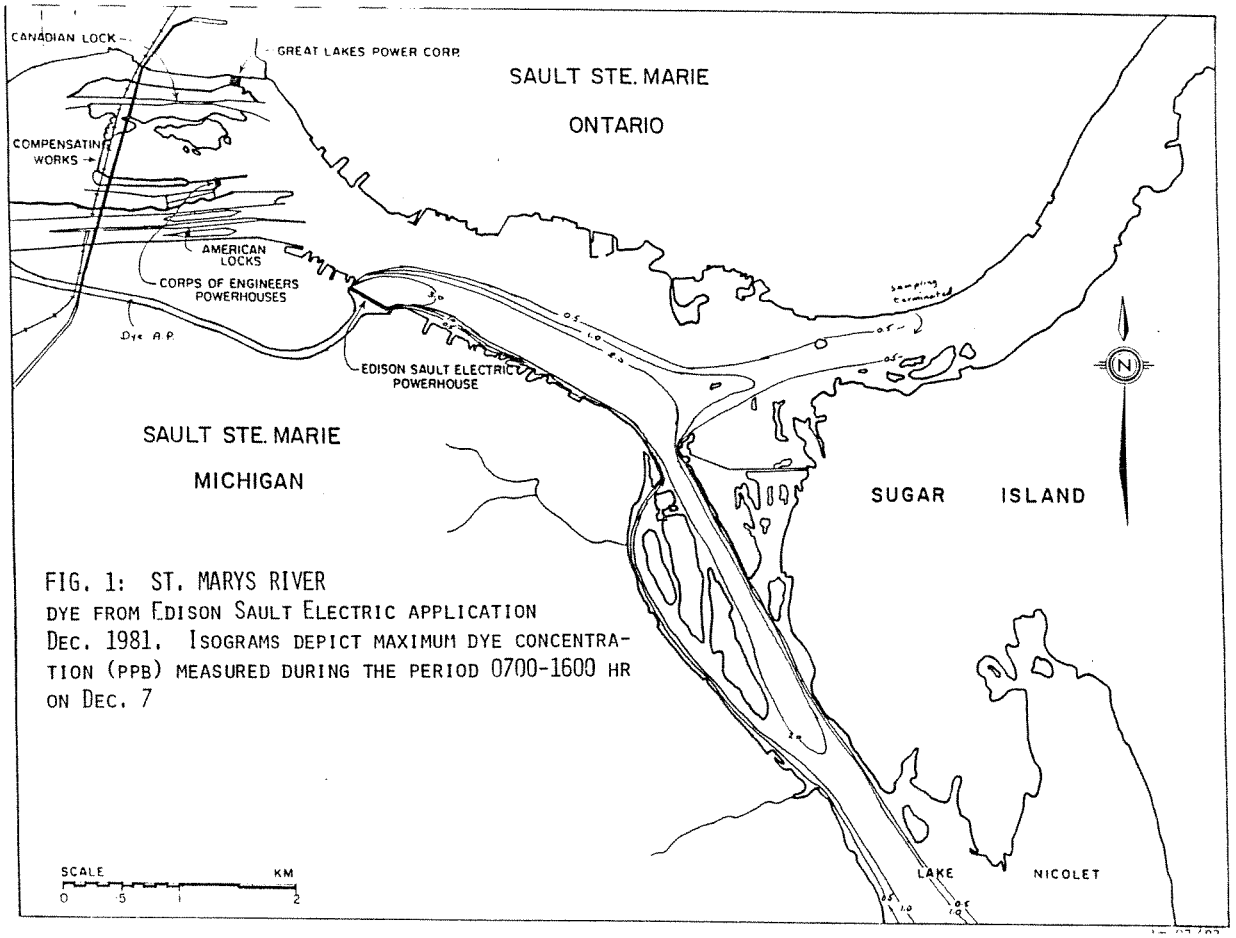

Figure 4.1: Maximum dye concentration observed for the period 0700-1600 hrs on Dec. 7 - Case 1

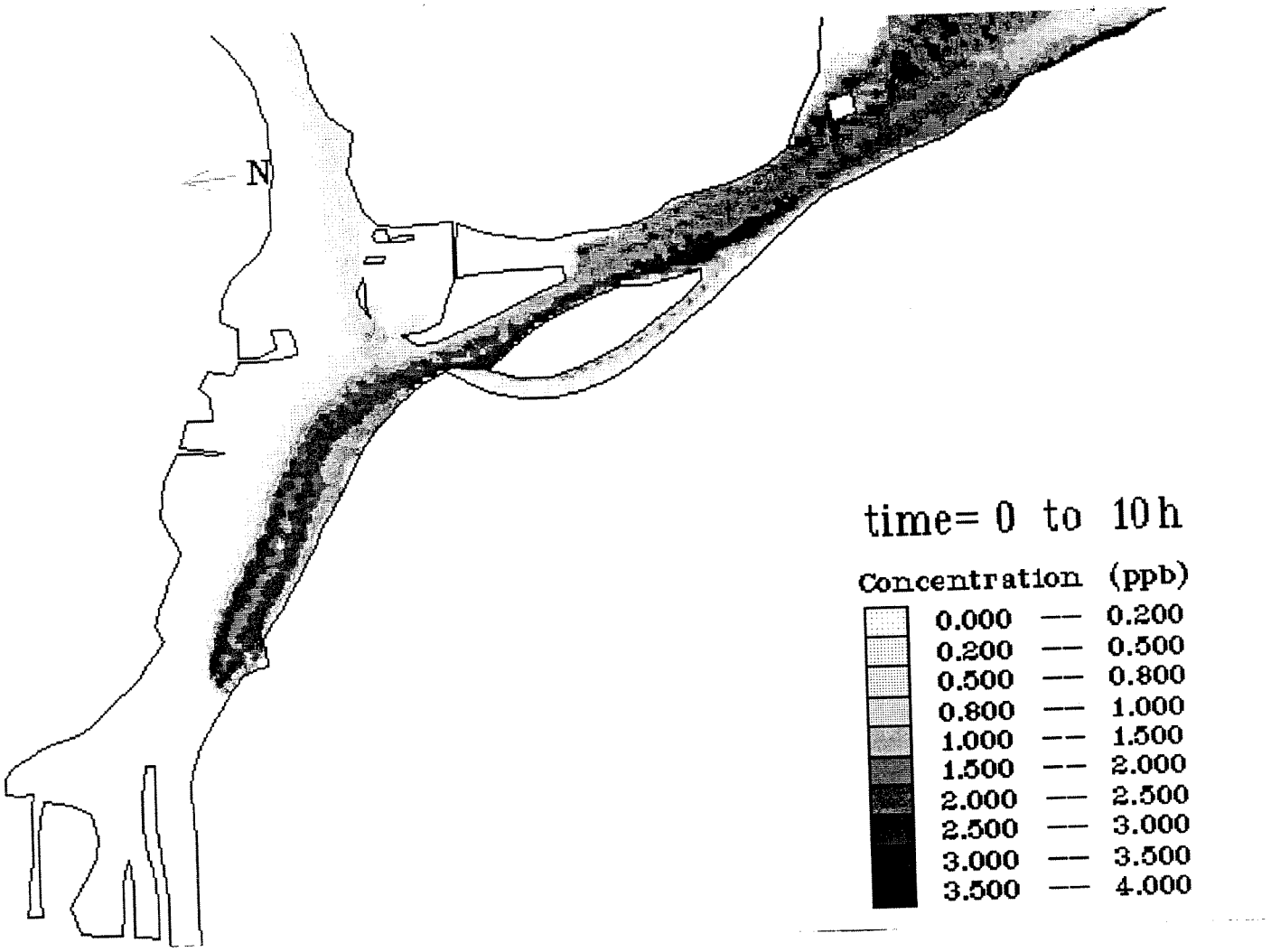

Figure 4.2: Maximum simulated dye concentration for the period 0600-1600 hrs on Dec. 7 during the 10 hours after the Edison Sault Electric application

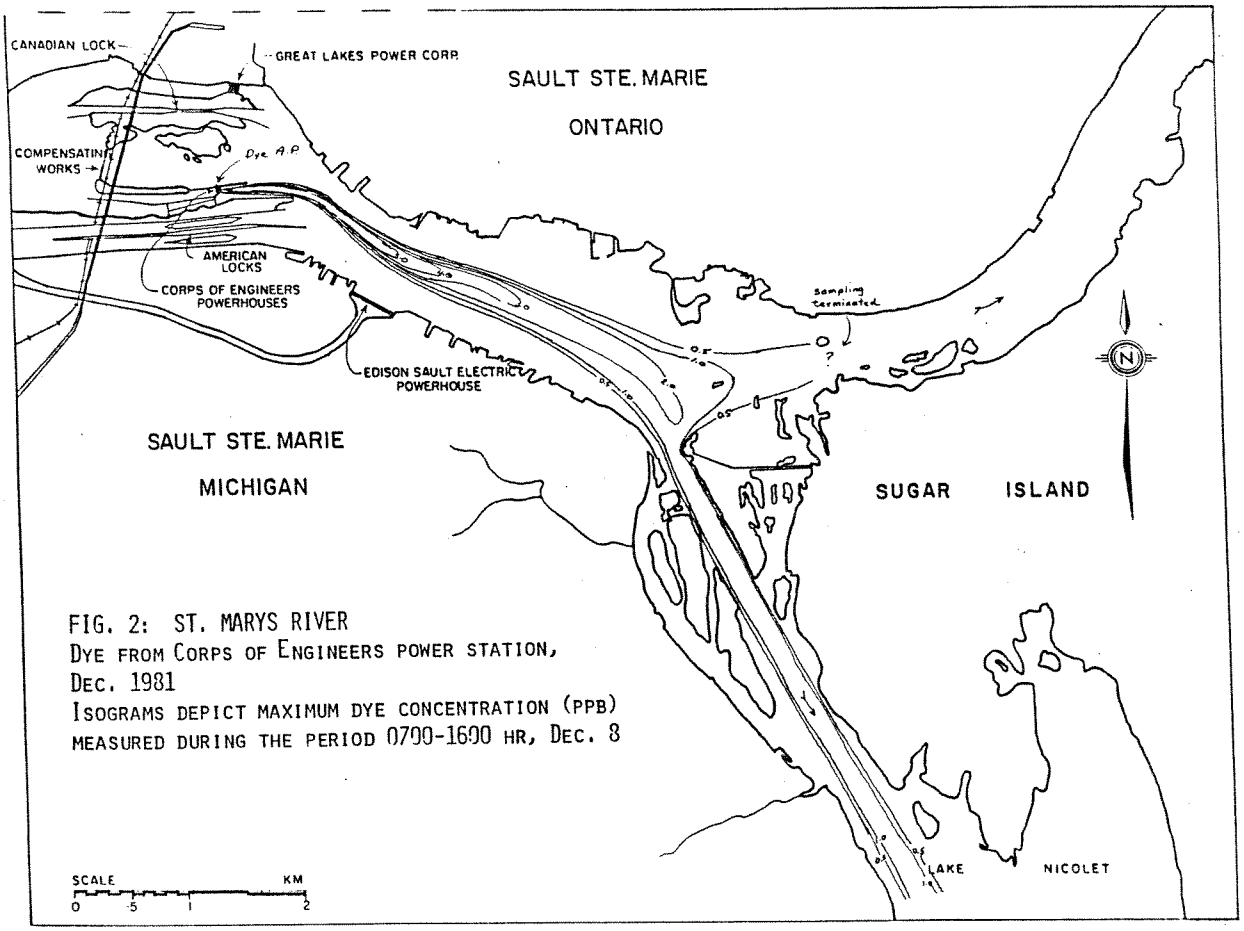

Figure 4.3: Maximum dye concentration observed for the period 0700-1600 hrs - Case 2

4.2 Case 2–Corps of Engineers Application

On December 8, 1981, a total of 26.8 liters of dye was applied at the Corps of Engineers Power House for a period of 5 hours from 0700 to 1200 hr. The average concentration of the dye discharge site was 3.46 ppb.

Maximum observed and simulated dye concentrations are shown in Figs. 4.3 and 4.4. The simulated results every hour are enclosed in the Appendix A from Figures 11 to 19. The dye released was split into two parts as it moved downstream. One part moved down the main shipping channel of south of Sugar Island. The other part moved down the Canadian side of Sugar Island. The simulated result agrees reasonably well with the observed data. One noticeable difference is that the dye distribution from the simulation tends to turn to the American shore between the American Lock and Edison Sault Electric Powerhouse. The reason is that the water discharge from the American Lock is very small.

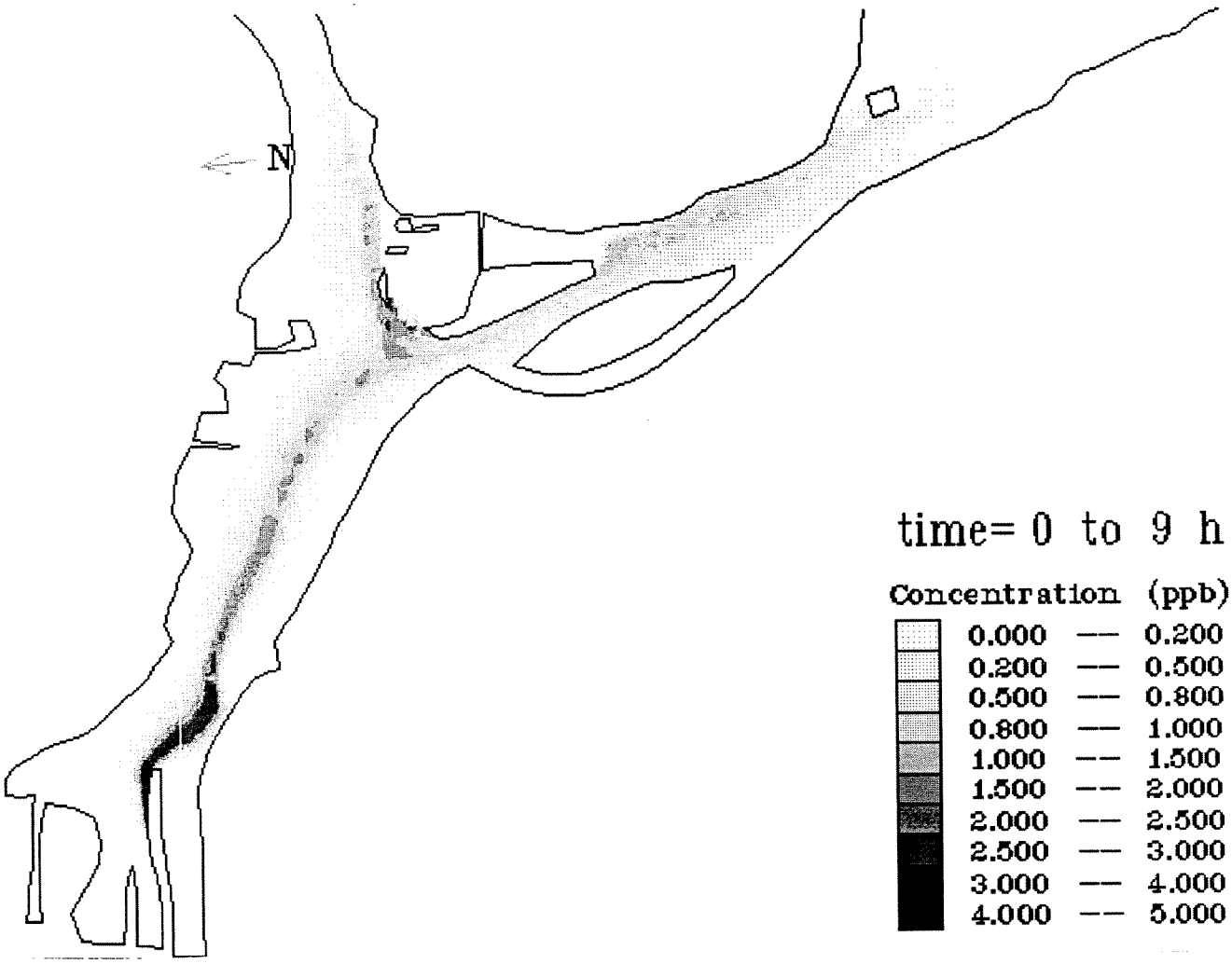

Figure 4.4: Maximum simulated dye concentration for the period 0700-1600 hrs on Dec. 8 during the 9 hours after the Corps of Engineer Application

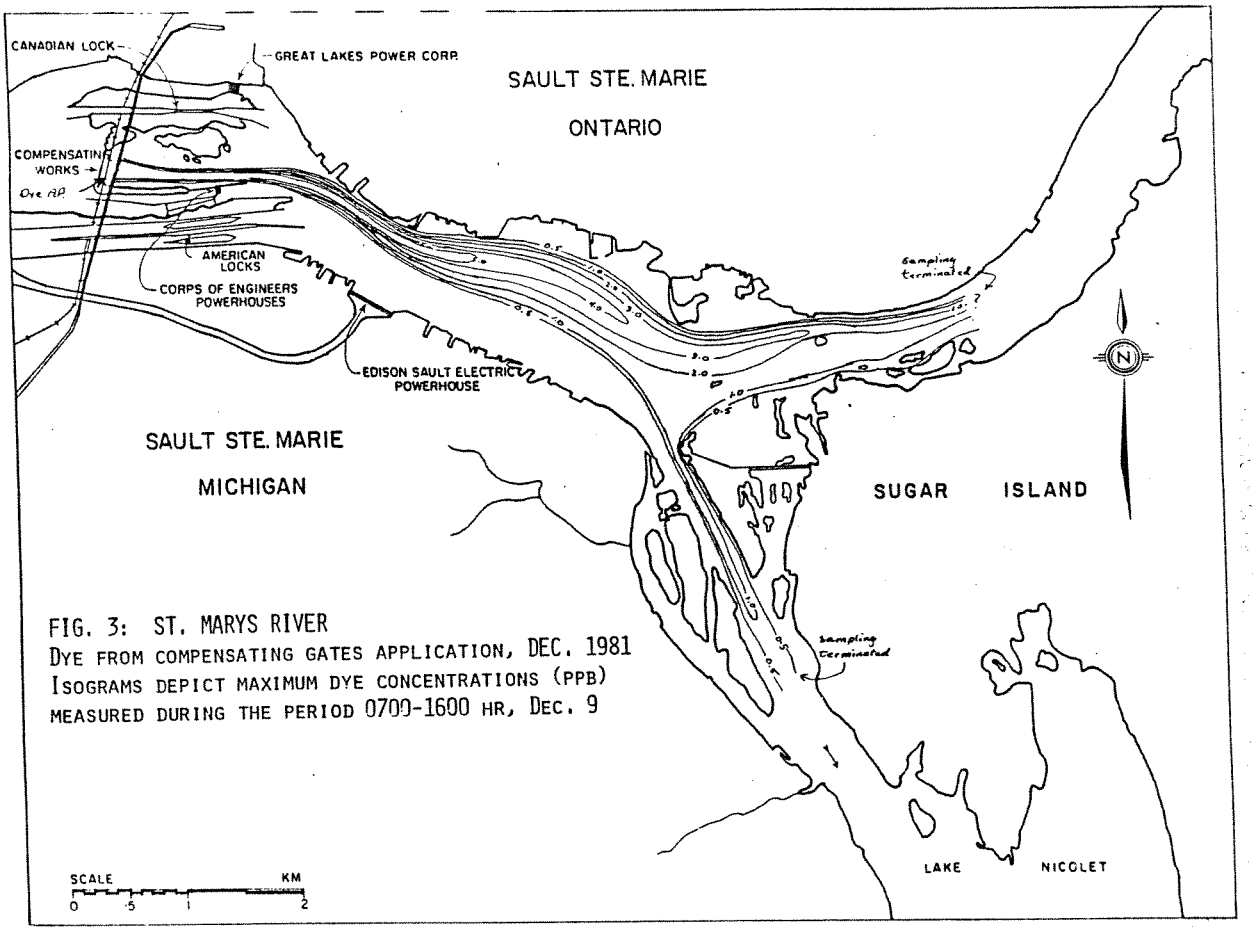

Figure 4.5: Maximum dye concentration observed for the period 0700-1600 hrs - Case 3

4.3 Case 3–Compensating Gates Application

On December 9, 1981, a total of 27 liters of dye was applied to the water passing over the St. Marys Rapids between the hours of 0730 and 1230. The average concentration of the dye discharge site was 4.81 ppb and the period of the discharge was 5 hours.

Maximum observed and simulated dye concentrations are shown in Figs. 4.5 and 4.6. The simulated results at every hour are shown in the Figures 20 to 28 of the Appendix A. Most of the dye from this source appears to go toward the Canadian Channel and moves a little slower than those from the two previous cases. The dye cloud stays near to the Canadian side.

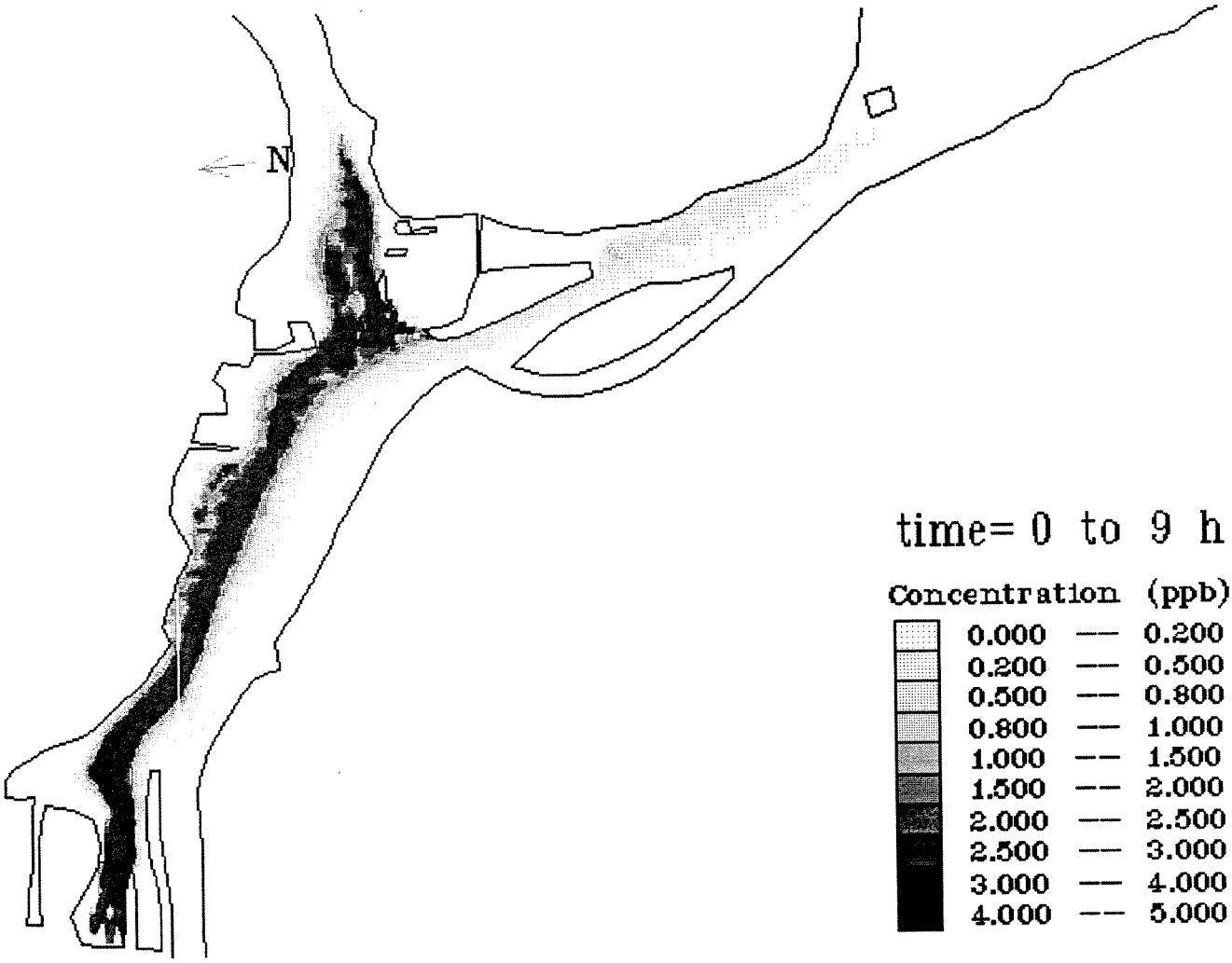

Figure 4.6: Maximum simulated dye concentration for the period 0700-1600 hrs on Dec. 9 during the 9 hours after the Compensating Gates Application

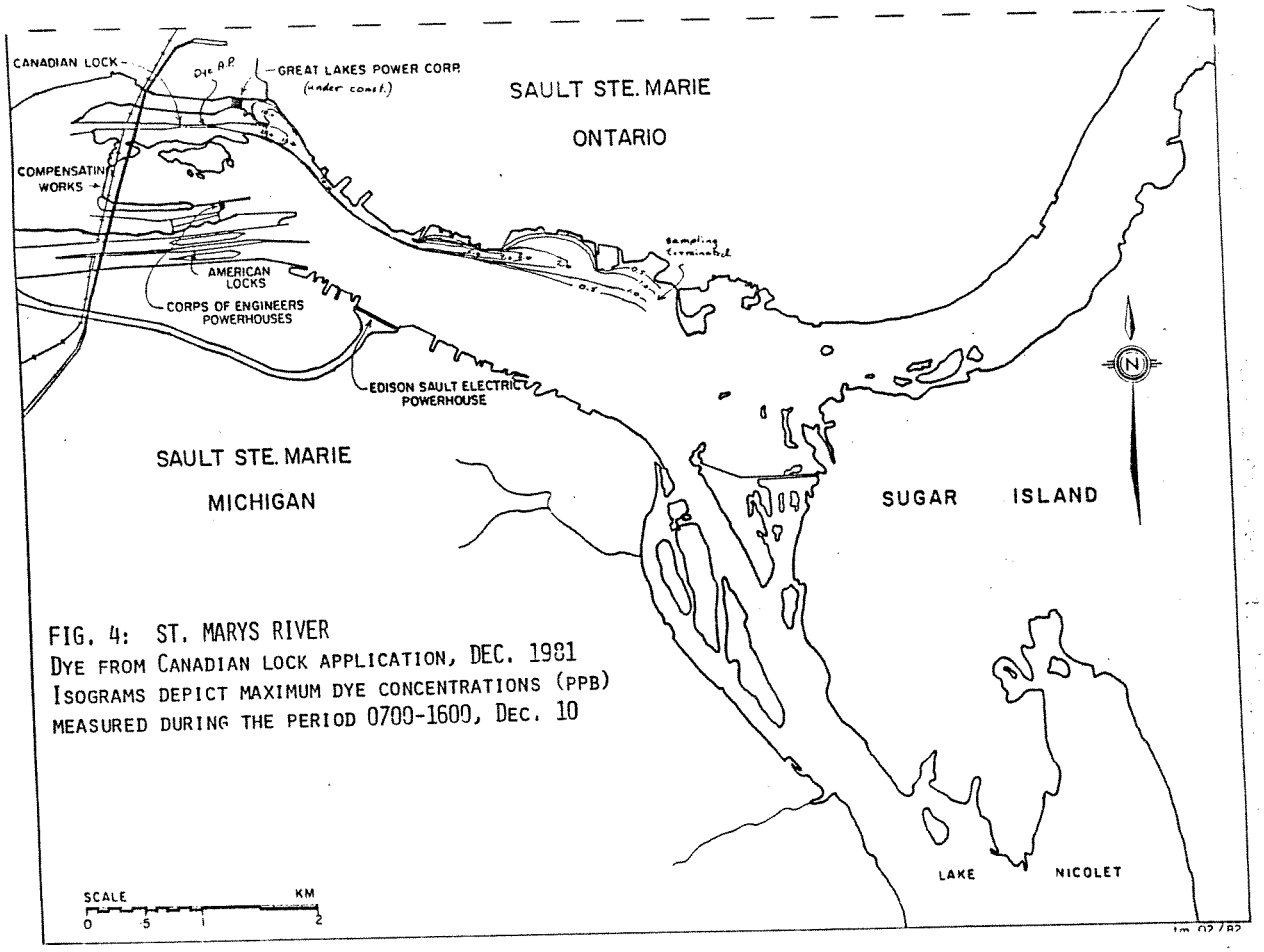

Figure 4.7: Maximum dye concentration observed for the period 0700-1600 hrs - Case 4

4.4 Case 4–Canadian Lock Application

On December 10, 1981, a total of 20.0 liters of dye was applied to the downstream valve outlets on each side of the Canadian shipping lock from 07:15 to 13:05 hrs. The average concentration of the dye at the discharge site was 27.0 ppb and the period of discharge was about 6 hours.

Maximum observed and simulated dye concentrations are shown in Figs. 4.7 and 4.8. The simulated results at every hour are included in Appendix A. This dye cloud tends to stay very close to the Canadian shore and fill in all the boat slips and bays. It takes a long time to get the dye down the channel between the mainland and the Sugar Island since the water flow is slow in the shallow region close to the shore.

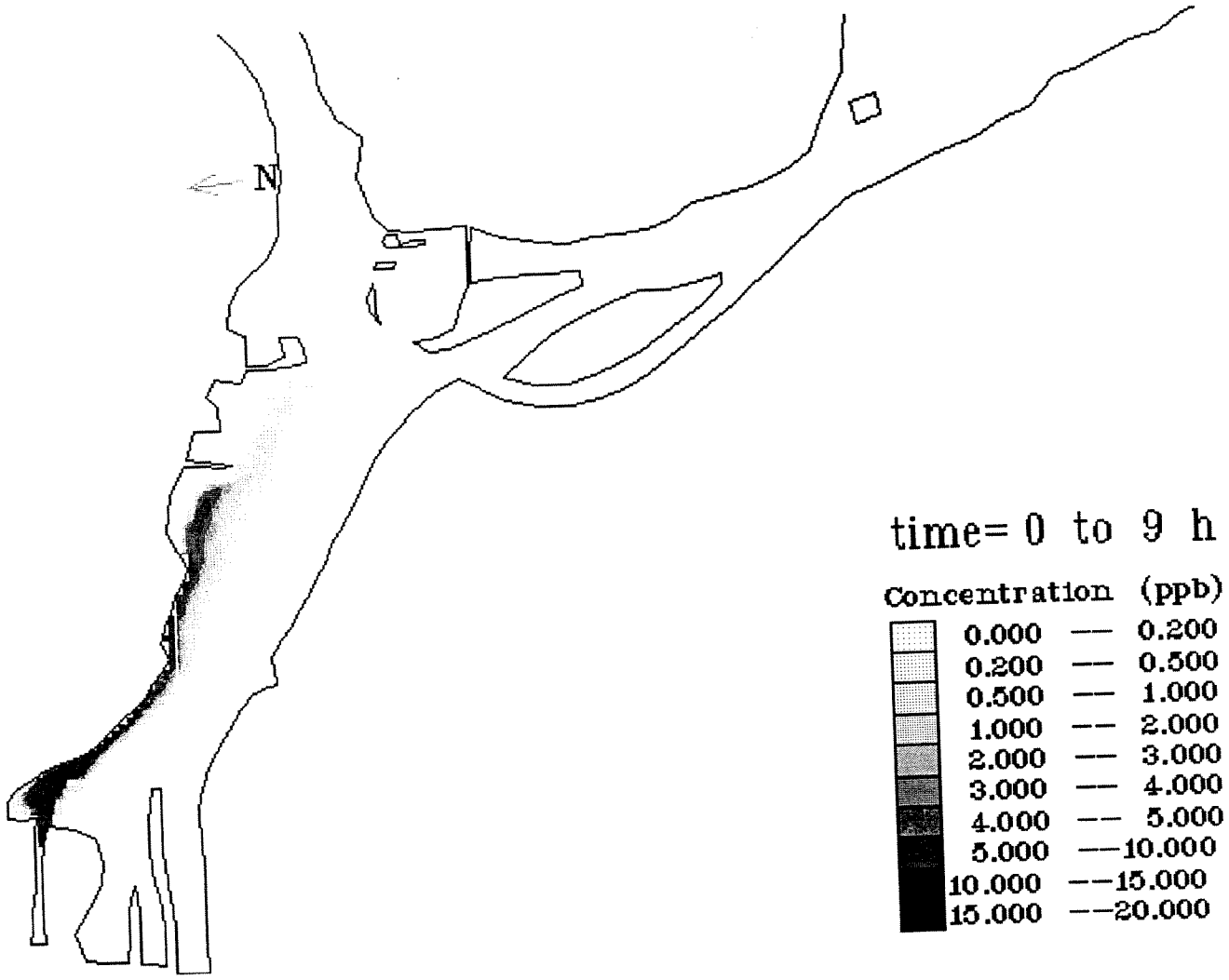

Figure 4.8: Maximum simulated dye concentration for the period 0700-1600 hrs on Dec. 10 during the 9 hours after the Canadian Lock application

Chapter 5

Case Studies

One important aspect of lampricide treatment in the St. Marys River is to apply the lampricide effectively. There are two important factors to be considered. Namely, the amount of lampricide and the accessability to application sites. A series of hydraulic structures in the St. Mary River, including compensating gates, navigation locks, and power generating facilities can be conveniently used as application sites.. These structures control entire outflow of Lake Superior. In order to eliminate lamprey larvae, the lampricide (TFM) must reach a lethal dosage.

In this simulation, we have used the general hydraulic conditions that existed during the fall of 1981, a more detail distribution of discharge of the St. Marys River was provided by the dye tests report[1]. The total discharge was 1315 m^3/s. The channels that remain functional at that time (December 1981) were the international Rapids (discharge = 300 m^3/s), the Edison Sault Electric Generating Station (discharge = $622m^3/s$), the U.S. Corps of Engineers Generating Station (discharge = 350 m^3/s) and the Canadian navigational lock (discharge = 28 m^3/s). According to the above hydrological conditions, the lampricide was applied to the four sites with the average concentration 10 ppm at the application sites. The duration for lampricide application is 13 hours. The lethal levels are assumed to be from a concentration of 3 or 9 ppm for 9 or 12 hours, respectively. The areas which reached the lethal dosage level are shown in Figure 5.1. Figure 1.1 shows larva distribution and density. The comparison of Fig. 1.1 with Fig. 5.1 shows that most of the areas with high density larvae are inflicted by the lethal dosage.

Five additional sample simulations were run under conditions of different hydrological situations and lampricide application. The distribution of water discharge at each application site was given in Table 5.1. Conditions of lampricide application are shown in Table 5.2. Lethal levels can vary from a low concentration applied over a long period to a relatively high one over a short period. Two lethal conditions are considered here. One used a concentration of 6.5 ppm for 9.00 hours; The other used a concentration of 5.5 ppm for 12 hours. For each simulation, the distributions of region reaching the lethal level were output for both the lethal levels. The Figure 5.2 to Figure 5.11 show the results.

The difference between the sample simulations I and II is the duration of lampricide application, 12 hours and 18 hours respectively. So is the the difference between sample simulations III and IV. The hydrological condition of sample simulation III and IV is an increase of 10,000 cfs of water discharge at Edison Sault Electric and Great Lakes Power Corps. Comparing the area reaching the first lethal level with the area reaching the second lethal level from the output results of five sample simulations, it is obvious that the area reaching the high concentration over a short

[1]Report of a study of current patterns in the Sault Ste. Marie Harbour area of St. Marys River using a tracer dye.

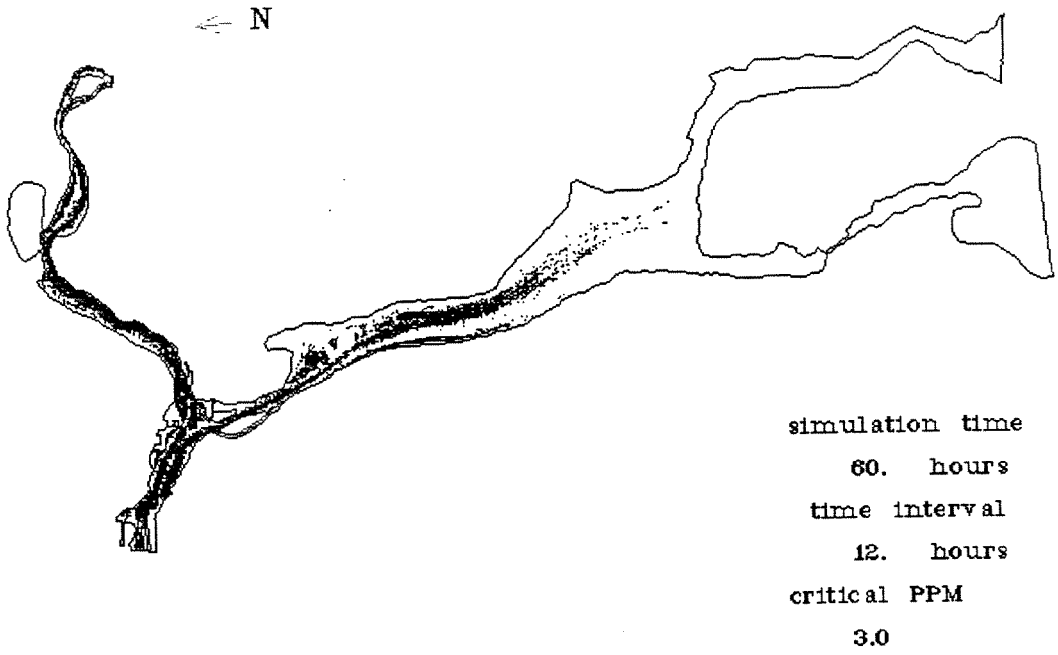

Figure 5.1: Area reaching the lethal dosage of 3 ppm for 12 hours

Table 5.1: **Water discharge at each application site for the sample tests**

Application sites	**Sample simulation I, II, V** Water discharge (cfs)	**Sample simulation III, IV** Water discharge (cfs)
American Lock	2,000	2,000
Compensation Works	2,500	2,500
Corps of Engineers power houses	11,500	11,500
Edison Sault Electric	13,750	23,750
Great Lakes Power Corps	25,250	35,250
Total discharge	55,000	75,000

Table 5.2: **Lamprecide application condition at each site**

NO. of sample tests	**Initial Concentration** (ppb)	**Application Duration** (hrs)	**Simulation Durati** (hrs)
I	10	12	60
II	10	18	60
III	10	12	60
IV	10	18	60
V	10	18 (+12)	36

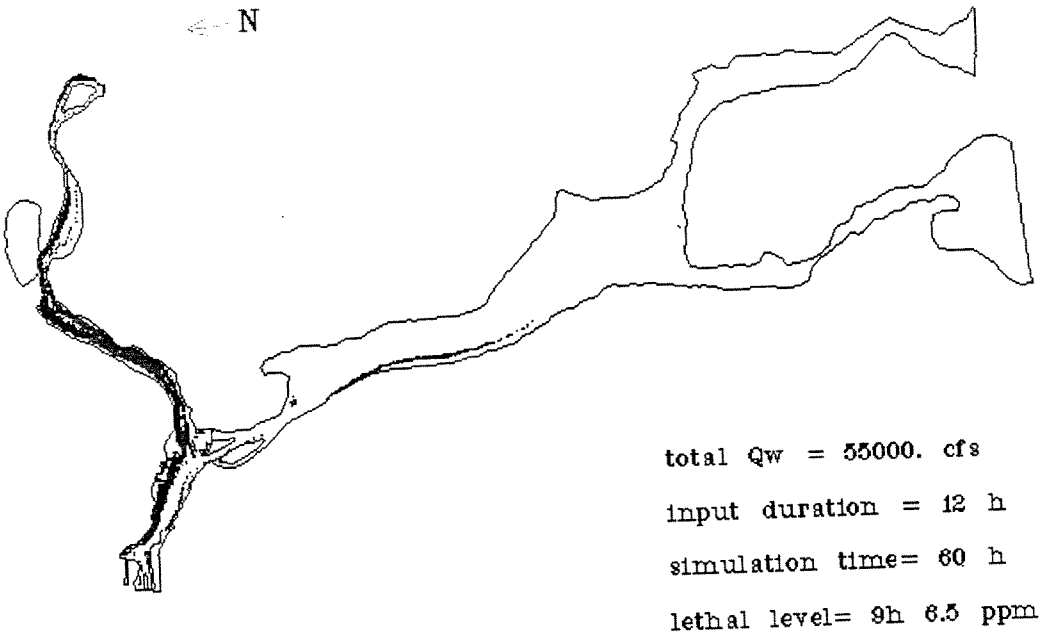

Figure 5.2: Area reaching the lethal dosage of 6.5 ppm for 9 hours in Sample simulation I

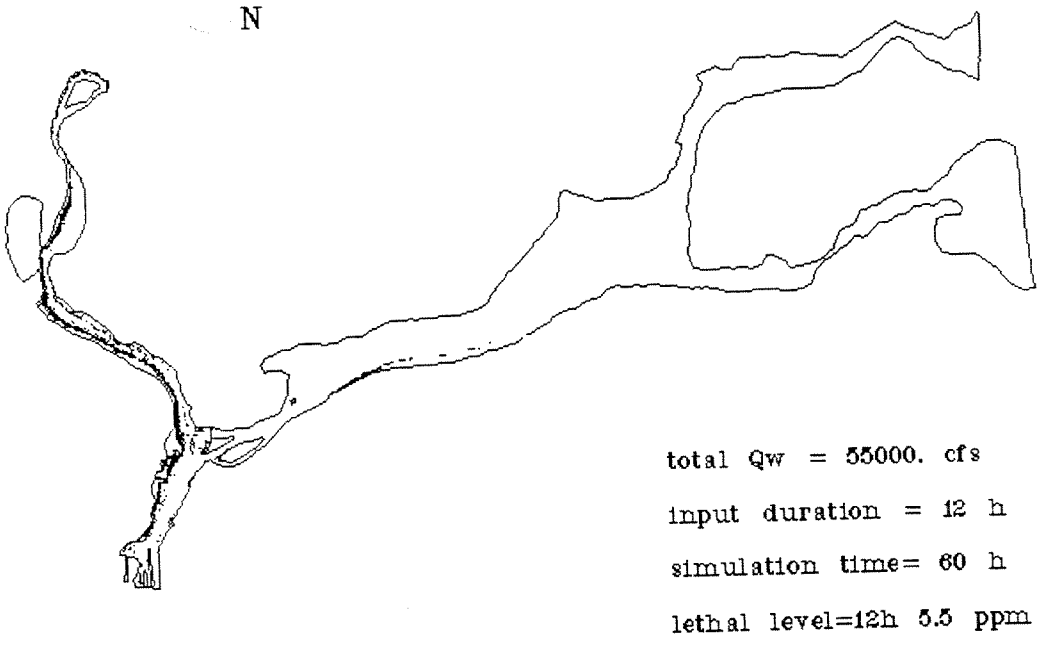

Figure 5.3: Area reaching the lethal dosage of 5.5 ppm for 12 hours in Sample simulation I

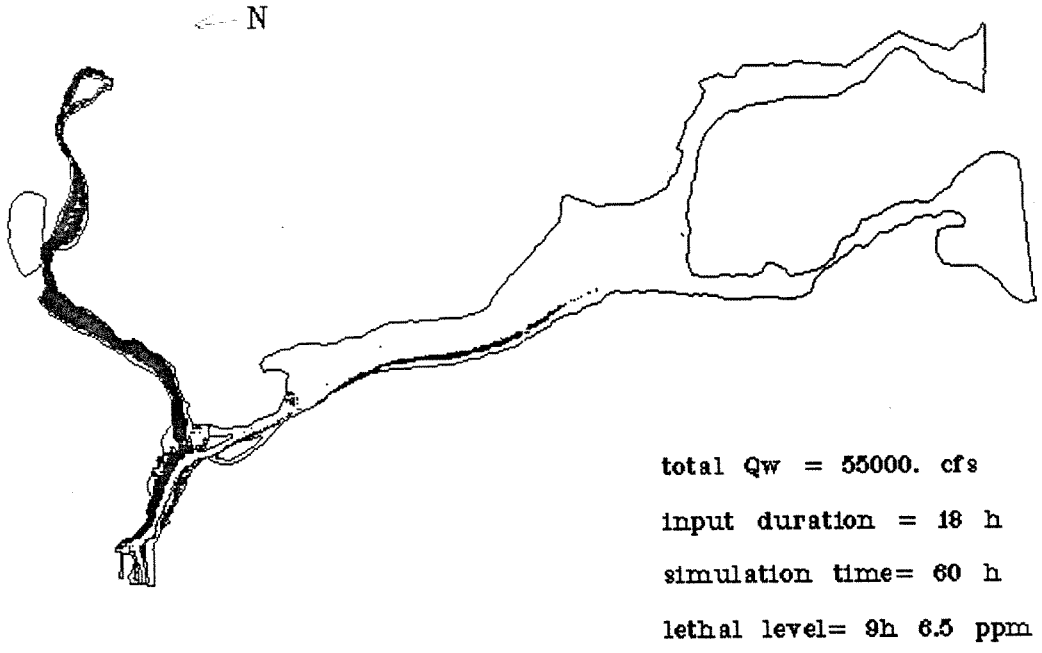

Figure 5.4: Area reaching the lethal dosage of 6.5 ppm for 9 hours in Sample simulation II

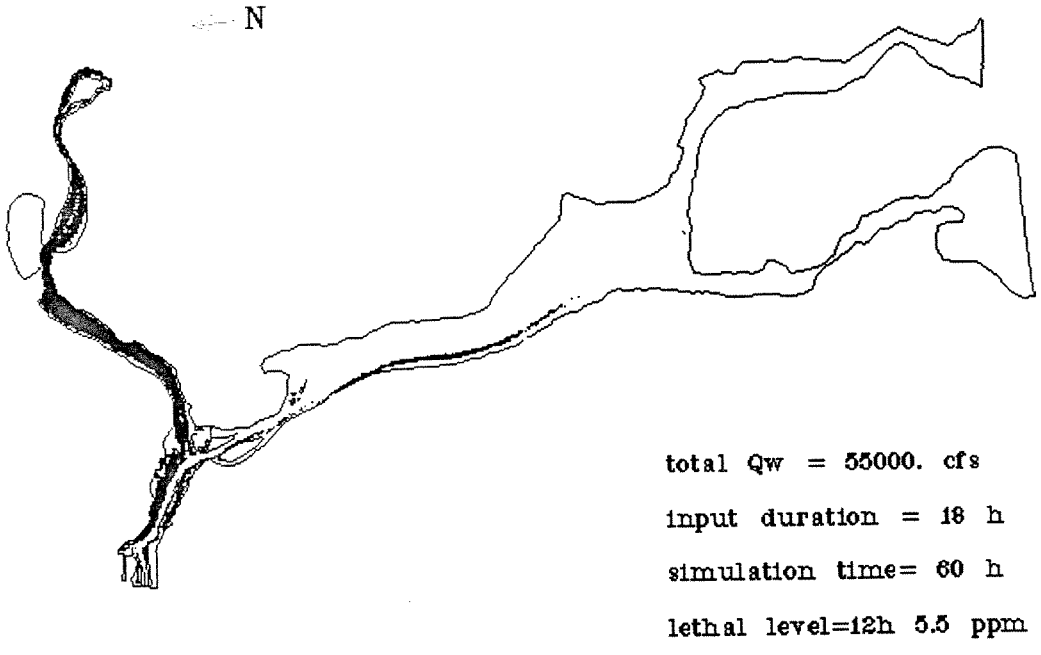

Figure 5.5: Area reaching the lethal dosage of 5.5 ppm for 12 hours in Sample simulation II

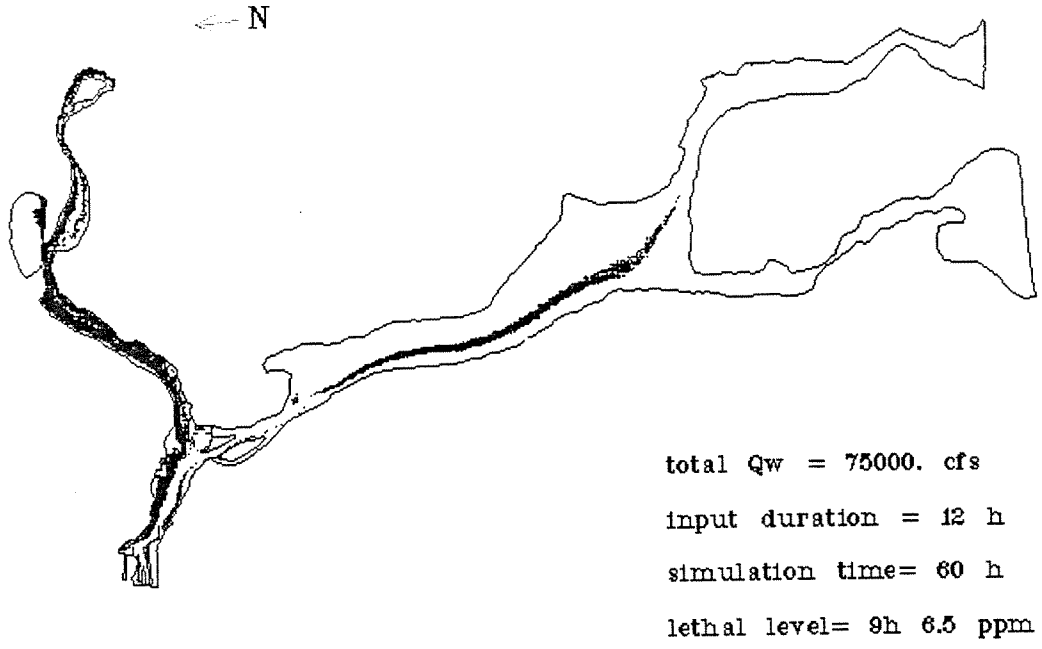

Figure 5.6: Area reaching the lethal dosage of 6.5 ppm for 9 hours in Sample simulation III

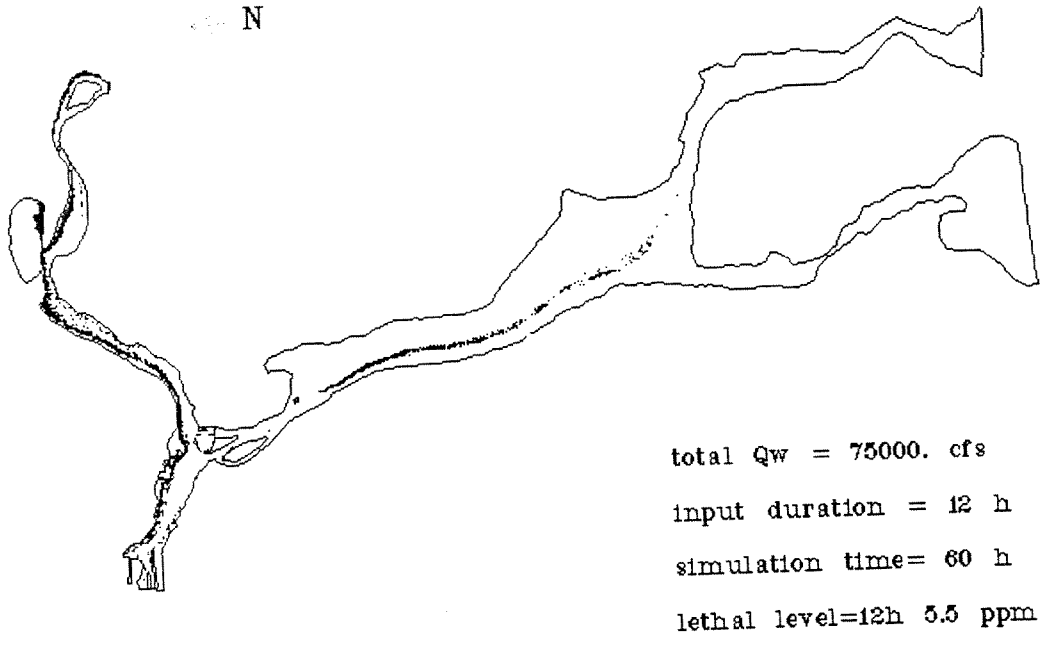

Figure 5.7: Area reaching the lethal dosage of 5.5 ppm for 12 hours in Sample simulation III

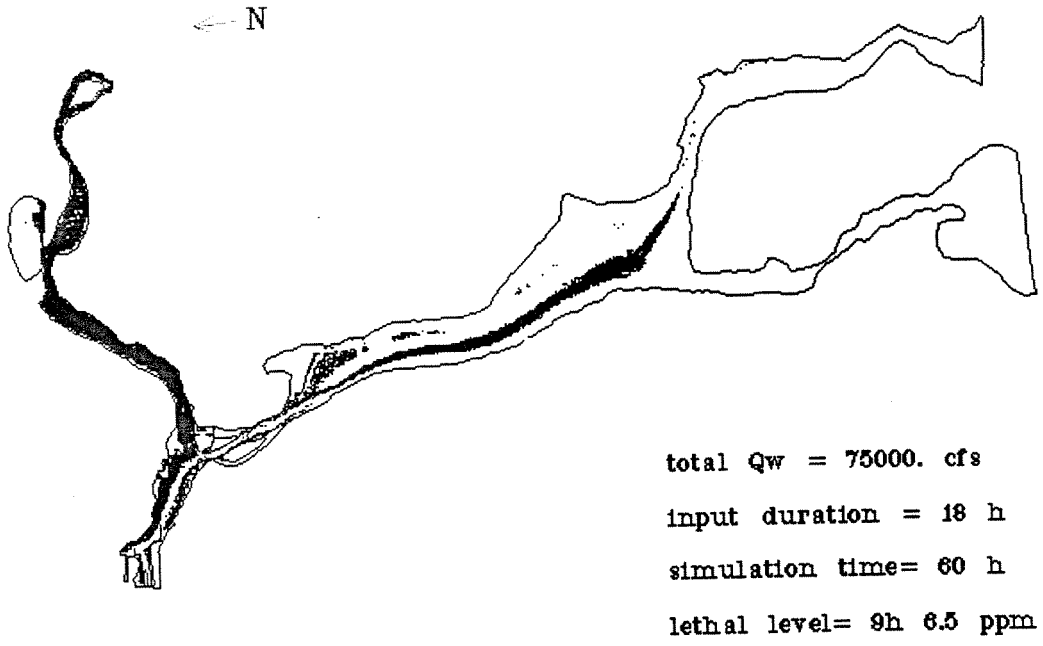

Figure 5.8: Area reaching the lethal dosage of 6.5 ppm for 9 hours in Sample simulation IV

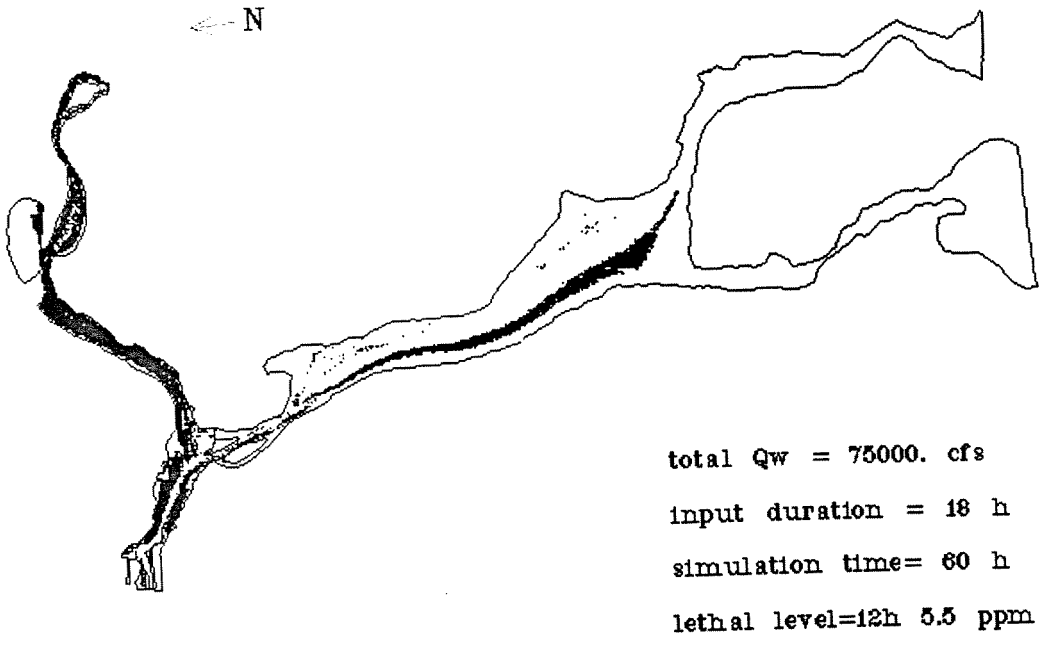

Figure 5.9: Area reaching the lethal dosage of 5.5 ppm for 12 hours in Sample simulation IV

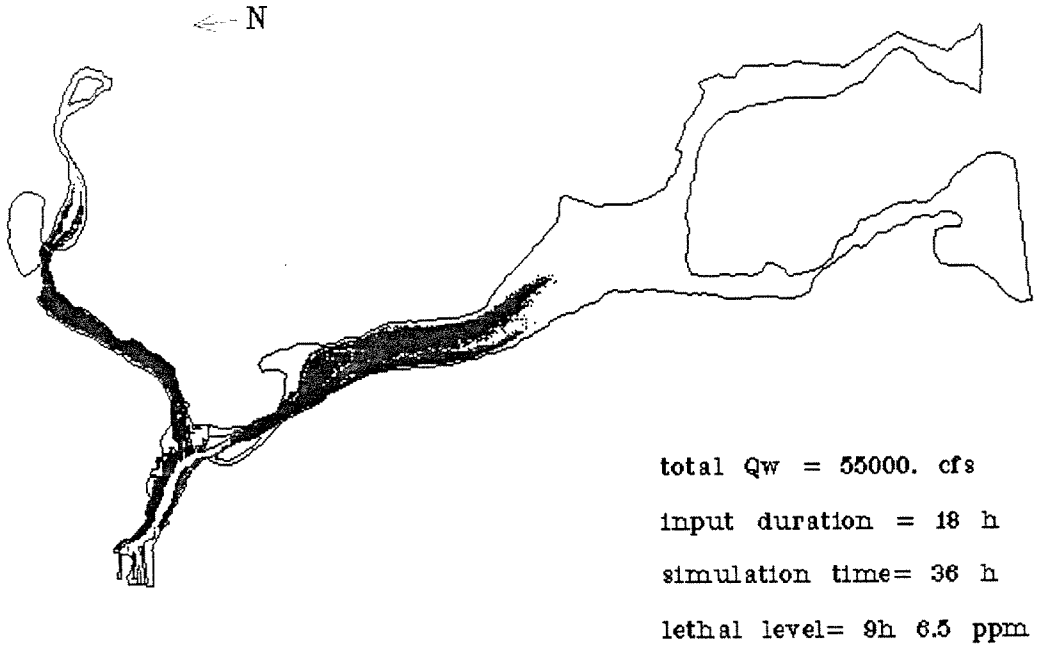

Figure 5.10: Area reaching the lethal dosage of 6.5 ppm for 9 hours in Sample simulation V

duration is larger than the area reaching the lower one with a long duration. In addition, most of the areas reaching the lethal level are along the Canadian Channel. Along the main shipping channel south of Sugar Island and in Lake Nicolet, the area reaching the lethal level is relatively small.

From Fig. 1.1, the north part of Lake Nicolet near the Sugar Island has a high density of sea lamprey population. This area can not be covered by the area reaching the lethal level from the above four simulations. An addition simulation, i.e. simulation V, with an addition local application of lampricide between Mission Point and Frechette Point when the leading edge of upstream lampricide travels there are made. The upstream condition of hydrology and lampricide application is same as that of the sample simulation II. From the output shown in Figs. 5.10 and 5.11, the area with high sea lamprey population density can be covered by a lethal dosage.

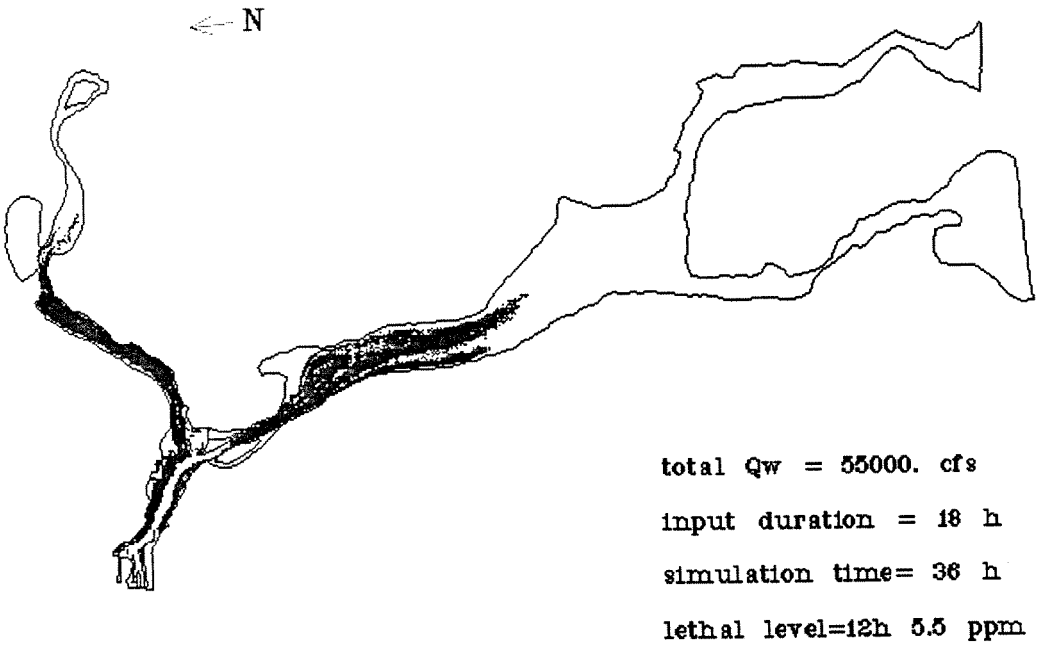

Figure 5.11: Area reaching the lethal dosage of 5.5 ppm for 12 hours in Sample simulation V

Chapter 6

Summary

This report describes the formulation and development of a chemical transport model for rivers. The model is applied to the upper St. Marys River to simulate the transport of lampricides. The hydrodynamics necessary for the model are computed based on a depth-averaged two dimensional finite element model.

Preliminary calibration of the model using the existing dye test results are made. Sample simulations for various lampricide applications under selected flow conditions are presented to demonstrate the general dispersion characteristics of the St. Marys River. The model shows the potential of being developed into a useful tool for evaluating alternative lampricide application strategies. The present model can be used to assist the design of an effective dye test to provide data for model calibration. Further calibration and refinement of the model with additional dye test data , when it becomes available, will improve the accuracy of the model. The refined model together with the sea lamprey population density distribution surveyed by the St. Marys River Control Tast Force will enable the design of effective and economical lampricide application plans.

Bibliography

[1] Ambrose, R. B., Hill, S. I. and Mulkey, L. A. (1983). "User's Manual for the Chemical Transport and Fate Model TOXIWASP." *EPA-600/3-83-005*, Environmental Research Laboratory, Athens, Georgia.

[2] Ambrose, R. B., Woll, T. A., Connolly, J. P., and Schang, R. W. (1988)." WASP4, A Hydrodynamic and Water Quality Model – Model Theory, Users Manual, and Programmer's Guide." *EPA/600/3-87/039*, USEPA, Athens, Georgia.

[3] Baker, R. A., ed. (1980)."Fate and Transport, Case Studies, Modeling, Toxicity," *Contaminants and sediments*, Vol. 1, Ann Arbor Science Publishers Inc., Ann Arbor, MI, 1-557.

[4] Chiou, C. T., Freed, D. W., Schmedding, D. W. and Kohnert, R. L. (1977). "Partition Coefficient and Bioaccumulation of Selected Organic Chemicals." *Env. Sci. Tech.*, Vol. 11 No.5, 475-478.

[5] Connor, J. J. and Brebbia, C. A. (1976)."Finite Element Techniques for Fluid Flow." Butterworths and Co., London, U.K.

[6] Callahan, M. A. et al. (1979). "Water-Related Environmental Fate of 129 Priority Pollutants" Vols. I and II. EPA-440/4-79-029a.

[7] Dickson, K. L., Maki, A. W. and Cairns, J. (1982)."Modeling the Fate of Chemical In the Aquatic Environment." Ann Arbor Science Publishers, Ann Arbor, Michigan, 1-346.

[8] Di Toro, D. M. (1985). "A Particle Interaction Model of Reversible Organic Chemical Sorption, " *Chemosphere* 14(10): 1503-1538.

[9] Di Toro, et al. (1981). "Analysis of Fate of Chemicals in Receiving Waters." Phase I. Chemical Manufact. Assoc., Washington, D. C., Prepared by HydroQual, Inc., Mahwah, NJ.

[10] Engelund, F. (1976). "A Sediment Transport Model for Straight Alluvial Channels." *Nordic Hydrology*, vol 7, 293-306.

[11] Egashira, S. and Ashida, K. (1991). " Unified View of the Mechanics of Debris Flow and Bed-Load." Proceedings, US-Japan Micromechanics of Granular Materials, Clarkson University, Potsdam, NY, 166-171.

[12] Garcia, M. and Parker, G. (1991). " Entrainment of Bed Sediment into Suspension." *Journal of Hydraulic Engineering*, ASCE, Vol. 117, No. 4, 414-435.

[13] Halfon, E. (1986)."Modeling the Pathways of Toxic Contaminants in the St. Clair-Detroit River System Using the Toxfate Model : The Fate of Perchlorothylene," *Water poll. res. J. Canada*, Vol.21, No.3, 213-252

[14] Halfon, E. and Brueggemann, R. (1990). "Simulation of Disulfoton Fate in the River with the Toxfate Model." The Science of Total Environment, 97/98, 385-394.

[15] Hamilton, G. D., Soileau C. W., and Stroud A. D. (1982)." Numerical Modeling Study of Lake Pontchautrain." *Journal of the Waterways, Ports, Coastal and Ocean Division, ASCE*, 108, 49-64.

[16] Herman, F. M. and Donald, F. O. et al. (1978). " Encyclopedia of Chemical Technology" 3rd edition, Wiley-Interscience Publication, NY.

[17] Karickhoff, S. W., et al. (1979). "Sorption of Hydrophobic Pollutants on Natural Sediments." *Water Research*, 13, 241-248.

[18] Leendretse, J. J. (1970)."A Water-quality Simulation Model for Well-mixed Estuaries and Coastal Seas," Vol I, Principles of computation, *Report RM-6230-RC*, The Rand Corporation, Santa Monica, California.

[19] Lyman, W. J. and Rosenblatt, D. H. (1982). "Handbook of Chemical Property Estimation Methods," McGraw-Hill Book Company, NY.

[20] McCorquodale, J. A., Ibrahim, K. and Hamdy, Y. (1986). "Fate and Transport Modeling of Perchloroethylene in the St. Clair River ." *Water Poll. Res. J. Canada* vol. 21, No. 3, 398-410.

[21] Mills, W. B. and Dean, J. D. (1982). "Water Quality Assessment: A Screening Procedure for Toxic and Conventional Pollutants." EPA-600/6-82-004a .

[22] Neely, W. B. and Lutz, R. W. (1985). "Environmental Exposure from a Chemical Spilled into a River." *Journal of Hazardous Materials*, 10, 33-41.

[23] Onishi, Y. and Wise, S. W. (1979). "Mathematical Model, SERATRA, for Sediment and Pesticide Transport in Rivers and Its Application to Pesticide Transport in Four Mile and Wolf Creek in Iowa," *Report to USEPA*, Battelle Pacific Northwest Laboratories, Richland, Washington, D.C.

[24] Schnoor, J. L. (1984)."Modeling Chemical Transport in Lake, River, and Estuarine Systems", in The Environmental Exposure From Chemicals, ed. Neely, W. B. and Blau, G. E. CRC Press, Inc.

[25] Shen, H. T. and Yapa, P. D., Wang, D.S. and Yang, X. Q. (1991). "A Mathematical Model for Oil Slick Transport and Mixing in River." *Report No. 91-1*, Clarkson University, Potsdam, NY.

[26] Shen, H. T. and Yapa, P. D. (1988). "Oil Slick Transport in Rivers." *Journal of Hydraulic Engineering*, ASCE, Vol. 114, No. 5, 529-543.

[27] Teisson, C. (1991). "Cohesive Suspended Sediment Transport : Feasibility and Limitations of Numerical Modeling." *Journal of Hydraulic Research*, IAHR, vol. 29, No. 6.

[28] Thomann, R. V. and Mueller, J. A. (1987)."Principles of Surface Water Quality Modeling and Control", Harper & Row Publishers, New York.

[29] Thomann, R. V. and Ditoro, D. M. (1983). "Physico Chemical Model of Toxic Substances in the Great Lakes," *Journal of Great Lakes Research*, Vol.9, No.4, 474-496.

[30] Thomann, R. V., and Salas, H. J. (1986). "Manual on Toxic Substances in Surface Waters, " Pan American Health Organization, CEPIS, Lima, Peru.

[31] Vanoni, V. A., ed. (1977). "Sedimentation Engineering", ASCE, NY.

[32] Verschueren, K. (1983). "Handbook of Environmental Data on Organic Chemicals" 2nd edition, Van Nostrand Reinhold Co., NY, 1-1310.

[33] Weast, R. C. (1981). " CRC Handbook of Chemistry and Physics" 61th Edition, 1980-1981. CRC Press, Cleveland, Ohio.

[34] Westrich, B. (1976). " Simulation of Mass Exchange in Dead Zones for Steady and Unsteady Flow Conditions," *International Symposium on Unsteady Flow in Open Channels*, Cranfield, Bedford, England, G3, 23-34.

[35] Valentine, E. M. and Wood, I. R. (1977). "Longitudinal Dispersion with Dead Zones." *Journal of the Hydraulics Division*, Vol. 103, No. HY9, 975-990.

[36] Yapa, P. D., Shen, H. T. (1994)." Modelling River Oil Spills: A Review" *Journal of Hydraulic Research*, Vol 32, No. 5, 765-782

[37] Yapa, P. D., Shen, H. T., Wang, D. S., and Angammana, K. S. (1992)." An Integrated Oil Spill Model for Upper St. Lawrence River," *Journal of Great Lakes Research*, .

[38] Yapa, P. D., Shen, H. T., Wang, D. S., and Angammana, K. S. (1993)." Modeling Oil Spills in a River-Lake System,"

Appendix A

Hourly simulation results for dye studies

CASE 1

Flow:

Total Flow = 1315 m^3/s

American Lock = 15 m^3/s

Compensation Works = 300 m^3/s

COE Powerhouse = 350 m^3/s

Edison Sault Electric = 622 m^3/s

Canadian Lock = 28 m^3/s

Input:

C_0= 2.84 ppb at Edison Sault Electric

Input duration =6 hrs

Output:

Maximum concentration during the 10 hrs

Concentration distribution every hour from 1 to 10 hrs


N
time= 1: 0 h
Concentration (ppb)
0.000 — 0.200
0.200 — 0.500
0.500 — 0.800
0.800 — 1.000
1.000 — 1.500
1.500 — 2.000
2.000 — 2.500
2.500 — 3.000
3.000 — 3.500
3.500 — 4.000

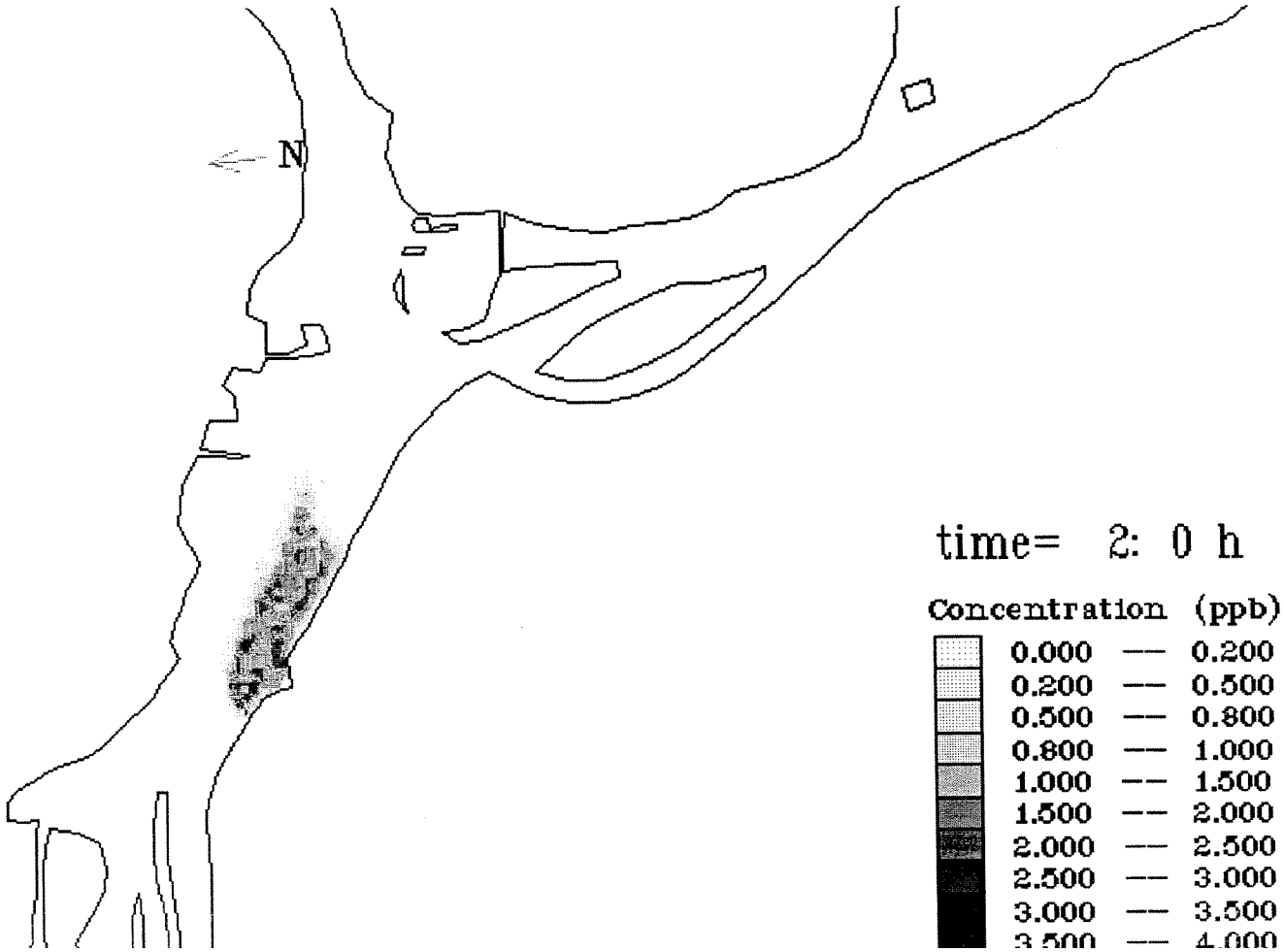
N
time= 2: 0 h
Concentration (ppb)
0.000 — 0.200
0.200 — 0.500
0.500 — 0.800
0.800 — 1.000
1.000 — 1.500
1.500 — 2.000
2.000 — 2.500
2.500 — 3.000
3.000 — 3.500
3.500 — 4.000

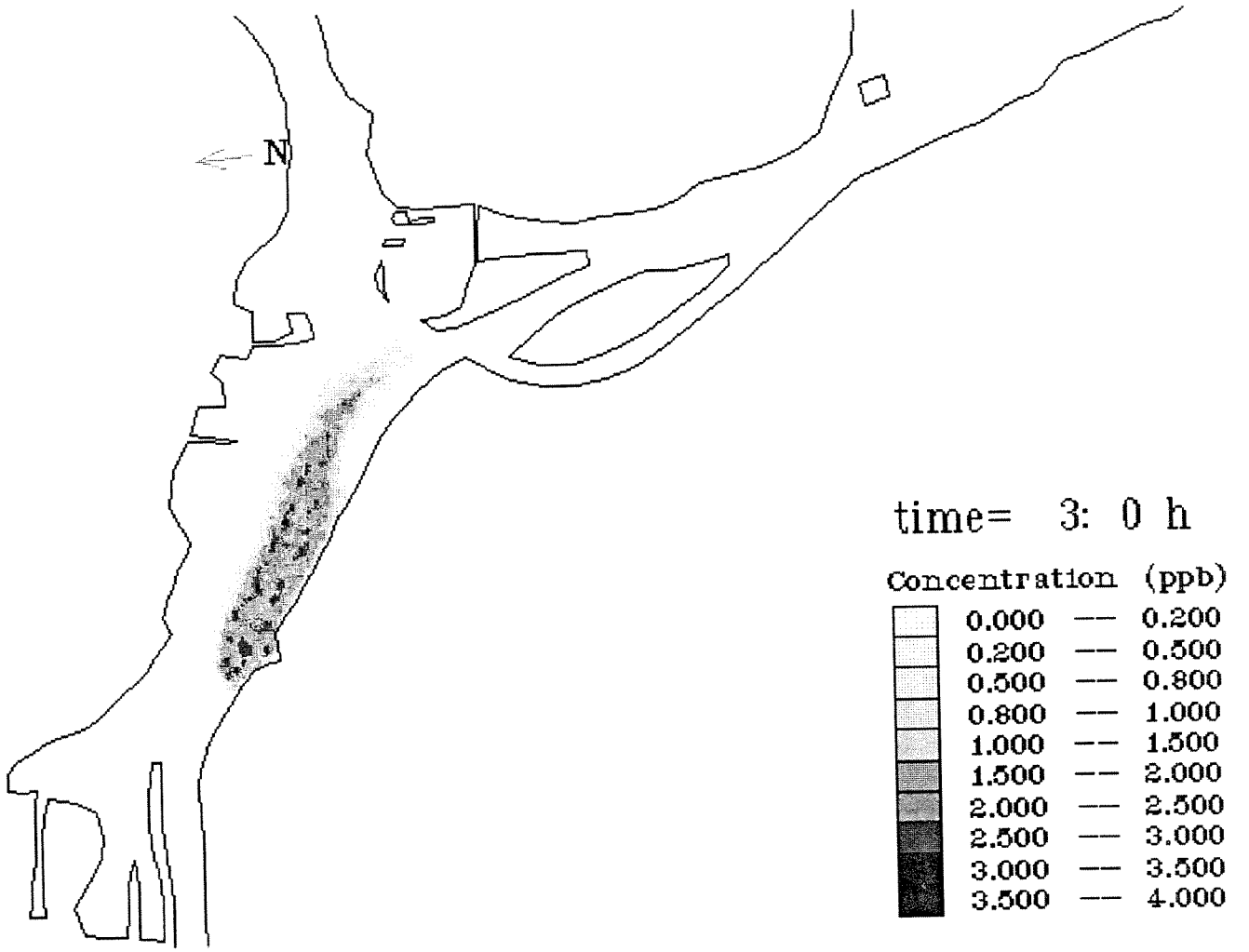
N
time= 3: 0 h
Concentration (ppb)
0.000 — 0.200
0.200 — 0.500
0.500 — 0.800
0.800 — 1.000
1.000 — 1.500
1.500 — 2.000
2.000 — 2.500
2.500 — 3.000
3.000 — 3.500
3.500 — 4.000

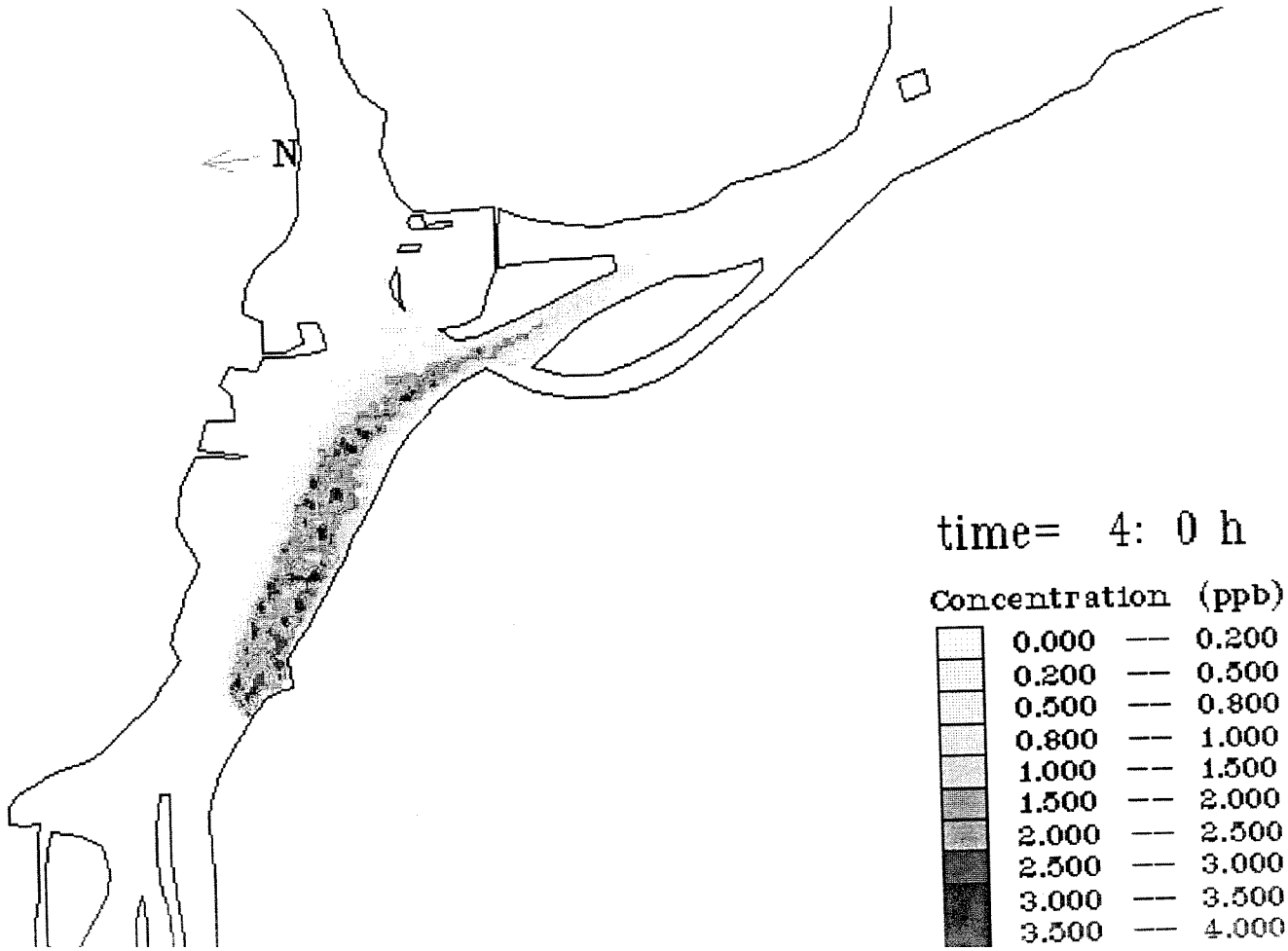
N
time= 4: 0 h
Concentration (ppb)
0.000 — 0.200
0.200 — 0.500
0.500 — 0.800
0.800 — 1.000
1.000 — 1.500
1.500 — 2.000
2.000 — 2.500
2.500 — 3.000
3.000 — 3.500
3.500 — 4.000

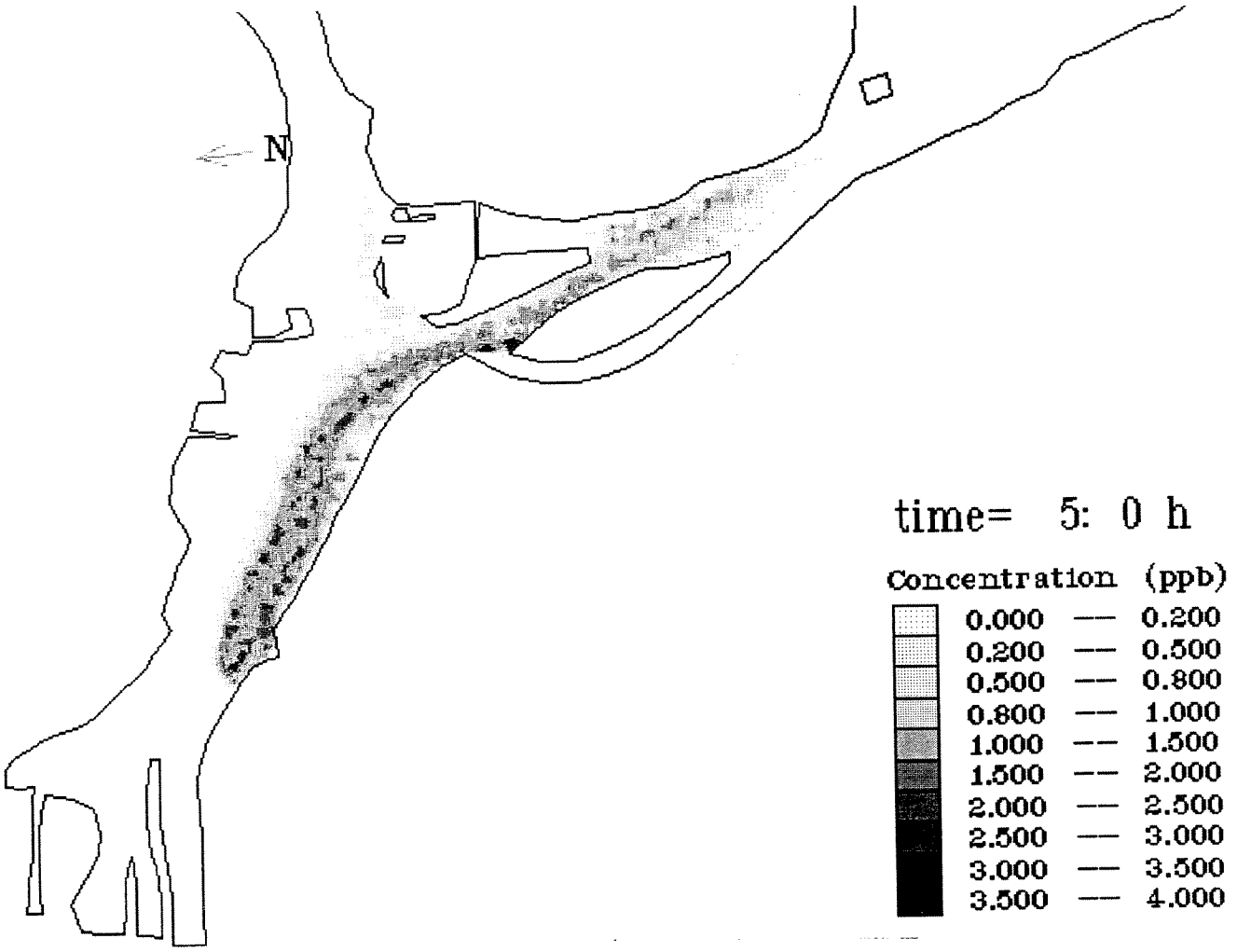
N
time= 5: 0 h
Concentration (ppb)
0.000 — 0.200
0.200 — 0.500
0.500 — 0.800
0.800 — 1.000
1.000 — 1.500
1.500 — 2.000
2.000 — 2.500
2.500 — 3.000
3.000 — 3.500
3.500 — 4.000

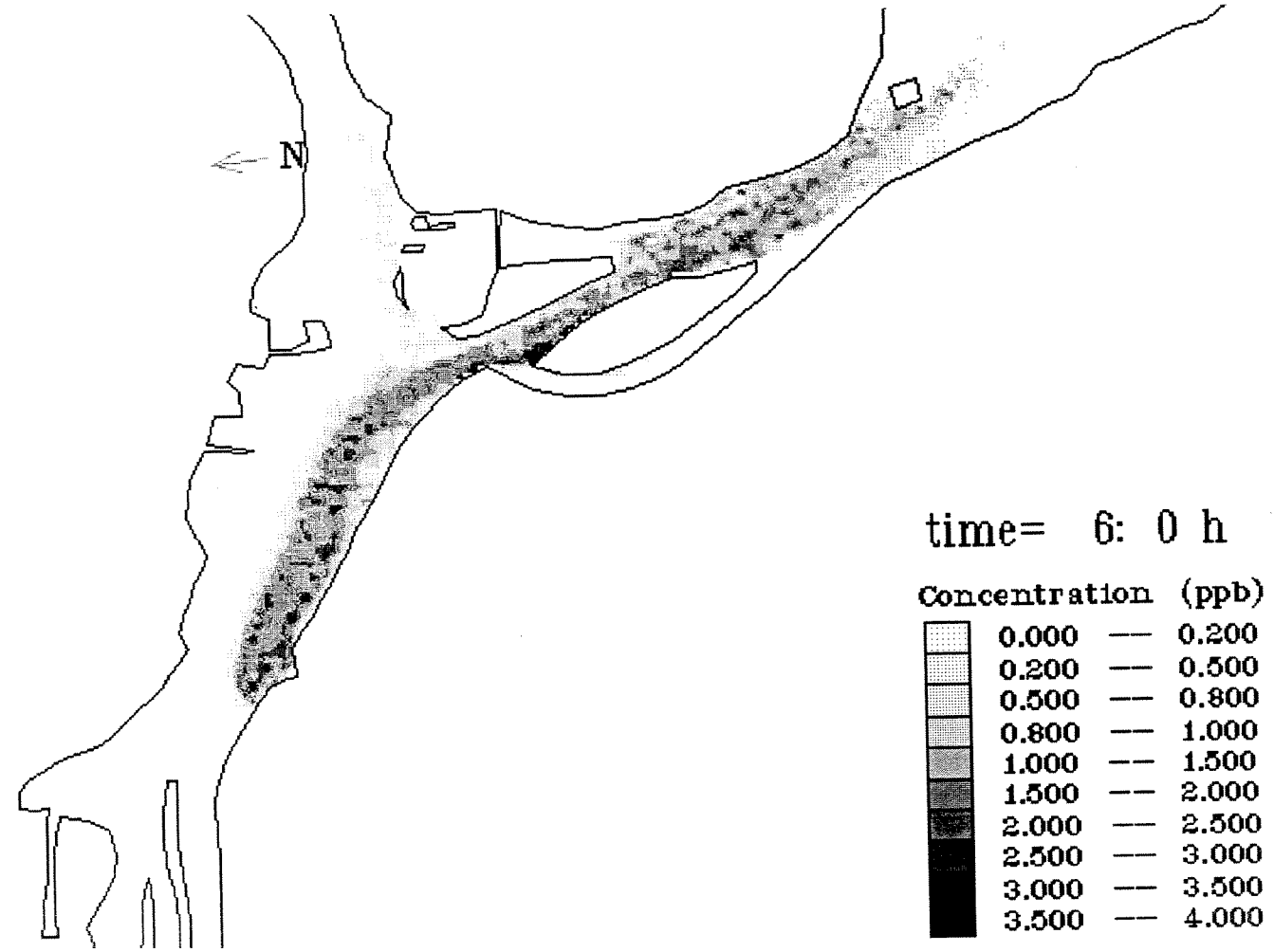
N
time= 6: 0 h
Concentration (ppb)
0.000 — 0.200
0.200 — 0.500
0.500 — 0.800
0.800 — 1.000
1.000 — 1.500
1.500 — 2.000
2.000 — 2.500
2.500 — 3.000
3.000 — 3.500
3.500 — 4.000

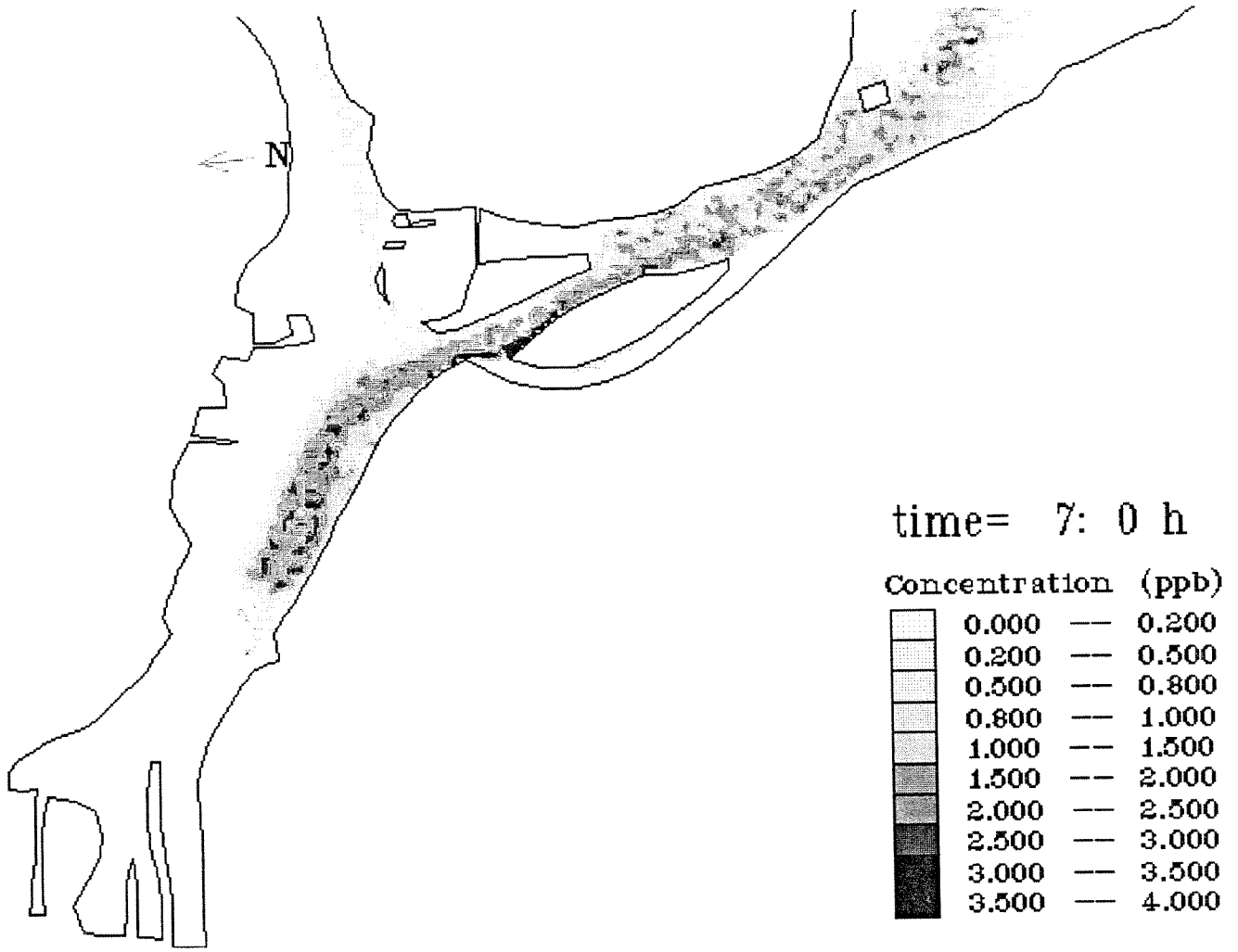
N
time= 7: 0 h
Concentration (ppb)
0.000 — 0.200
0.200 — 0.500
0.500 — 0.800
0.800 — 1.000
1.000 — 1.500
1.500 — 2.000
2.000 — 2.500
2.500 — 3.000
3.000 — 3.500
3.500 — 4.000

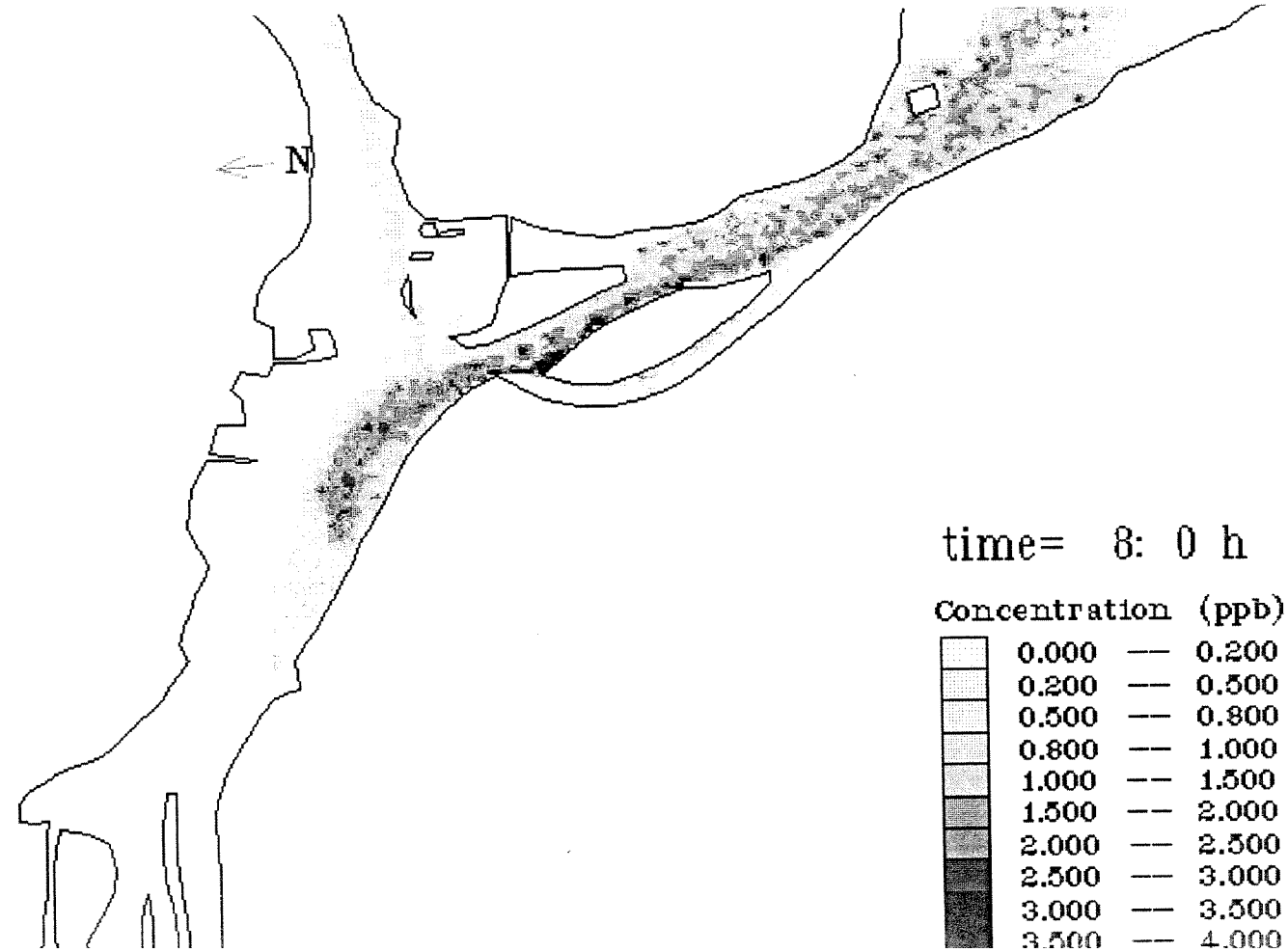
N
time= 8: 0 h
Concentration (ppb)
0.000 — 0.200
0.200 — 0.500
0.500 — 0.800
0.800 — 1.000
1.000 — 1.500
1.500 — 2.000
2.000 — 2.500
2.500 — 3.000
3.000 — 3.500
3.500 — 4.000

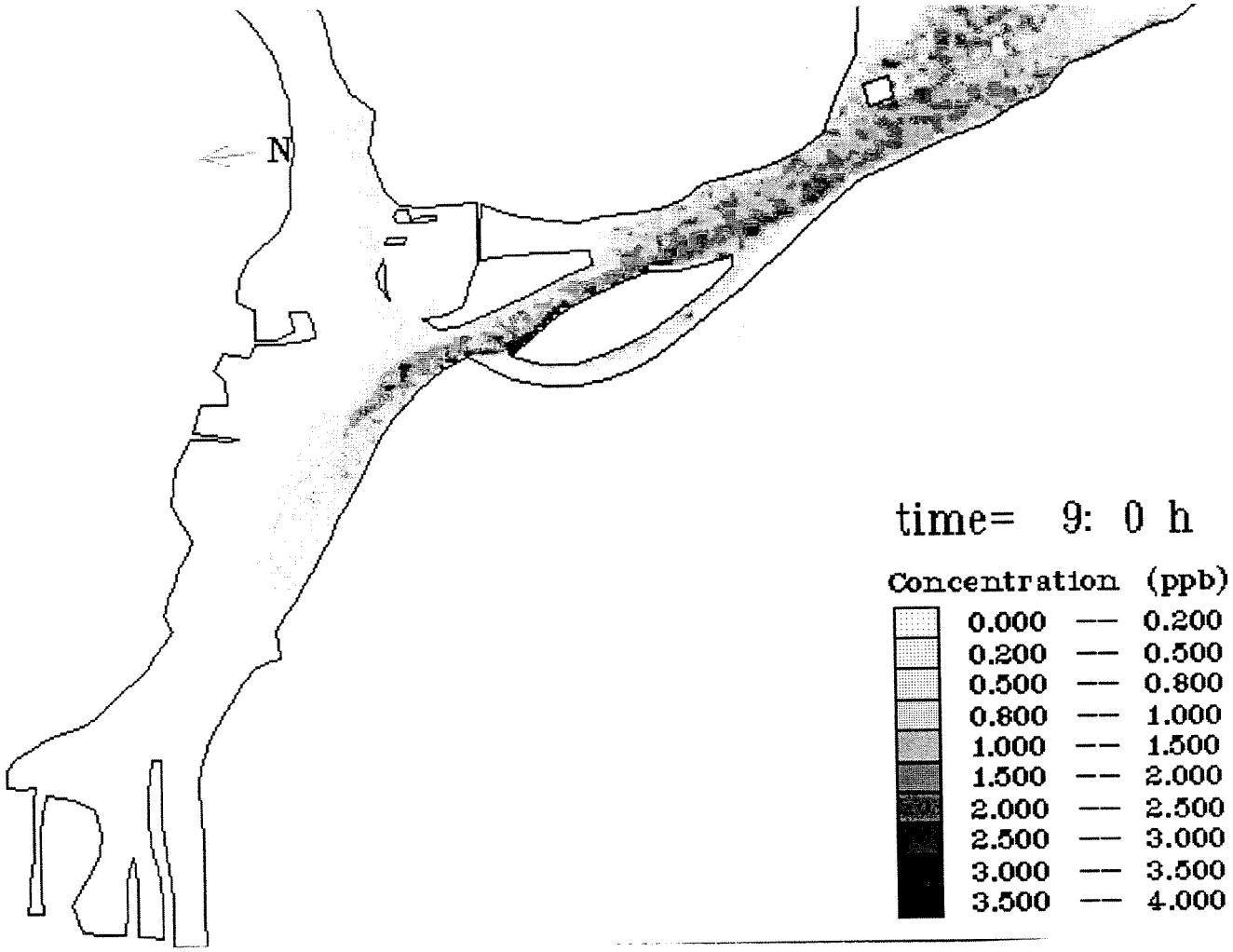
N
time= 9: 0 h
Concentration (ppb)
0.000 — 0.200
0.200 — 0.500
0.500 — 0.800
0.800 — 1.000
1.000 — 1.500
1.500 — 2.000
2.000 — 2.500
2.500 — 3.000
3.000 — 3.500
3.500 — 4.000

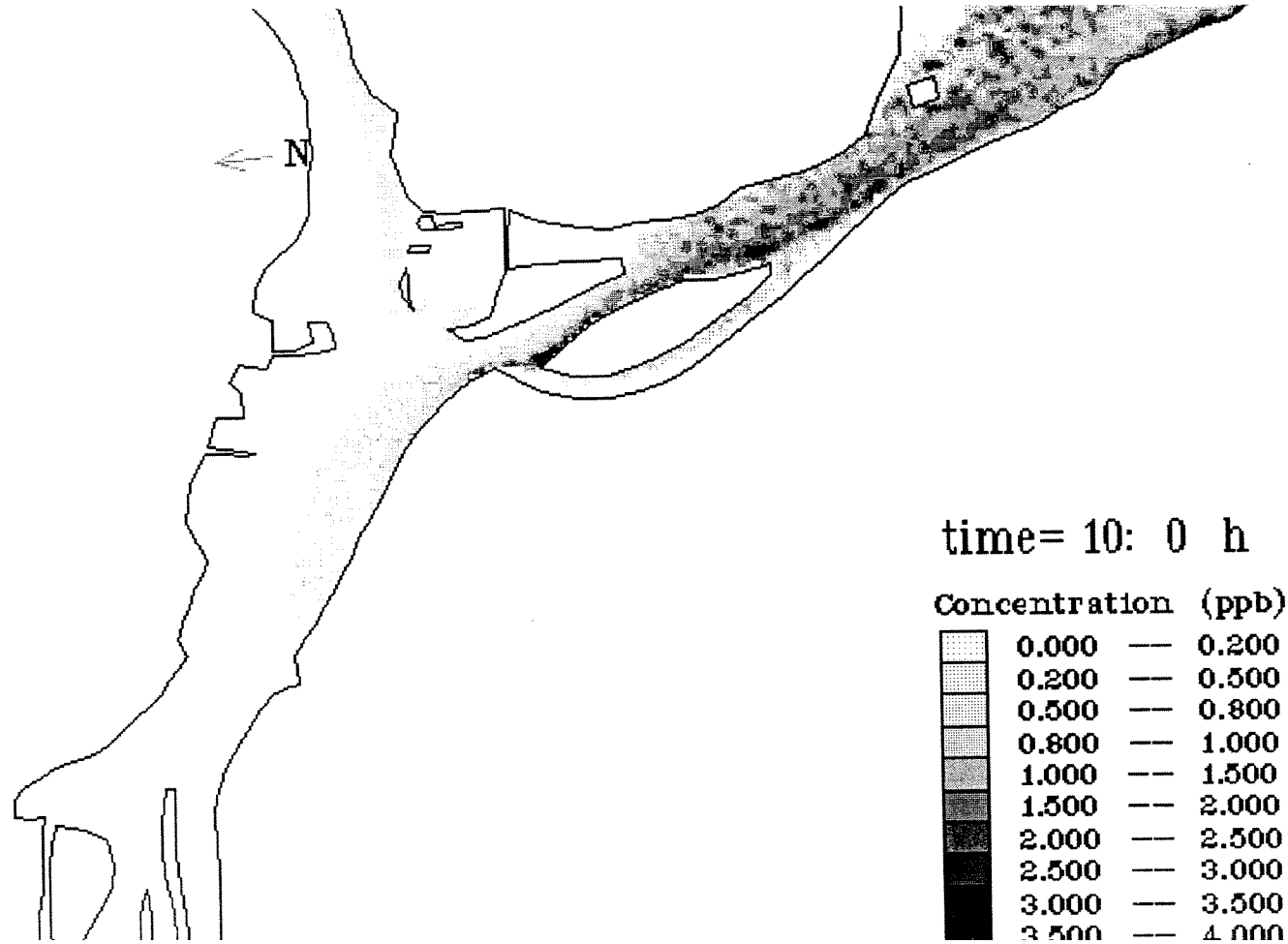
N
time= 10: 0 h
Concentration (ppb)
0.000 — 0.200
0.200 — 0.500
0.500 — 0.800
0.800 — 1.000
1.000 — 1.500
1.500 — 2.000
2.000 — 2.500
2.500 — 3.000
3.000 — 3.500
3.500 — 4.000

CASE 2

Flow:

Total Flow = 1315 m^3/s

American Lock = 15 m^3/s

Compensation Works = 300 m^3/s

COE Powerhouse = 350 m^3/s

Edison Sault Electric = 622 m^3/s

Canadian Lock = 28 m^3/s

Input:

C_0= 3.46 ppb at COE Powerhouse

Input duration = 5 hrs

Output:

Maximum concentration during the 9 hrs

Concentration distribution every hour from 1 to 9 hrs

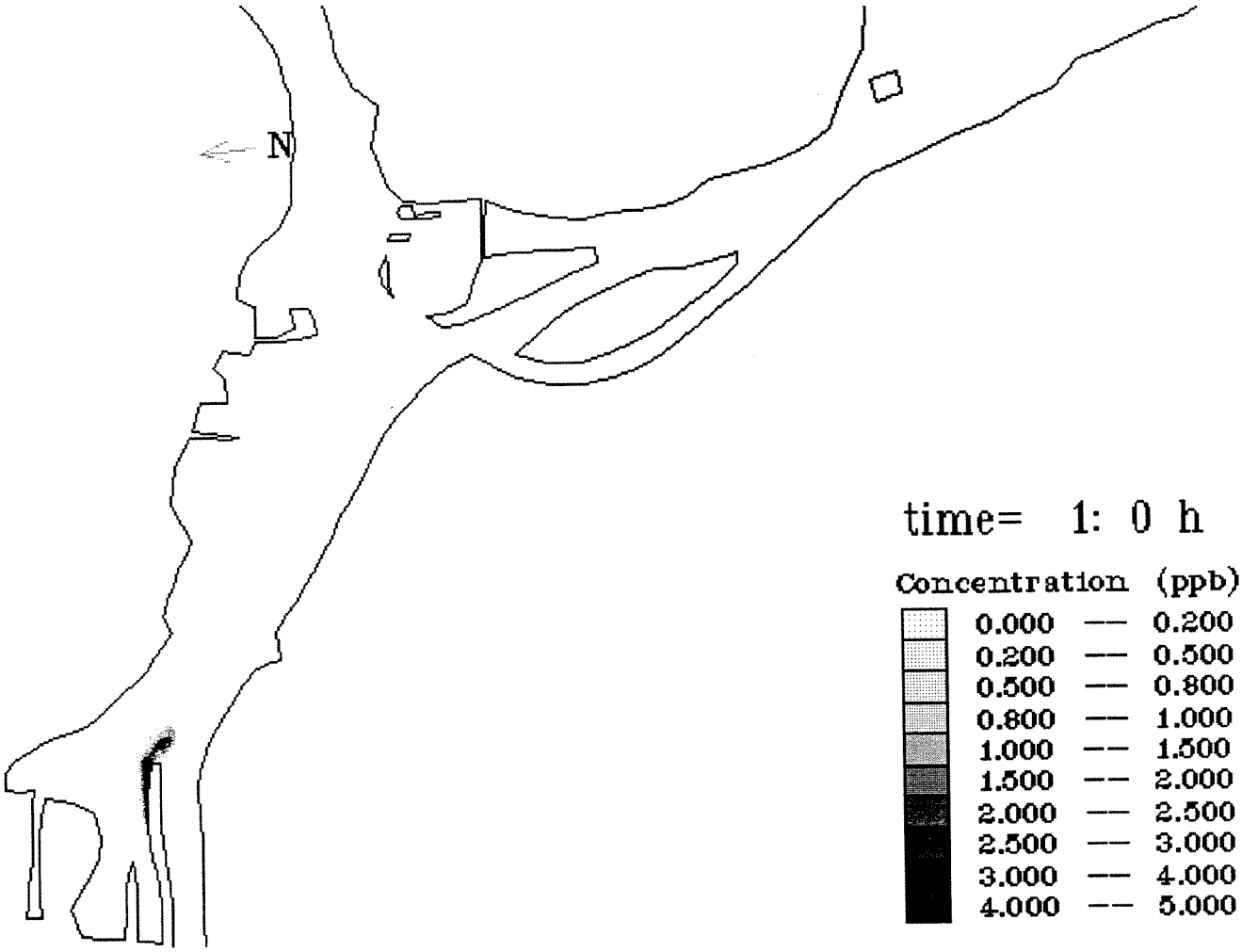
N
time= 1: 0 h
Concentration (ppb)
0.000 — 0.200
0.200 — 0.500
0.500 — 0.800
0.800 — 1.000
1.000 — 1.500
1.500 — 2.000
2.000 — 2.500
2.500 — 3.000
3.000 — 4.000
4.000 — 5.000

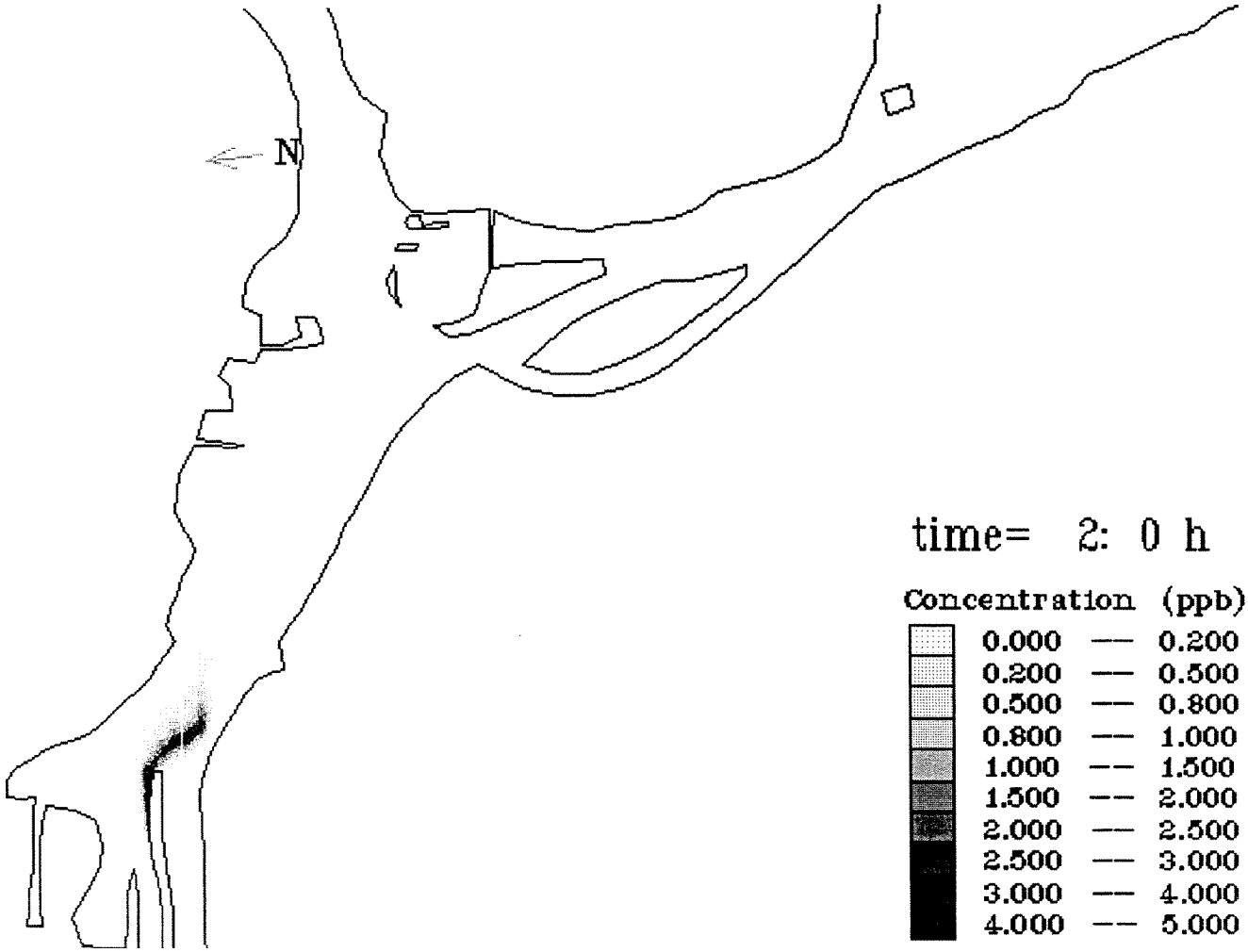
N
time= 2: 0 h
Concentration (ppb)
0.000 — 0.200
0.200 — 0.500
0.500 — 0.800
0.800 — 1.000
1.000 — 1.500
1.500 — 2.000
2.000 — 2.500
2.500 — 3.000
3.000 — 4.000
4.000 — 5.000

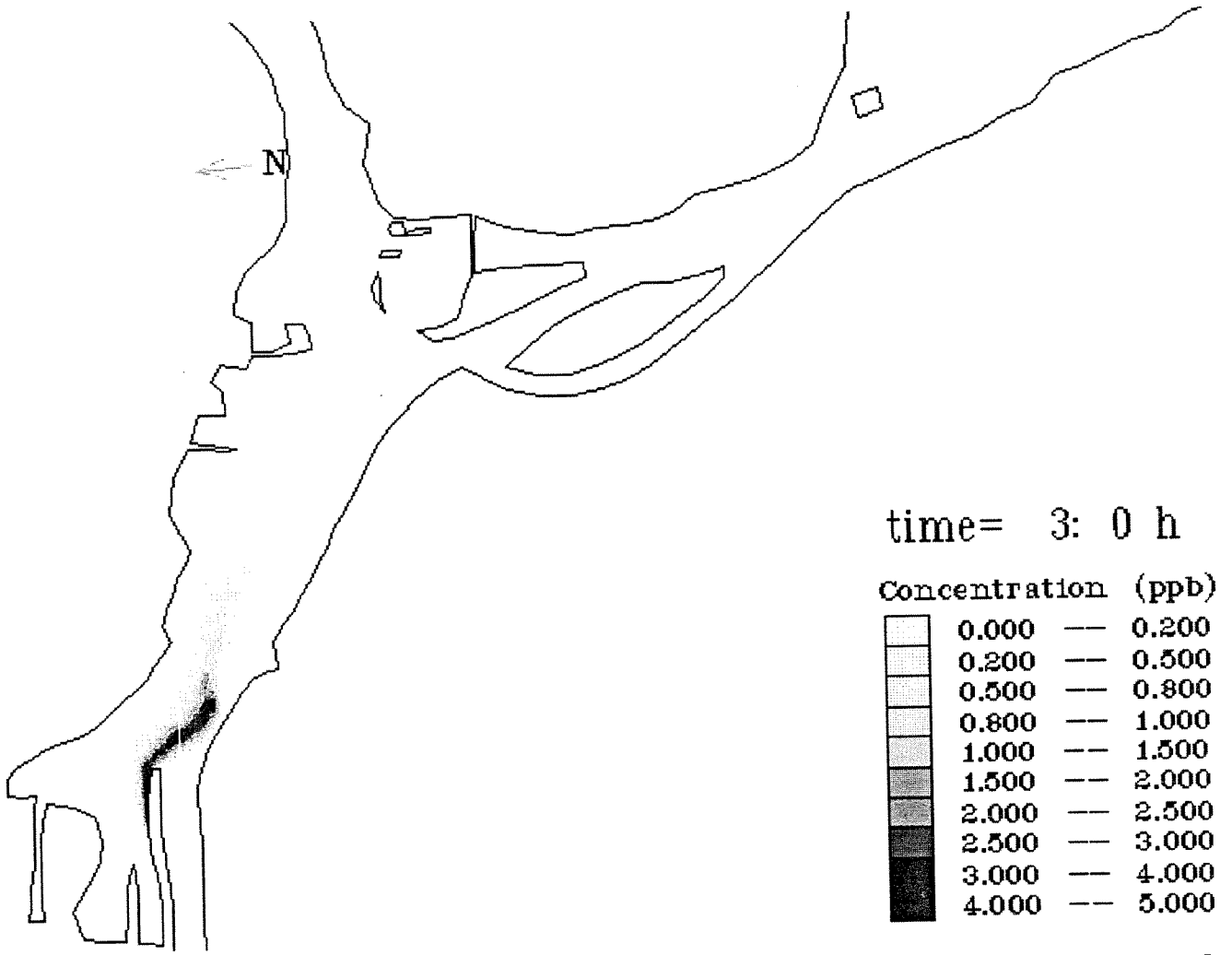
N
time= 3: 0 h
Concentration (ppb)
0.000 — 0.200
0.200 — 0.500
0.500 — 0.800
0.800 — 1.000
1.000 — 1.500
1.500 — 2.000
2.000 — 2.500
2.500 — 3.000
3.000 — 4.000
4.000 — 5.000

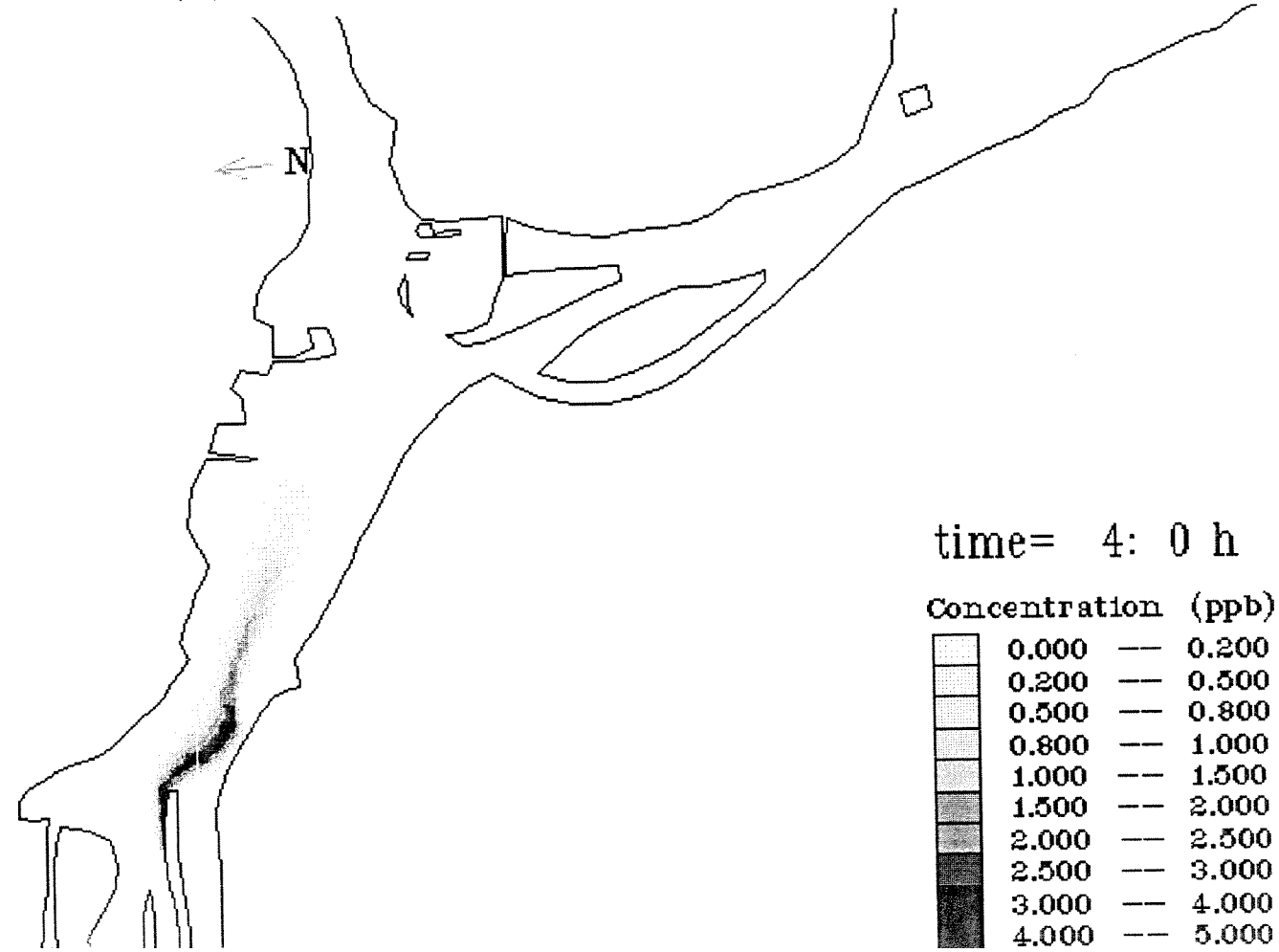
N
time= 4: 0 h
Concentration (ppb)
0.000 — 0.200
0.200 — 0.500
0.500 — 0.800
0.800 — 1.000
1.000 — 1.500
1.500 — 2.000
2.000 — 2.500
2.500 — 3.000
3.000 — 4.000
4.000 — 5.000

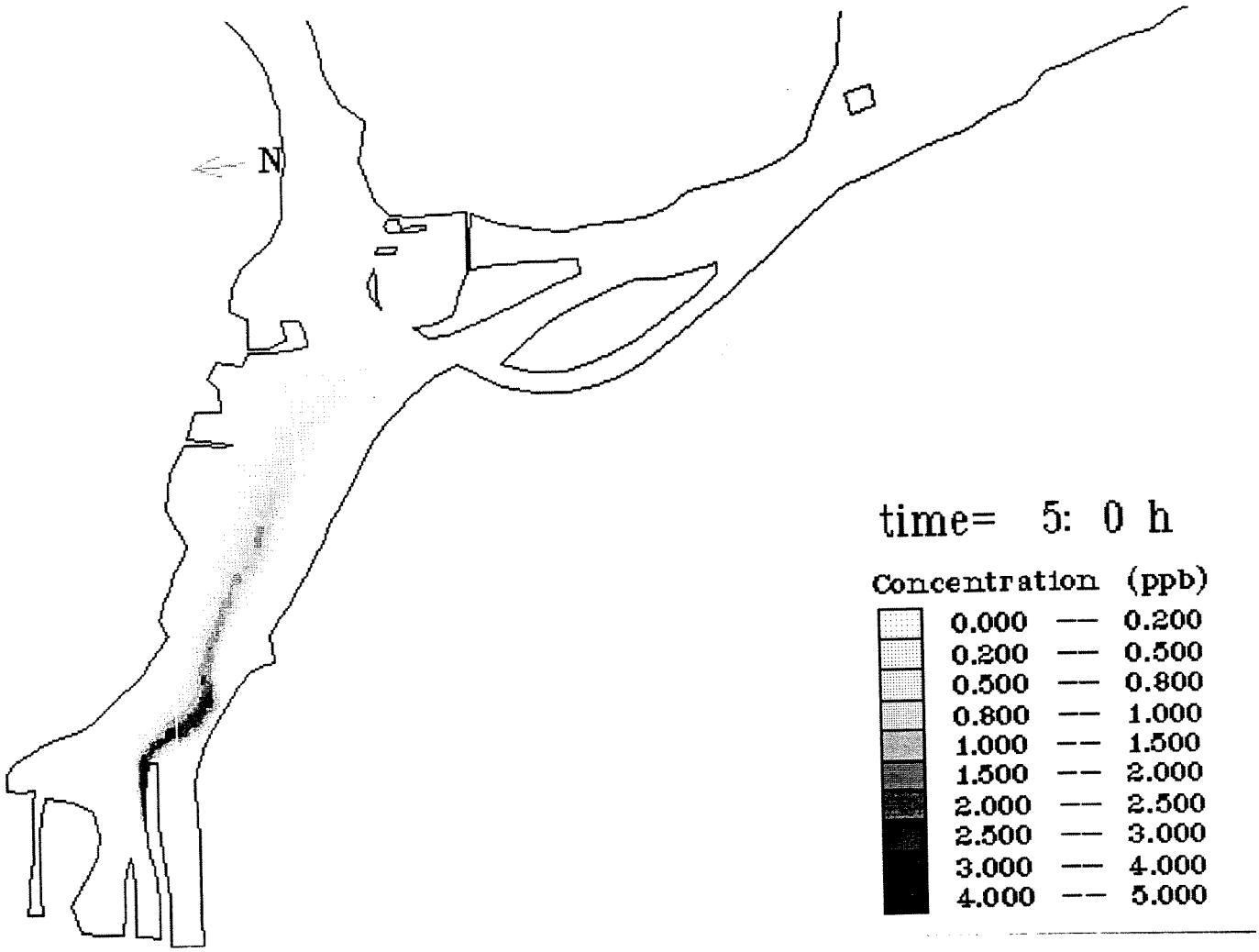
N
time= 5: 0 h
Concentration (ppb)
0.000 — 0.200
0.200 — 0.500
0.500 — 0.800
0.800 — 1.000
1.000 — 1.500
1.500 — 2.000
2.000 — 2.500
2.500 — 3.000
3.000 — 4.000
4.000 — 5.000

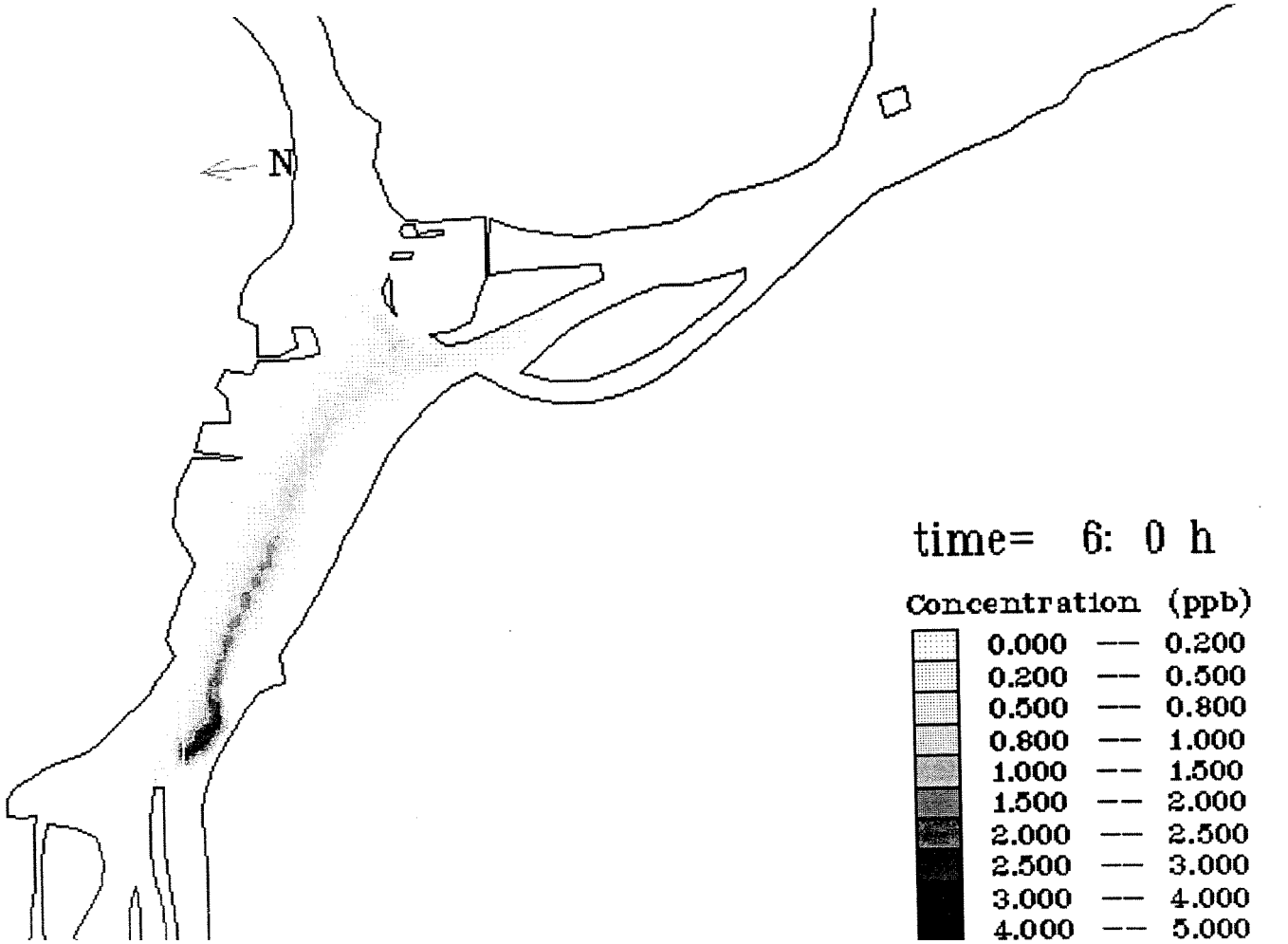
N
time= 6: 0 h
Concentration (ppb)
0.000 — 0.200
0.200 — 0.500
0.500 — 0.800
0.800 — 1.000
1.000 — 1.500
1.500 — 2.000
2.000 — 2.500
2.500 — 3.000
3.000 — 4.000
4.000 — 5.000

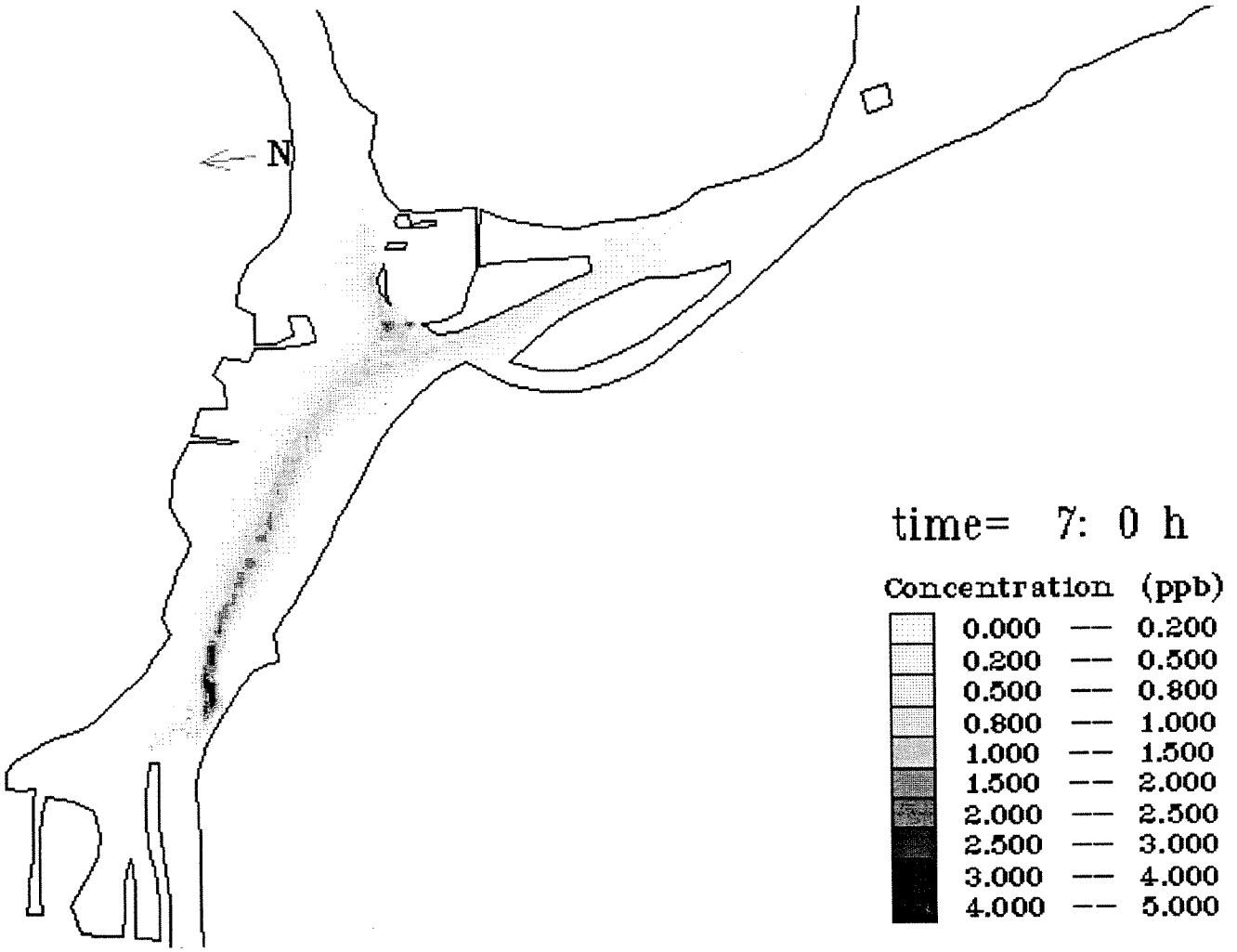
N
time= 7: 0 h
Concentration (ppb)
0.000 — 0.200
0.200 — 0.500
0.500 — 0.800
0.800 — 1.000
1.000 — 1.500
1.500 — 2.000
2.000 — 2.500
2.500 — 3.000
3.000 — 4.000
4.000 — 5.000

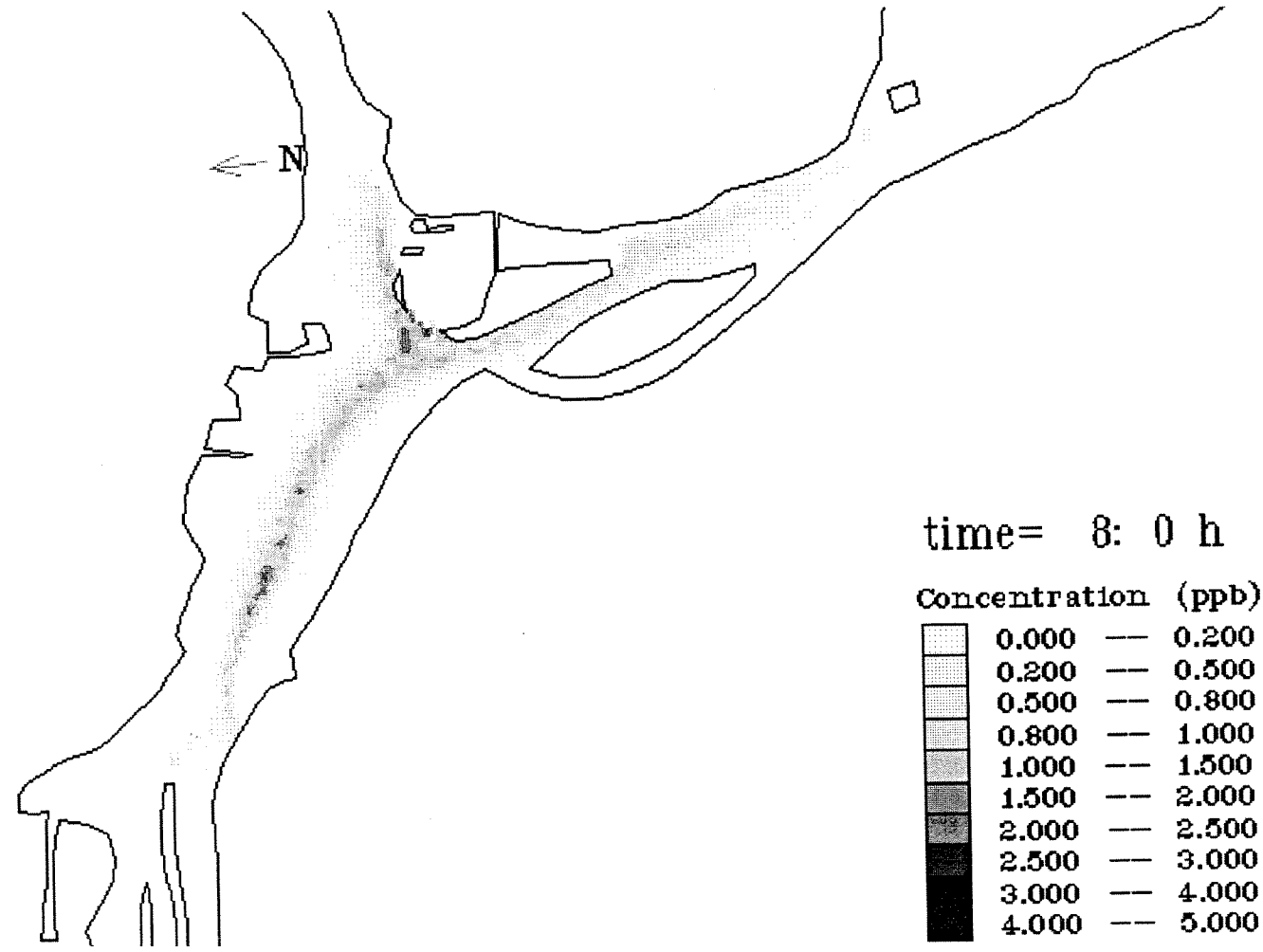
N
time= 8: 0 h
Concentration (ppb)
0.000 — 0.200
0.200 — 0.500
0.500 — 0.800
0.800 — 1.000
1.000 — 1.500
1.500 — 2.000
2.000 — 2.500
2.500 — 3.000
3.000 — 4.000
4.000 — 5.000

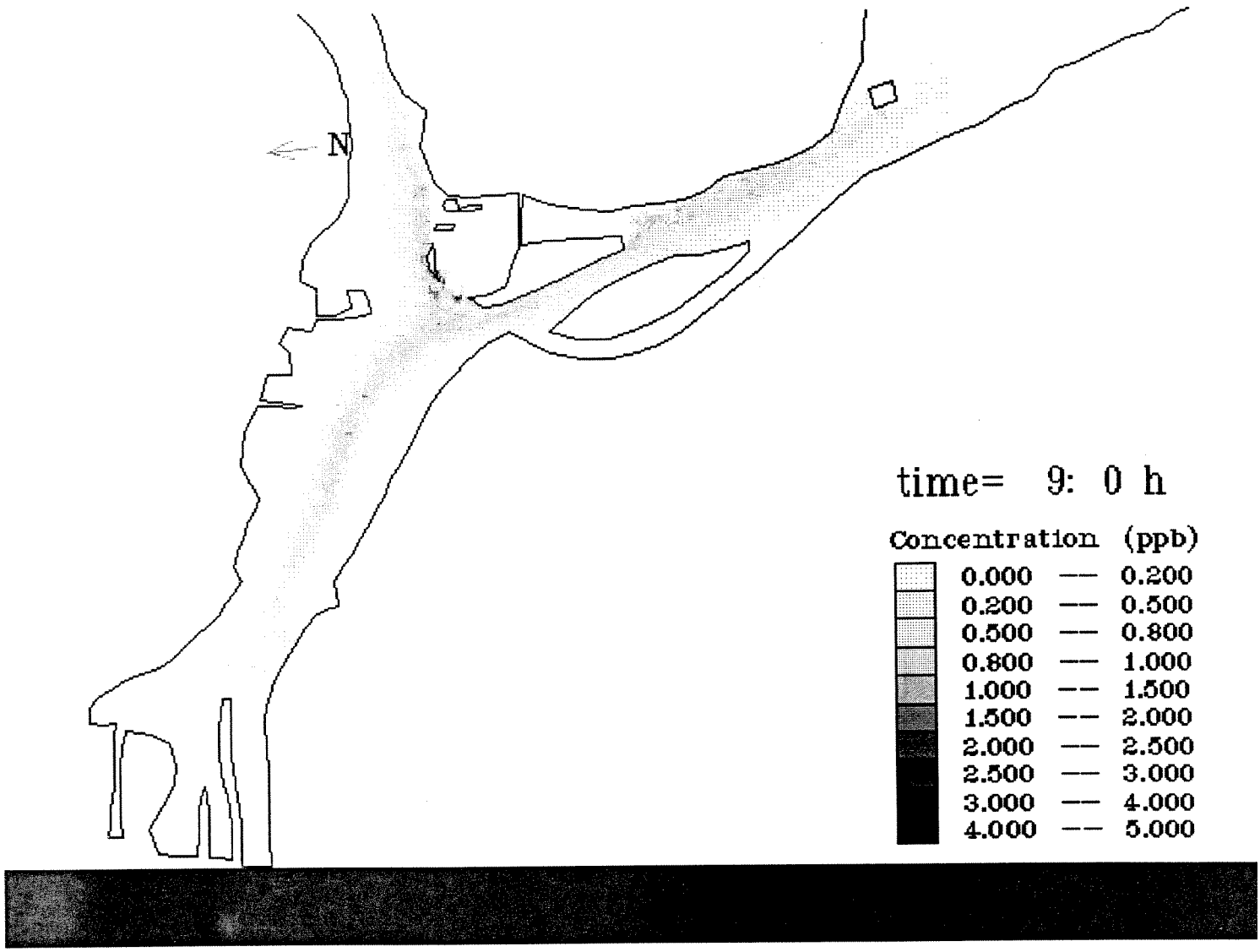
N
time= 9: 0 h
Concentration (ppb)
0.000 — 0.200
0.200 — 0.500
0.500 — 0.800
0.800 — 1.000
1.000 — 1.500
1.500 — 2.000
2.000 — 2.500
2.500 — 3.000
3.000 — 4.000
4.000 — 5.000

CASE 3

Flow:

Total Flow = 1315 m^3/s

American Lock = 15 m^3/s

Compensation Works = 300 m^3/s

COE Powerhouse = 350 m^3/s

Edison Sault Electric = 622 m^3/s

Canadian Lock = 28 m^3/s

Input:

C_0= 4.81 ppb at Compensation Works

Input duration = 5 hrs

Output:

Maximum concentration during the 9 hrs

Concentration distribution every hour from 1 to 9 hrs

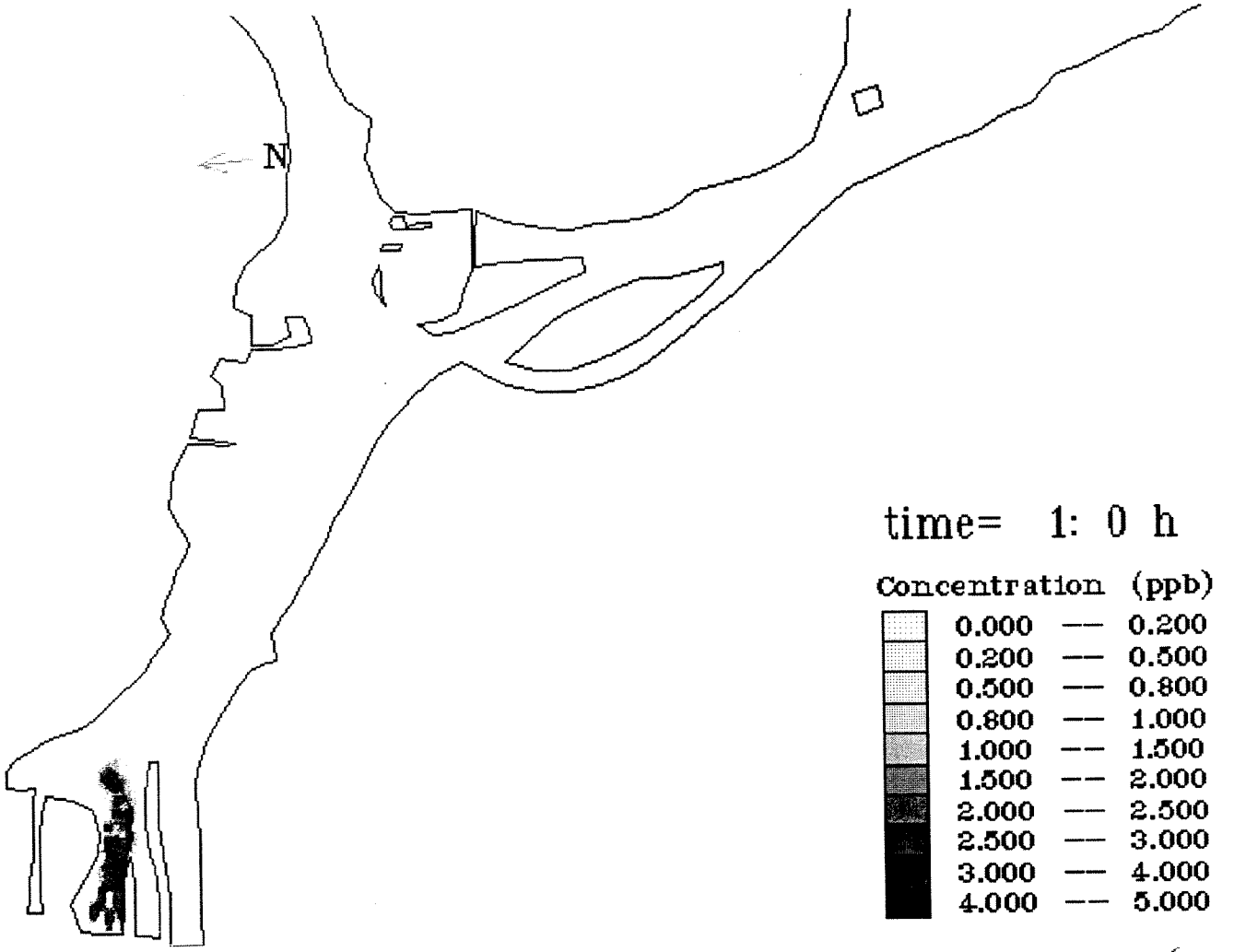
N
time= 1: 0 h
Concentration (ppb)
0.000 — 0.200
0.200 — 0.500
0.500 — 0.800
0.800 — 1.000
1.000 — 1.500
1.500 — 2.000
2.000 — 2.500
2.500 — 3.000
3.000 — 4.000
4.000 — 5.000

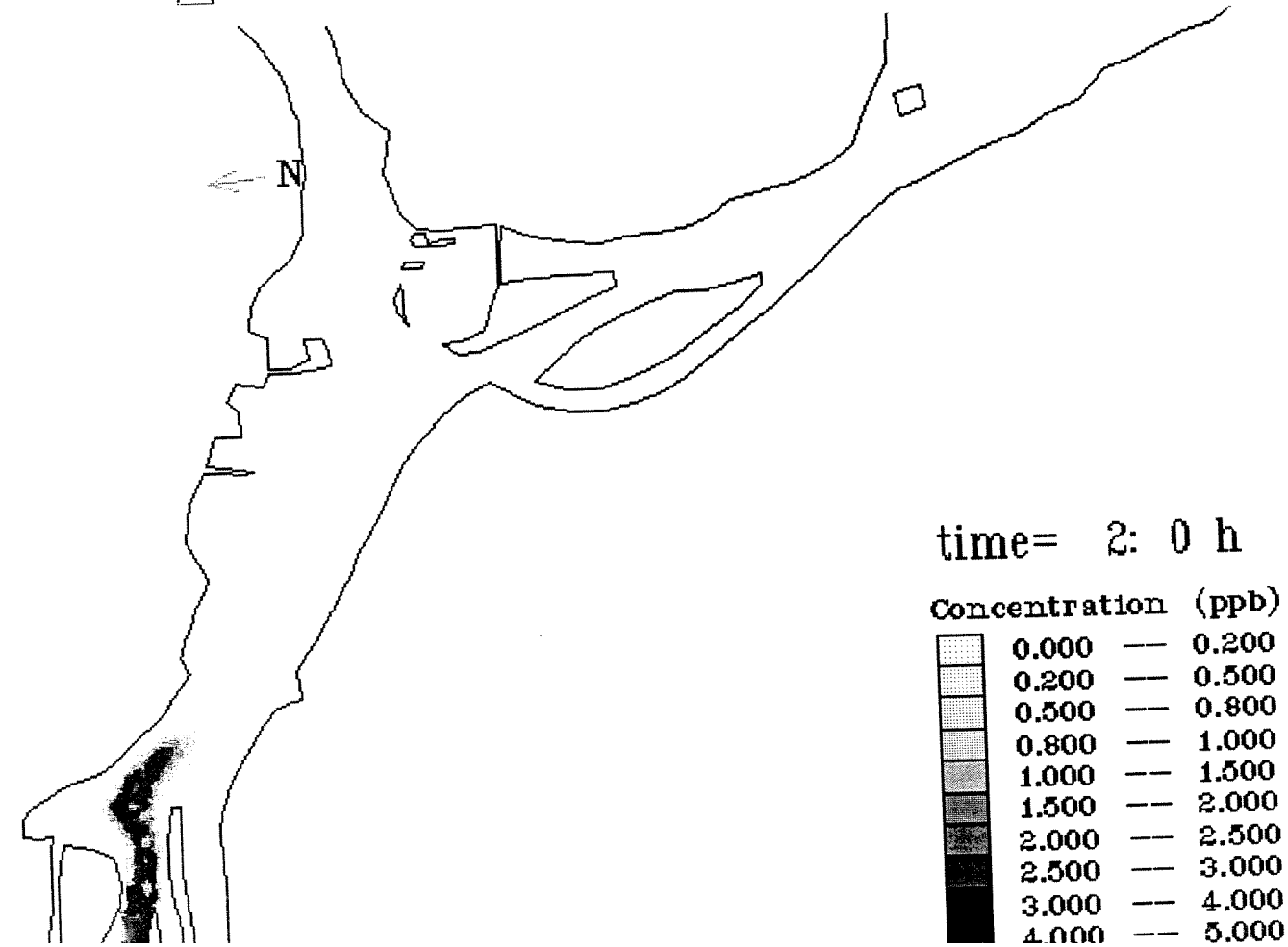
N
time= 2: 0 h
Concentration (ppb)
0.000 — 0.200
0.200 — 0.500
0.500 — 0.800
0.800 — 1.000
1.000 — 1.500
1.500 — 2.000
2.000 — 2.500
2.500 — 3.000
3.000 — 4.000
4.000 — 5.000

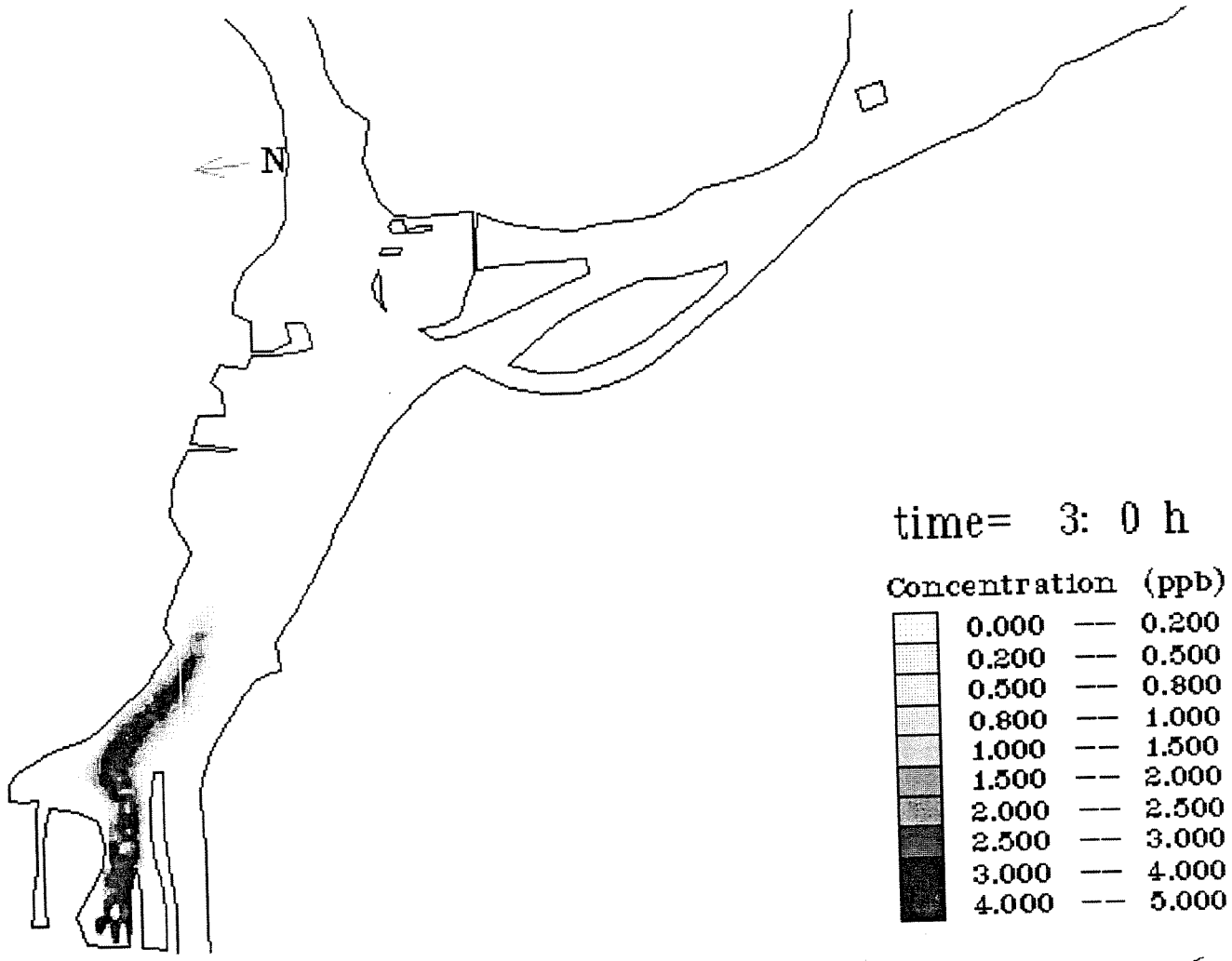
N
time= 3: 0 h
Concentration (ppb)
0.000 — 0.200
0.200 — 0.500
0.500 — 0.800
0.800 — 1.000
1.000 — 1.500
1.500 — 2.000
2.000 — 2.500
2.500 — 3.000
3.000 — 4.000
4.000 — 5.000

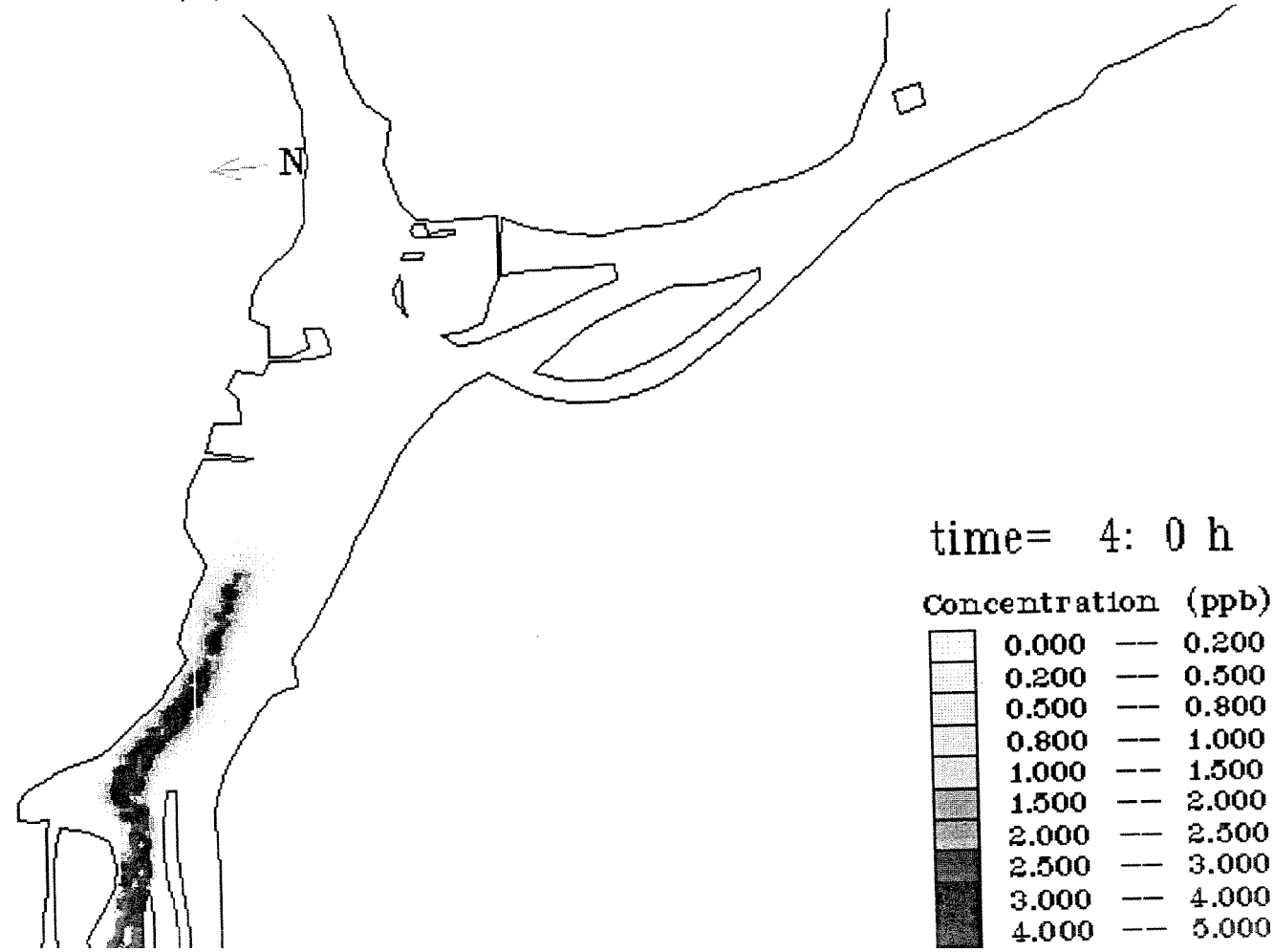
N
time= 4: 0 h
Concentration (ppb)
0.000 — 0.200
0.200 — 0.500
0.500 — 0.800
0.800 — 1.000
1.000 — 1.500
1.500 — 2.000
2.000 — 2.500
2.500 — 3.000
3.000 — 4.000
4.000 — 5.000

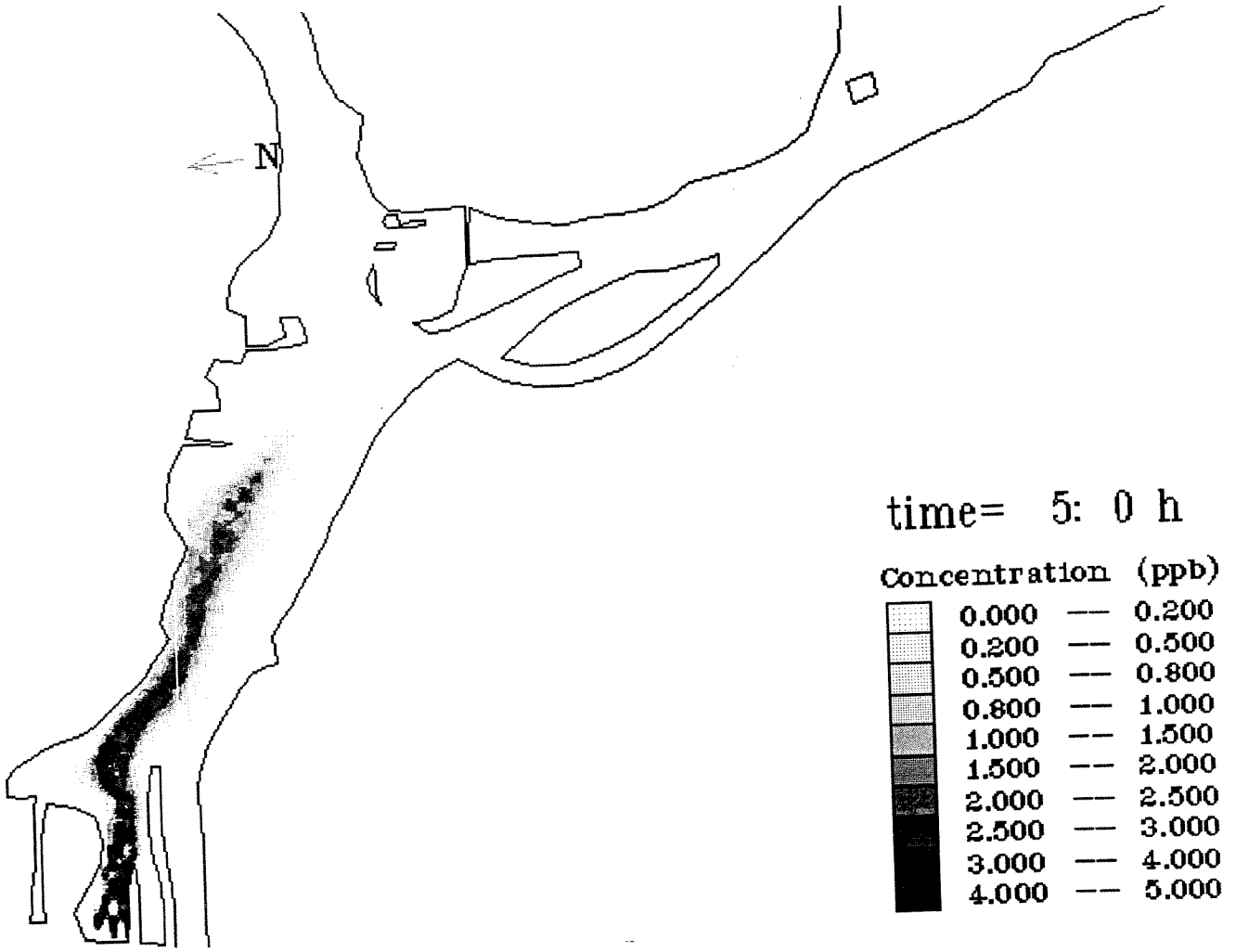
N
time= 5: 0 h
Concentration (ppb)
0.000 — 0.200
0.200 — 0.500
0.500 — 0.800
0.800 — 1.000
1.000 — 1.500
1.500 — 2.000
2.000 — 2.500
2.500 — 3.000
3.000 — 4.000
4.000 — 5.000

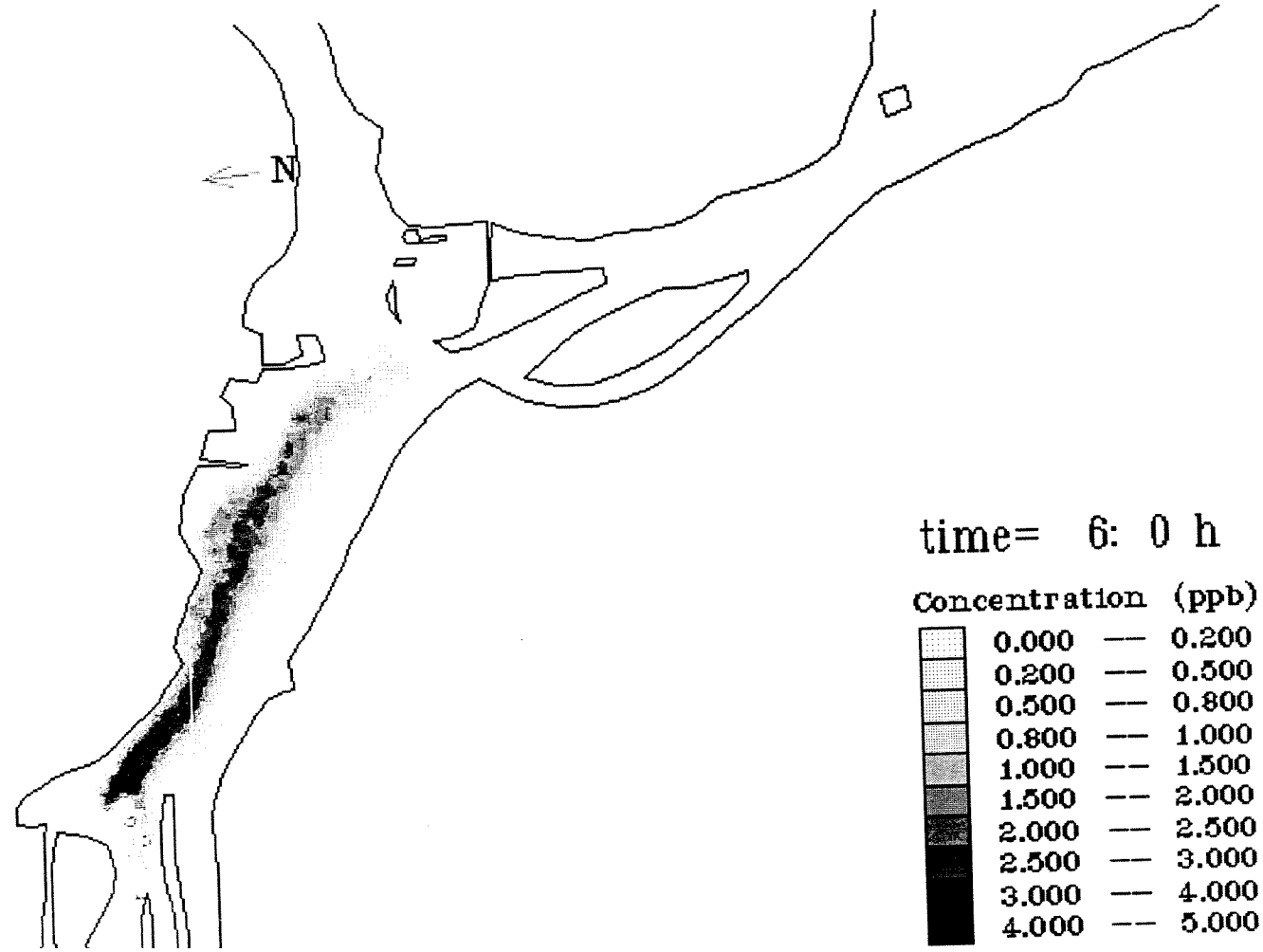
N
time= 6: 0 h
Concentration (ppb)
0.000 — 0.200
0.200 — 0.500
0.500 — 0.800
0.800 — 1.000
1.000 — 1.500
1.500 — 2.000
2.000 — 2.500
2.500 — 3.000
3.000 — 4.000
4.000 — 5.000

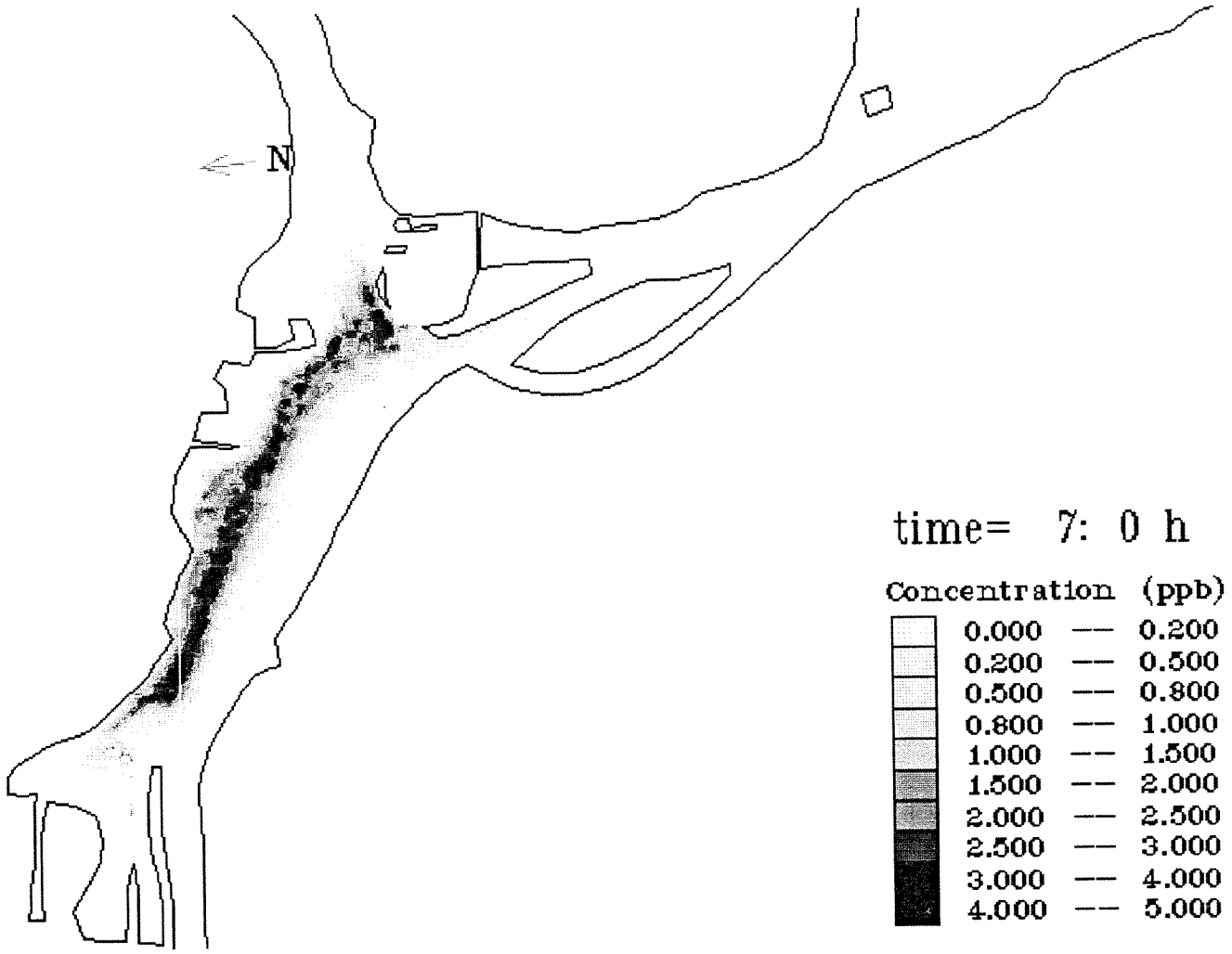
N
time= 7: 0 h
Concentration (ppb)
0.000 — 0.200
0.200 — 0.500
0.500 — 0.800
0.800 — 1.000
1.000 — 1.500
1.500 — 2.000
2.000 — 2.500
2.500 — 3.000
3.000 — 4.000
4.000 — 5.000

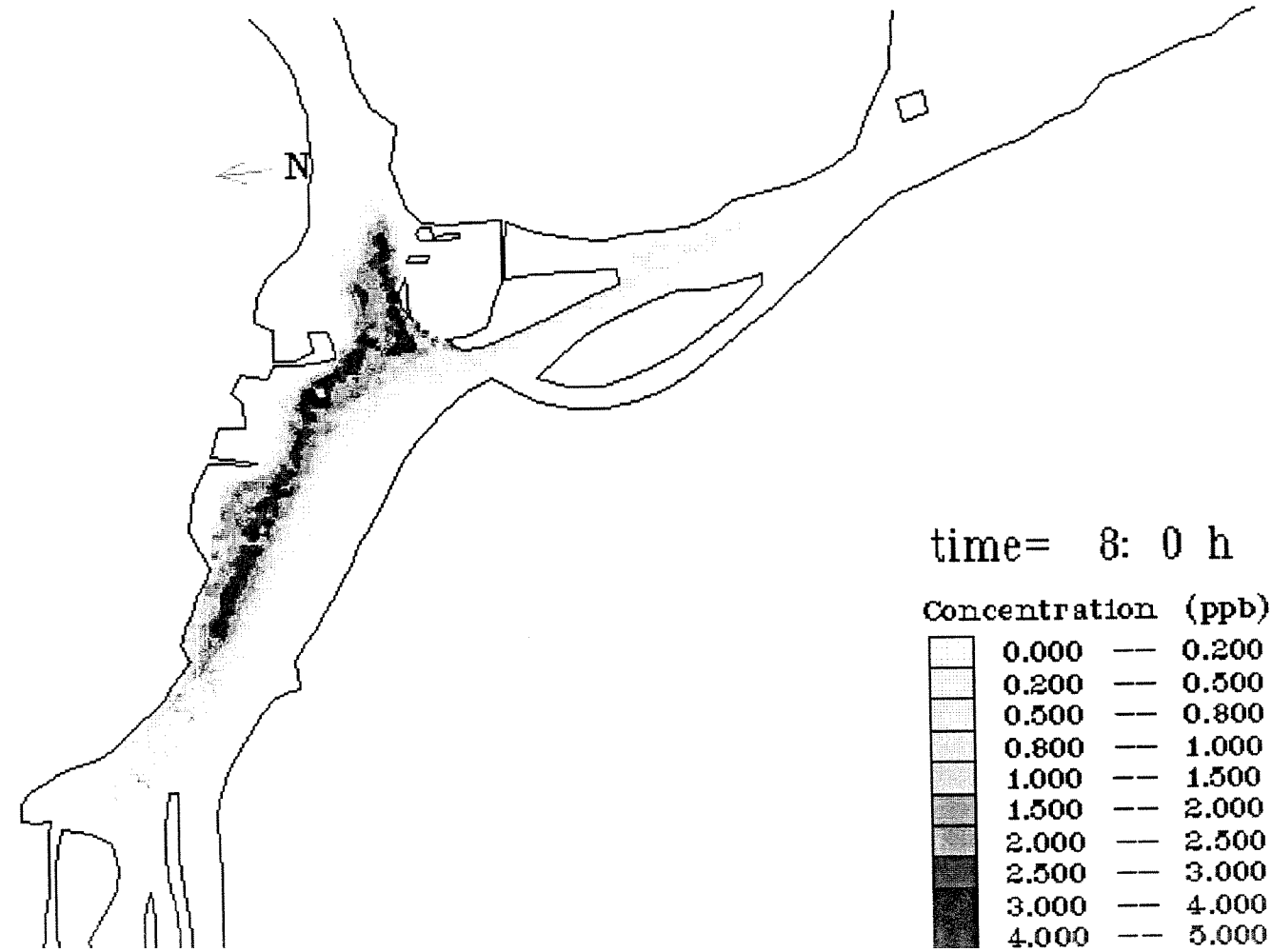
N
time= 8: 0 h
Concentration (ppb)
0.000 — 0.200
0.200 — 0.500
0.500 — 0.800
0.800 — 1.000
1.000 — 1.500
1.500 — 2.000
2.000 — 2.500
2.500 — 3.000
3.000 — 4.000
4.000 — 5.000

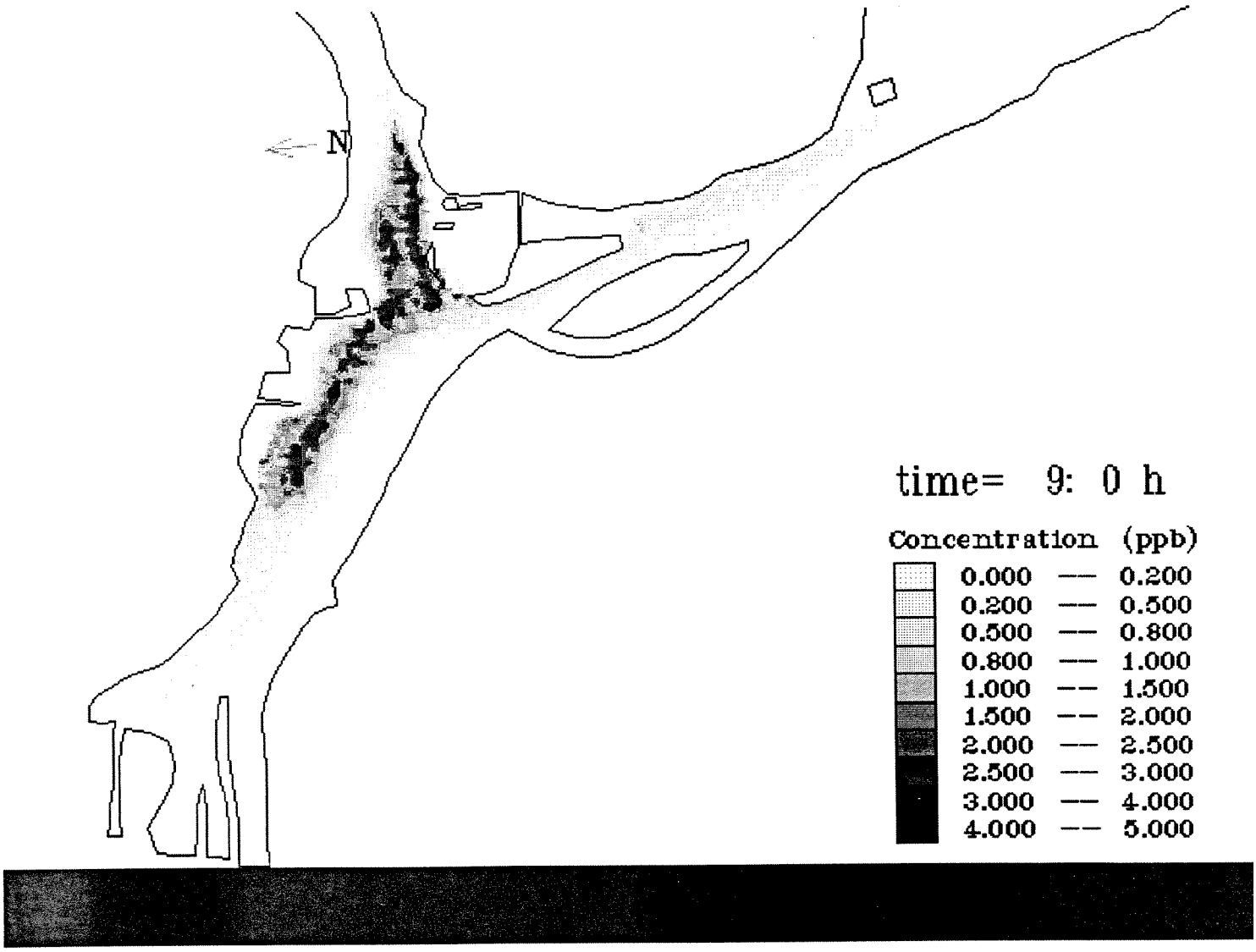
N
time= 9: 0 h
Concentration (ppb)
0.000 — 0.200
0.200 — 0.500
0.500 — 0.800
0.800 — 1.000
1.000 — 1.500
1.500 — 2.000
2.000 — 2.500
2.500 — 3.000
3.000 — 4.000
4.000 — 5.000

CASE 4

Flow:

Total Flow = 1315 m^3/s

American Lock = 15 m^3/s

Compensation Works = 300 m^3/s

COE Powerhouse = 350 m^3/s

Edison Sault Electric = 622 m^3/s

Canadian Lock = 28 m^3/s

Input:

C_0= 27.0 ppb at Compensation Works

Input duration = 5:50 hrs

Output:

Maximum concentration during the 9 hrs

Concentration distribution every hour from 1 to 9 hrs

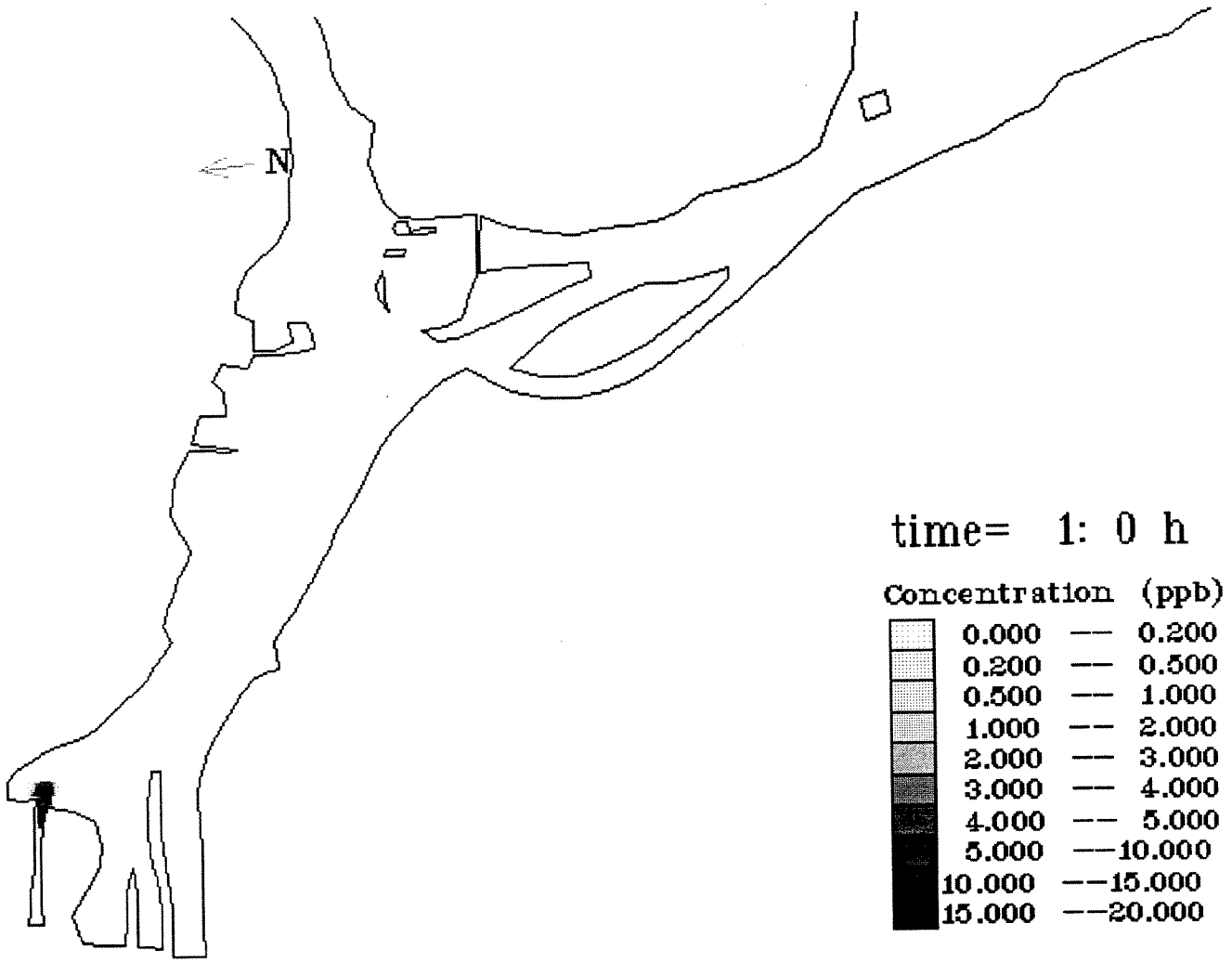
N
time= 1: 0 h
Concentration (ppb)
0.000 — 0.200
0.200 — 0.500
0.500 — 1.000
1.000 — 2.000
2.000 — 3.000
3.000 — 4.000
4.000 — 5.000
5.000 —10.000
10.000 —15.000
15.000 —20.000

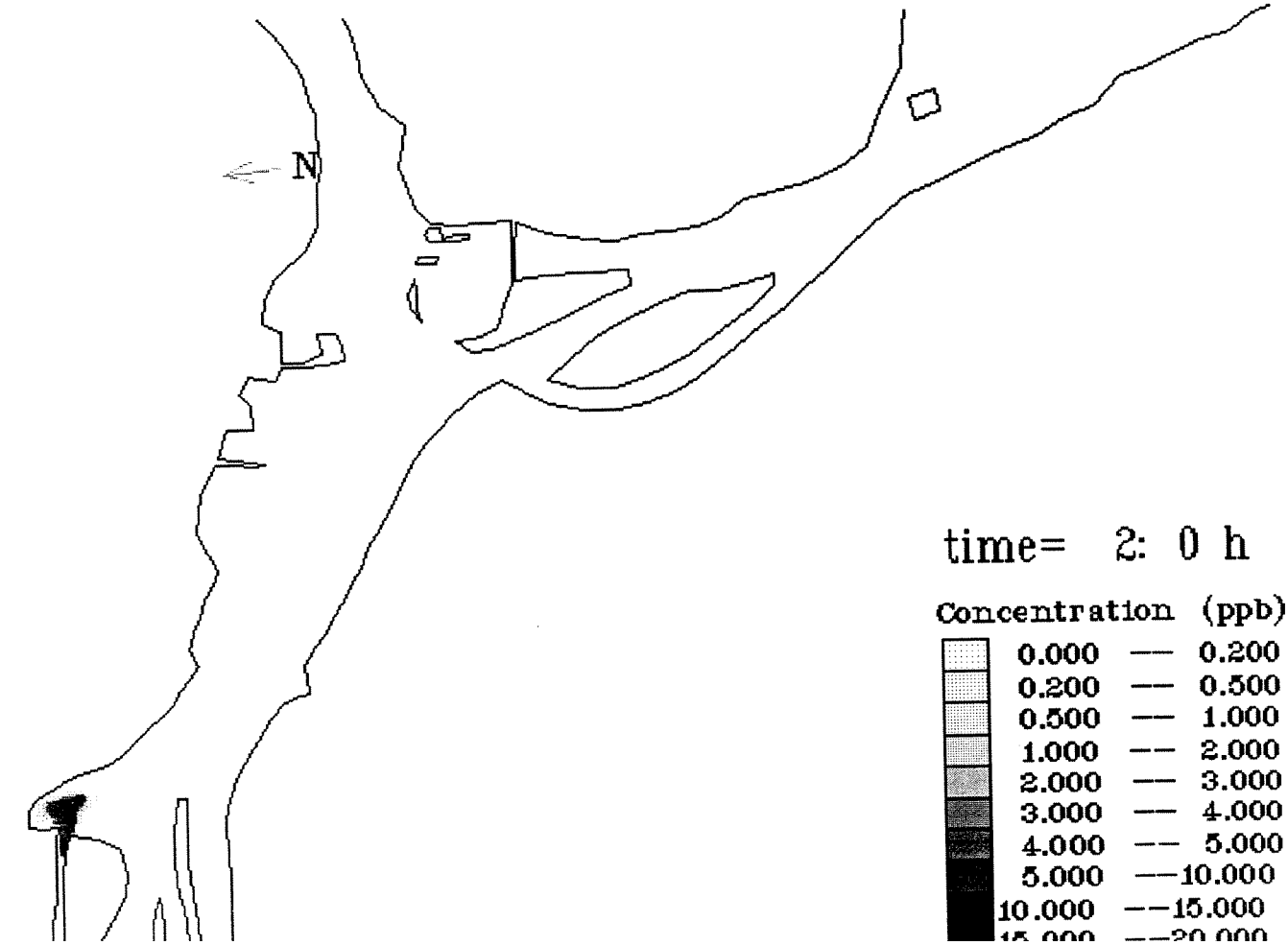
N
time= 2: 0 h
Concentration (ppb)
0.000 — 0.200
0.200 — 0.500
0.500 — 1.000
1.000 — 2.000
2.000 — 3.000
3.000 — 4.000
4.000 — 5.000
5.000 —10.000
10.000 —15.000

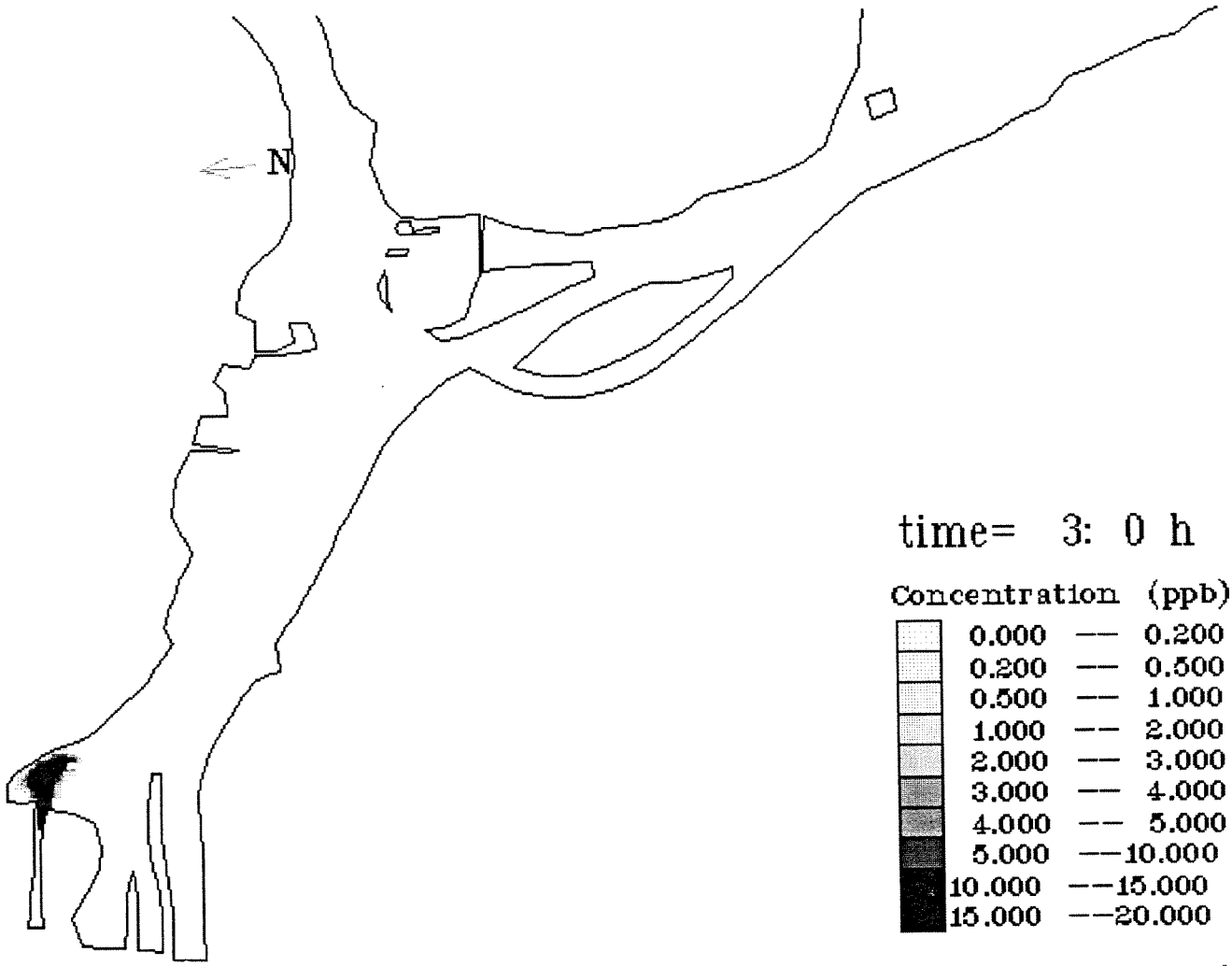
N
time= 3: 0 h
Concentration (ppb)
0.000 — 0.200
0.200 — 0.500
0.500 — 1.000
1.000 — 2.000
2.000 — 3.000
3.000 — 4.000
4.000 — 5.000
5.000 —10.000
10.000 —15.000
15.000 —20.000


N
time= 4: 0 h
Concentration (ppb)
0.000 — 0.200
0.200 — 0.500
0.500 — 1.000
1.000 — 2.000
2.000 — 3.000
3.000 — 4.000
4.000 — 5.000
5.000 —10.000
10.000 —15.000

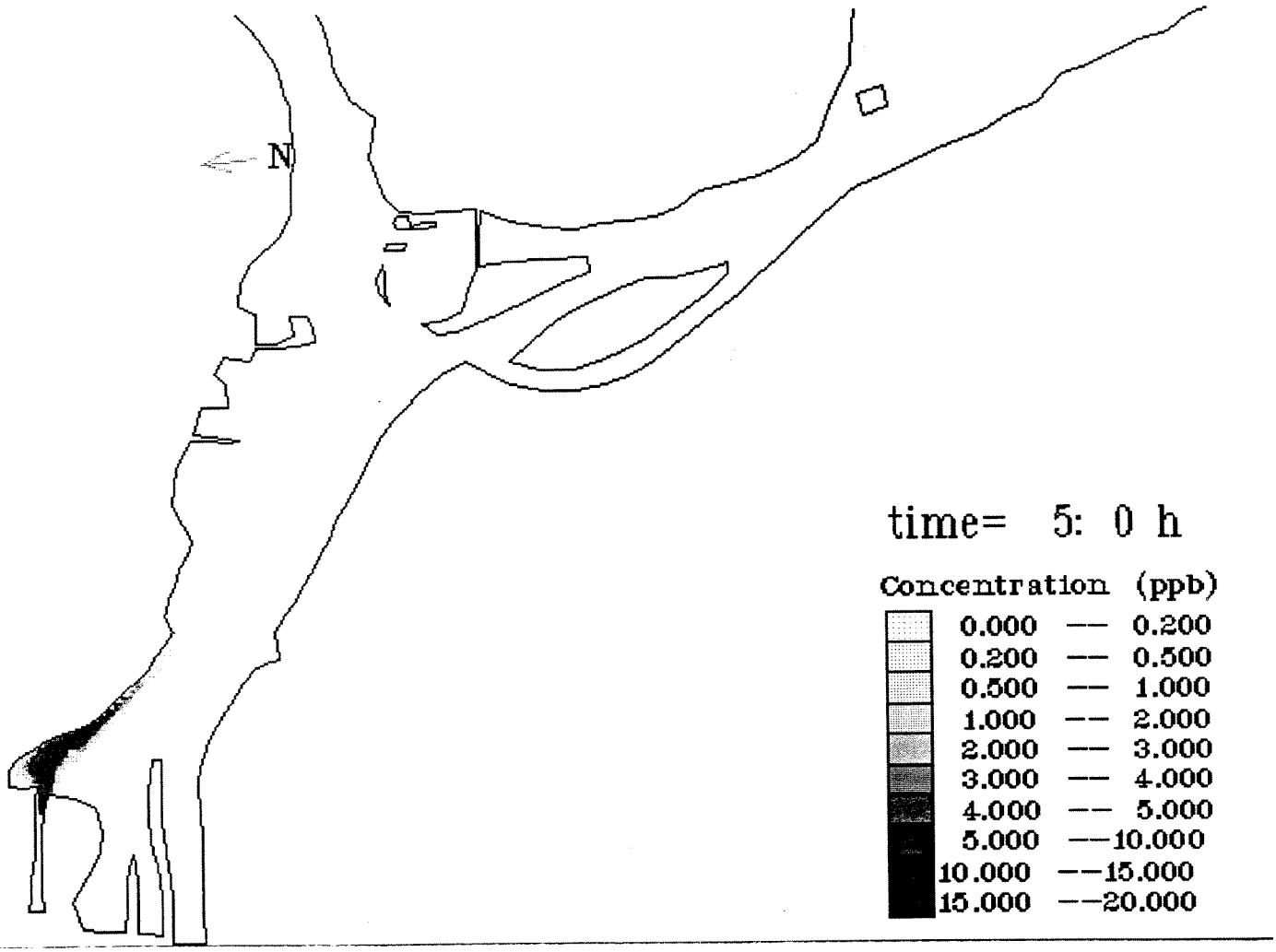
N
time= 5: 0 h
Concentration (ppb)
0.000 — 0.200
0.200 — 0.500
0.500 — 1.000
1.000 — 2.000
2.000 — 3.000
3.000 — 4.000
4.000 — 5.000
5.000 —10.000
10.000 —15.000
15.000 —20.000

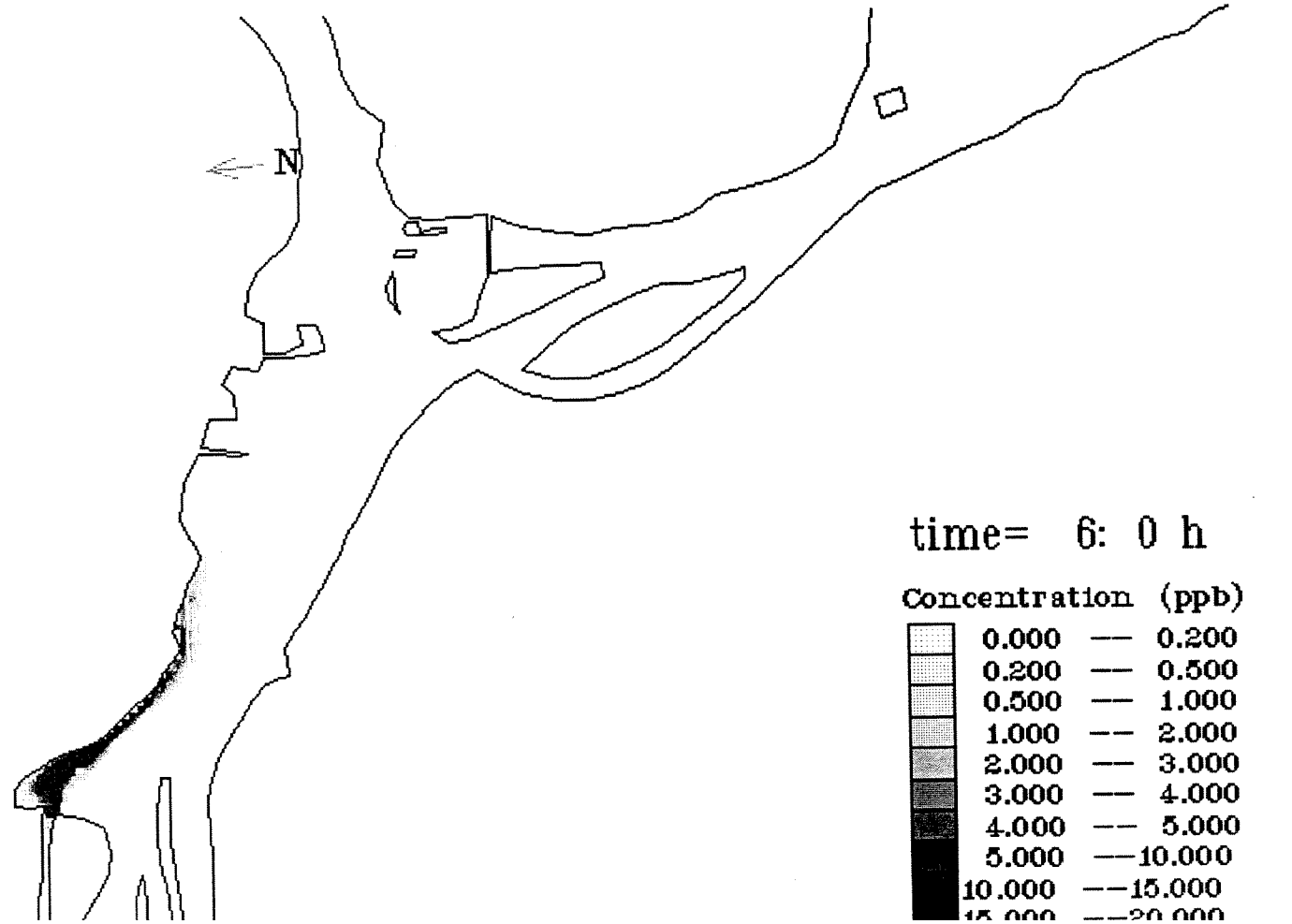
N
time= 6: 0 h
Concentration (ppb)
0.000 — 0.200
0.200 — 0.500
0.500 — 1.000
1.000 — 2.000
2.000 — 3.000
3.000 — 4.000
4.000 — 5.000
5.000 —10.000
10.000 —15.000
15.000 —20.000

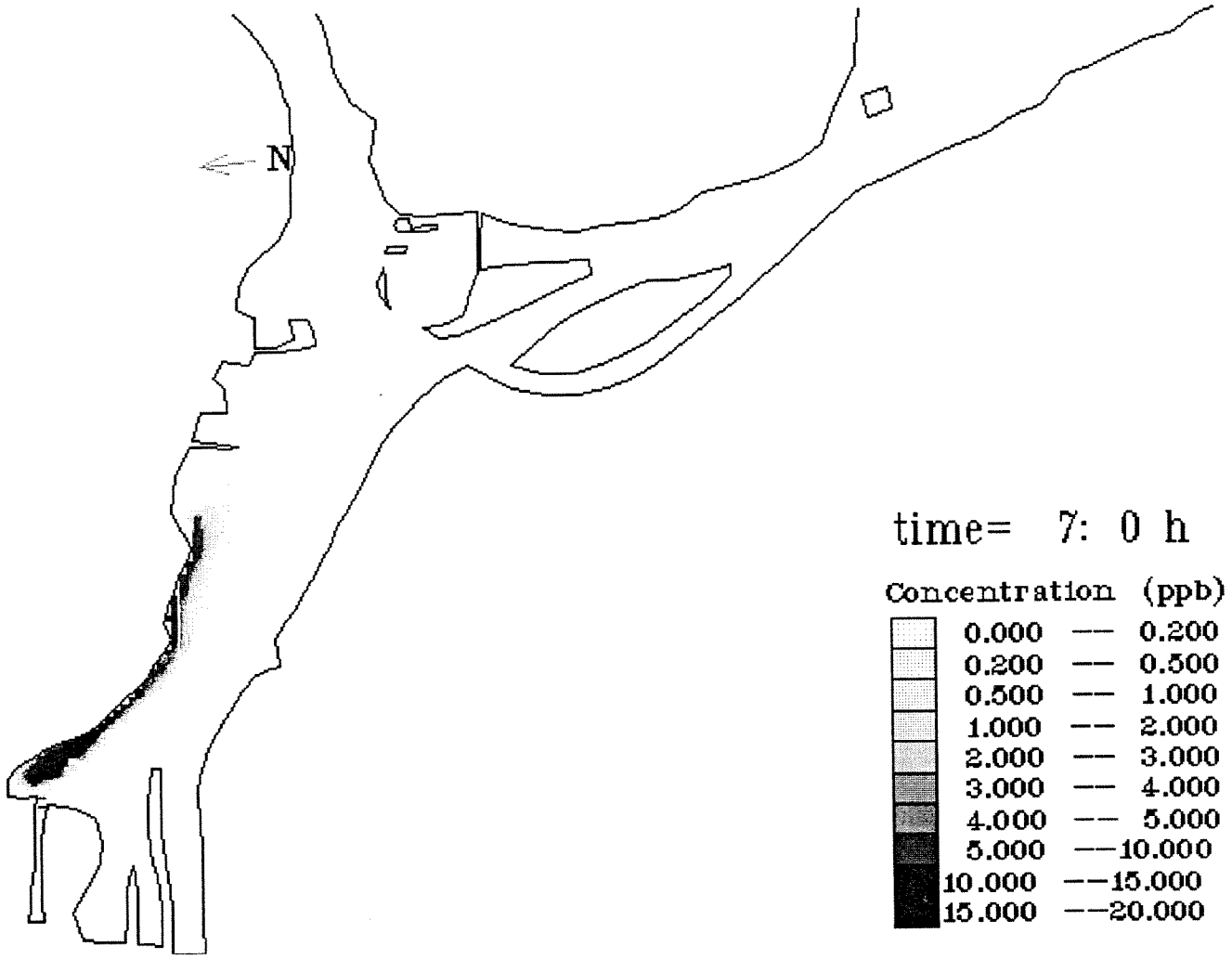
N
time= 7: 0 h
Concentration (ppb)
0.000 — 0.200
0.200 — 0.500
0.500 — 1.000
1.000 — 2.000
2.000 — 3.000
3.000 — 4.000
4.000 — 5.000
5.000 —10.000
10.000 —15.000
15.000 —20.000

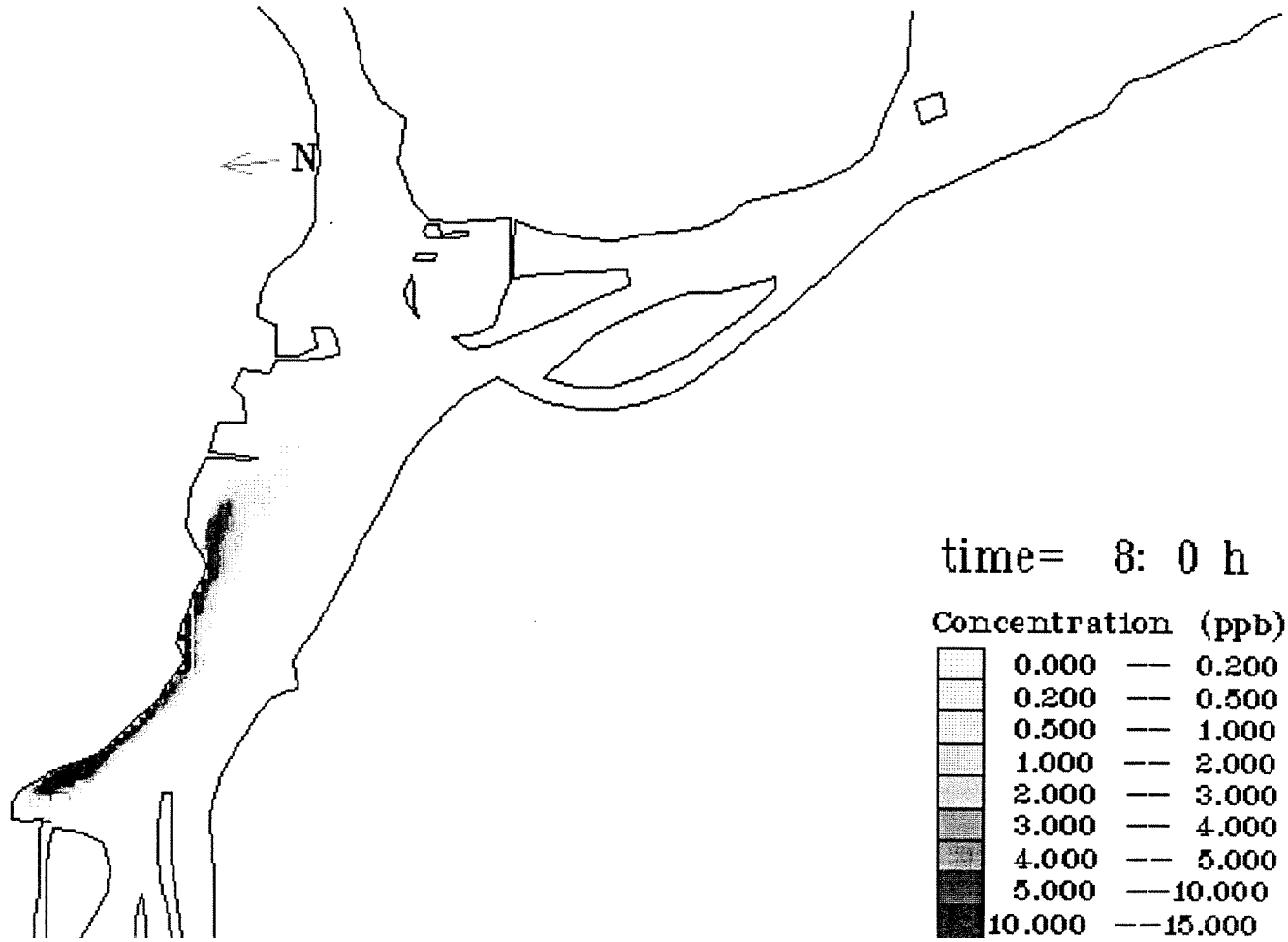
N
time= 8: 0 h
Concentration (ppb)
0.000 — 0.200
0.200 — 0.500
0.500 — 1.000
1.000 — 2.000
2.000 — 3.000
3.000 — 4.000
4.000 — 5.000
5.000 —10.000
10.000 —15.000


N
time= 9: 0 h
Concentration (ppb)
0.000 — 0.200
0.200 — 0.500
0.500 — 1.000
1.000 — 2.000
2.000 — 3.000
3.000 — 4.000
4.000 — 5.000
5.000 —10.000
10.000 —15.000
15.000 —20.000